FACULTY OF SCIENCES

Towards molecular communication between hydrogels

Emiel Pattyn

Promotor: Prof. Dr. Richard Hoogenboom
Co-promotor: Prof. Dr. Patrice Woisel
Supervisor: Dr. Yann Bernhard

A dissertation submitted to Ghent University in partial fulfilment of the requirements for the degree of Master of Science in Chemistry

GHENT UNIVERSITY

FACULTY OF SCIENCES

Towards molecular communication between hydrogels

Emiel Pattyn
Student number: 01507499

Promotor: Prof. Dr. Richard Hoogenboom
Co-promotor: Prof. Dr. Patrice Woisel
Supervisor: Dr. Yann Bernhard

A dissertation submitted to Ghent University in partial fulfilment of the requirements for the degree of Master of Science in Chemistry

Academic year: 2019 - 2020

GHENT UNIVERSITY

Acknowledgements

Writing the acknowledgment of my master thesis does not only mark the end of a thrilling, challenging, interesting, stressful and above all amazing project. It also means that an important chapter of my life has come to an end. The past five years have been an incredible journey with a lot of ups and unfortunately also some downs, which have taught me so many personal and academic skills. The route was not always easy but in the end I am extremely proud to say that I (almost) hold a master degree in the most beautiful subject there is: chemistry.

This thesis would never have seen the light of day if it weren't for the support of several people and I would like to express my sincerest gratitude towards all of them.

First and foremost, I would like to thank prof. dr. Richard Hoogenboom for the opportunity to become a part of the Supramolecular Chemistry group and for giving me the chance to work on this project. Secondly, I wish to thank my supervisor Yann for his guidance and willingness to always share his expertise with me. I learned a great deal from you and can only hope to become an equally skilled researcher in the further. Many thanks as well to the current group members of the Supramolecular Chemistry group for making me feel welcome and letting me work and learn in a fun and professional environment.

There is however more in life than chemistry and with that in mind, I would like to thank my friends for brightening up my days. A special shout out, in the context of my thesis, goes out to Gilles, Rinus and Sigo for there not so professional but nevertheless invaluable feedback. Thanks to you Sigo, I will never again write the word job plot without a capital letter.

A special thanks goes out to my lovely girlfriend Louise for her unconditional support and love. You are an incredible women and I love you with all my heart.

Last but definitely not least, the biggest thank you by far, to my parent who gave me the greatest gift they could ever give by giving me the chance to pursue my dreams.

Abbreviation

ΔG	Change in Gibbs free energy
ΔH	Change in Enthalpy
ΔS	Change in Entropy
AROP	Anionic Ring-Opening Polymerization
BBox	Blue Box Cyclobis(paraquat-p-phenylene)
CuAAC	Cu(I)-catalyzed azide-alkyne cycloaddition
CROP	Cationic Ring-Opening Polymerization
CRP	Controlled Radical Polymerization
DCE	1,2-Dichloroethane
DCM	Dichloromethane
DMF	*N,N*-Dimethylformamide
DNP	1,5-Dialkyloxynaphthalene
DOSY	Diffusion-Ordered Spectroscopy
DP	Degree of Polymerization
HPβCD	Hydroxypropylated β-cyclodextrin
Ka	Thermodynamic association constant
LCST	Lowest Critical Solution Temperature
LS	Light Scattering
MALS	Multi Angle Light Scattering
MeCN	Acetonitrile

MeOH	Methanol
MeOTs	Methyl Tosylate
PAOx	Poly(2-oxazoline)s
PNAGA	Poly(*N*-acryloyl glycinamide)
PNIPAM	Poly(*N*-isopropylacrylamide)
RAFT	Reversible Addition Fragmentation chain-Transfer
ROMP	Ring-Opening Metathesis Polymerization
ROP	Ring Opening Polymerization
SEC	Size Exclusion Chromatography
Tcp	Cloud point Temperature
THF	Tetrahydrofuran
UCST	Upper Critical Solution Temperature
UV	Ultraviolet

Contents

1 Introduction 1

1.1 Supramolecular Chemistry 1

1.1.1 Non-covalent interactions 2

1.1.2 Host-guest chemistry 4

1.1.2.1 Principle 4

1.1.2.2 Characterization of Host-Guest complexes 5

1.1.2.3 Solvent effects 6

1.1.2.4 Pillar[n]arene hosts 7

1.1.2.4.1 The structure 7

1.1.2.4.2 Synthesis 8

1.1.2.4.3 Host-guest properties of pillar[n]arenes 10

1.1.2.4.4 Applications of pillar [n]arenes 12

1.2 Polymers 13

1.2.1 General 13

1.2.2 Polymerization techniques 14

1.2.2.1 Ring opening polymerization (ROP) and CROP of 2-alkyl-2-oxazolines 15

1.2.3 Stimuli-responsive polymers 16

1.2.3.1 Thermo-responsive polymers 17

1.2.3.2 Thermo-responsive polymers in aqueous solution 17

1.2.3.2.1 Polymers with LCST behaviour 18

1.2.3.2.2 Polymers with UCST behaviour 18

1.2.4 Host-guest-thermo-responsive polymers 18

1.3 Hydrogels 20

1.3.1 Smart hydrogels 20
1.3.2 Host-guest-responsive-hydrogels 21
2 Thesis goal and strategy 23
3 Results and discussion 25
3.1 Model system 25
3.1.1 Synthesis of the viologen end-capped 2-n-propyl-2-oxazoline (PropOx) 26
3.1.2 Synthesis of the water-soluble pillar[n]arenes 29
3.1.2.1 Synthesis from the dimethoxybenzene .**Fout! Bladwijzer niet gedefinieerd.**
3.1.2.2 Alternative synthetic route 32
3.1.3 Host guest complexation 33
3.1.3.1 Determination of the association constant of the complexation in water 33
3.1.3.2 Influence of the complexation on the LCST behaviour of **4** 34
3.1.3.3 Job plot 35
3.1.3.4 Observation of the complexation by ^{1}H NMR spectroscopy 36
3.1.3.5 ^{1}H-NMR and DOSY monitoring of the release of **6** from the **[4**-**6]** complex 37
3.1.3.6 Reversibility of the threading-dethreading process 39
3.1.4 Conclusions 40
3.2 One Hydrogel system 40
3.2.1 Synthesis of the viologen monomer 40
3.2.2 Alternative viologen monomer synthesis 41
4 Conclusion and outlook 43
5 Extra assignment 45
5.1 Chemical communication between supramolecular systems 45
5.1.1 Molecular communication based on metal coordination 45

5.1.2 Molecular communication based on hydrogen bonding arrays 49
5.1.3 Molecular communication based on host-guest chemistry 49
5.1.4 Molecular communication based on cascades 52
5.1.4.1 Simulations on different multicomponent cascade systems 53
5.2 Conclusion 60
6 Bibliography 61
7 Appendix and Experimental section 69
7.1 Materials 69
7.2 Equipment 69
7.3 Methods 71
7.3.1 Synthesis of 1-methyl-4,4'-bipyridin-1-ium iodide (**1**) 71
7.3.2 Synthesis of the poly (2-*n*-propyl-2-oxazoline) end capped with the 1-methyl-4,4'-bipyridinium group (poly-(nPropOx-viologen) 71
7.3.3 Synthesis of decamethoxy pillar[5]arenes (**9**) 72
7.3.4 Synthesis of decahydroxypillar[5]arene (**10**) 72
7.3.5 Synthesis of triethylene glycol monomethyl ether p-toluenesulfonate (**12**) 72
7.3.6 Synthesis of deca(2-(2-(2-methoxyethoxy)ethoxy)pillar[5]arenes (**7**) 73
7.3.7 Synthesis of 1,4-bis(2-(2-(2-methoxyethoxy)ethoxy)ethoxy)benzene (**14**) 73
7.3.8 Attempt at the synthesis of pillar[5]arenes (**7**) from the 1,4-bis(2-(2-(2-methoxyethoxy)ethoxy)ethoxy)benzene (**14**) 73
7.3.9 Synthesis of 1-(2-aminoethyl-)-1'-methyl-[4,4'-bipyridine]-1,1'-diium dibromide iodide (**15**) 74
7.3.10 Synthesis of the 1-methyl-1'-(4-vinylbenzyl)-4,4'-bipyridinium salt (**17**) 74
7.4 Measurements 74
7.4.1 Measuring the binding constant in water by fluorescence spectroscopy 74
7.4.2 Measuring the Job plot by fluorescence spectroscopy 75

7.4.3 Measuring the Job plot by UV-vis spectroscopy 75

7.4.4 Turbidimetry 75

8 Scientific article 76

1 Introduction

1.1 Supramolecular Chemistry

For a long time, chemists tried to understand nature on a purely molecular level, considering only structures and functions involving the strong covalent bonds. However biological systems are generally made from supramolecular superstructures of many molecules that are held together by weak non-covalent interactions. These interactions have a dynamic nature and are responsible for a great majority of processes occurring in biological systems.[1] The double helical structure of DNA for example, is held together through, amongst other, hydrogen bonding between the complementary nucleotides.[2] Hemoglobin uses metal-ligand interactions to transport oxygen through the body[3] and proteins are able to change their assemblies to perform specific functions such as temperature regulation,[4] the focussing of the eye[5] and the process of wound healing.[6]

Inspired by these impressive but highly complex natural phenomena, chemist started to mimic them. From the seminal studies on crown-ether alkali metal ion interactions,[7] the field of supramolecular chemistry was created. The term was introduced by one of its founding fathers, Jean-Marie Lehn in 1969. He defined supramolecular chemistry as "the chemistry of the intermolecular bond". Just like molecules are built by connecting atoms with covalent bonds, supramolecular systems are built by linking molecules through intermolecular interactions.[8] In 1987 was Lehn awarded the Nobel prize in Chemistry together with Donald J. Cram and Charles J. Pedersen for "*their syntheses of molecules that mimic important biological processes*" emphasizing the significance and potential of supramolecular chemistry and stimulating further developments. Ever since, the field has seen profound developments and has evolved into a mature active domain of research that is still vibrant today. A prime example is the fact that in 2016 Jean-Pierre Sauvage, James F. Stoddart and Bernard L. Feringa have been awarded the Nobel Prize in Chemistry "*for the design and synthesis of molecular machines*", which was made possible through supramolecular chemistry.

Today supramolecular chemistry is a highly interdisciplinary field, ranging from inorganic and organic chemistry, to physical chemistry and computer modelling that is applied in a brought

range of applications such as catalysis, [9] nanotechnology,[10] smart materials,[11] data storage and processing,[12] biomaterials,[13] and drug delivery.[14]

1.1.1 Non-covalent interactions

Non-covalent interactions are the corner stone of supramolecular chemistry, as they are modular and reversible, thereby giving adaptive and cooperative motion to the supramolecular systems. They can be subdivided in five main classes: 1) electrostatic interactions, 2) hydrogen bonds 3) Van der Waals interactions 4) the metal ligand coordination and 5) π interactions (Figure1).

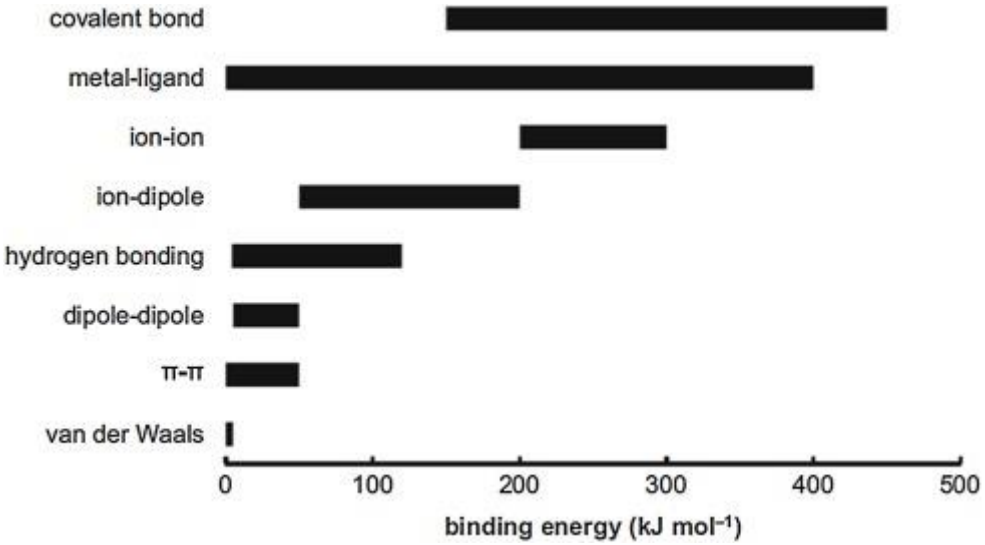

Figure 1: Overview of the (non)covalent binding energy[15]

In the general term **"electrostatic interactions"** include all the interactions hold by electric force between two (partially) charged molecules.[16] Under this broad term fall ion-ion interaction, ion-dipole interaction, dipole-dipole interactions and induced dipole interactions. **Hydrogen bonding** on the other hand is a special type of dipole-dipole interaction that results from the attractive force between an electron deficient hydrogen atom and an electron rich heteroatom such as oxygen, sulphur or nitrogen. Hydrogen bonding is one of the most important types of non-covalent interactions in the supramolecular field, because of its great binding strength and high degree of directionality.[17] The **Van der Waals interactions** are the weakest of all the non-covalent interactions, but can nevertheless be of great importance. The **metal to ligand coordination** interaction consists of a central metal ion that is surrounded by molecules that are known as ligands. The binding strength of this interaction is dependent on the type and number of ligands as well as the oxidation state of the central metal ion. Binding strengths up to and even higher than covalent bonds are possible with this highly directional

type of non-covalent interactions.[18] The **π interactions** occur between two or multiple π-systems, such as aromatic rings, but also between a π-system and a functional group.[19] Thus, the class can be subdivided into three categories: the π-π stacking, the cation-π interactions and the anion-π interactions. The **π-π stacking** is occurring between two aromatic moiety's that have no obvious electron donating or accepting character.[20] In case of simple benzene rings, many different stacking arrangements are possible, and some of them are illustrated in (Figure 2).

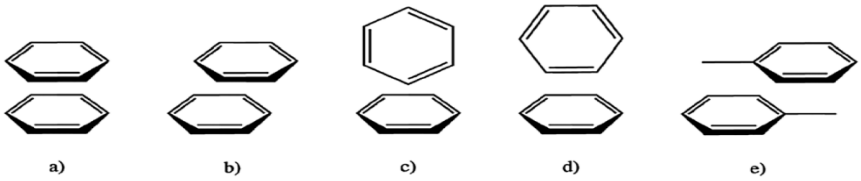

Figure 2: Possible aromatic stacking arrangements for benzene. (a) Parallel face-centred.(b) Parallel offset. (c) Perpendicular t-shaped. (d) Perpendicularly-shaped. (e) Parallel offset for toluene[21]

The **donor-acceptor π-π stacking** is a special type of π-π stacking. The nature and strength of the interaction are related to the electron density of the π-system. Molecules that have a high electron density π-system are called electron donors, when electron acceptors have a π-system with a low electron density. The donor/acceptor character is generally related to the presence of electrons donating/accepting groups that are attached to the π system. The apparent electronical benefit of interactions between the donor and acceptor will result from the formation of the non-covalent bond. As an example, π-π interactions are favoured between the nitrobenzene and the dimethylaniline, as they form donor acceptor π-π stacking interactions based on the electron rich-electron aromatic pair (Figure 3).

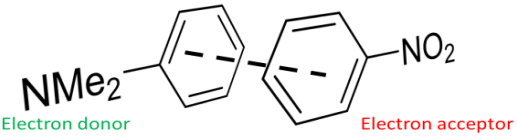

Figure 3: An illustration of a π interaction between an electron rich and an electron poor aromatic ring

The **cation-π interaction** occurs between an electron-rich π-system and a cation. Forces that play a role in this case are ion-induced dipolar interactions, dispersion and electrostatic interactions.[21] Many examples of cation-π interactions exist in nature, in proteins for example, where cationic side chain groups (from lysine or arginine) interact with aromatic side chain groups (such as in phenylalanine, tyrosine or tryptophan). These types of interactions play an essential role in biological systems, for biological recognition for instance, for example for

binding in glycine receptors, which is mediated by interactions with phenylalanine residues. The **anion-π interaction** involves an electron deficient aromatic system and an anion,[22] which interact through electrostatic force and anion-induced polarization.[23] They are also found in biological systems, for instance between phenylalanine and chloride or phosphate.[24]

1.1.2 Host-guest chemistry

1.1.2.1 Principle

Host-guest chemistry is one of the key concepts in the field of supramolecular chemistry, as it was first explored during the pioneer work of Cram,[25] Lehn,[26] and Pedersen [27], and is all about the formation of host-guest complexes. These are inclusion structures that are defined by IUPAC as *: "A complex in which one component (the host) forms a cavity or, in the case of a crystal, a crystal lattice containing spaces in the shape of long tunnels or channels in which molecular entities of a second chemical species (the guest) are located. There is no covalent bonding between guest and host, the attraction being generally due to van der Waals forces."* [28] In the seminal works, several macrocyclic cryptands, cavitands and carcerands host molecules were created, and their interactions with various guests studied. Ever since, numerous types and families of macrocycle have been further developed, giving a wide variety of host molecules. An overview of commonly employed hosts and their structure is given in Figure 4.

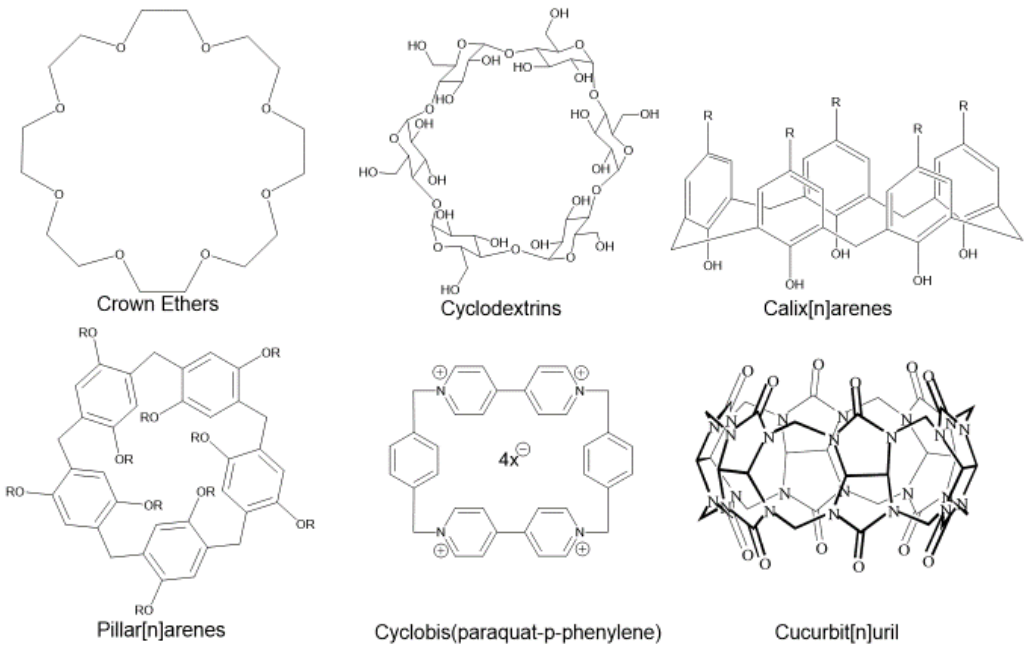

Figure 4: Structures of commonly used host molecules

From these examples, it can be noted that the majority of host molecules share common features: they have a rigid framework and are preorganized cyclic structures, meaning that no significant conformational changes are needed for the host to bind a guest, resulting in stronger complexes.[29]

1.1.2.2 Characterization of Host-Guest complexes

The host-guest complex is a dynamic equilibrium between the associated complex and the dissociated host and guest molecules (Figure 5). Within this context, the binding or association constant K_a is an important term. The K_a value permits to quantify the affinity of the host and guest molecules for making a host-guest complex. Its formula is described in the first equation and it is directly related to the concentration of the different entities present in solution. This concentration, and consequently the K_a value can be determined by a broad range of techniques such as ^{1}H-NMR spectroscopy,[30] UV-vis spectroscopy,[31] isothermal titration calorimetry,[32] and fluorescence spectroscopy[33].

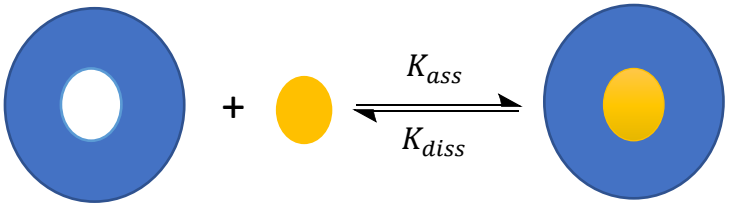

$$K_a = \frac{[host-guest\ complex]}{[host]*[guest]} = \frac{K_{ass}}{k_{diss}} \qquad (1)$$

$$\Delta G = -RTln(K_a) \qquad (2)$$

$$\Delta G = \Delta H - T\Delta S \qquad (3)$$

Figure 5: Scheme and equations describing the thermodynamics of a host guest complex

The K_a is also linked to the thermodynamics of the system through the second equation, where the enthalpic term (ΔH) is related to the interaction energies between the different moieties and the solvent and the entropic term (ΔS) is linked to the degrees of freedom the system has. The process of complexation will be spontaneous and favoured, when it results in a negative change of the Gibbs free energy ΔG, *i.e.* when ΔH decrease and/or ΔS increase.

Another important property of host-guest complexes is their binding stoichiometry. Various techniques exist to determine it, but the Job's method is by far the most popular one, albeit it also has its limitations.[34] In this method, equimolar solutions containing different molar ratios of host/guest are prepared and a signal proportional to the concentration of the complex is

measured. This is done for example by integration of the NMR signal,[35] UV-VIS absorbance[35] or fluorescence measurements.[35] This response is then plotted against the mole fraction of the host or guest, resulting in a graph called the Job plot. From the maximum of this plot, corresponding to the highest concentration of complex, it is possible to subtract the binding stoichiometry, which is for example 1:1: in case of the Job plot presented on Figure 6.

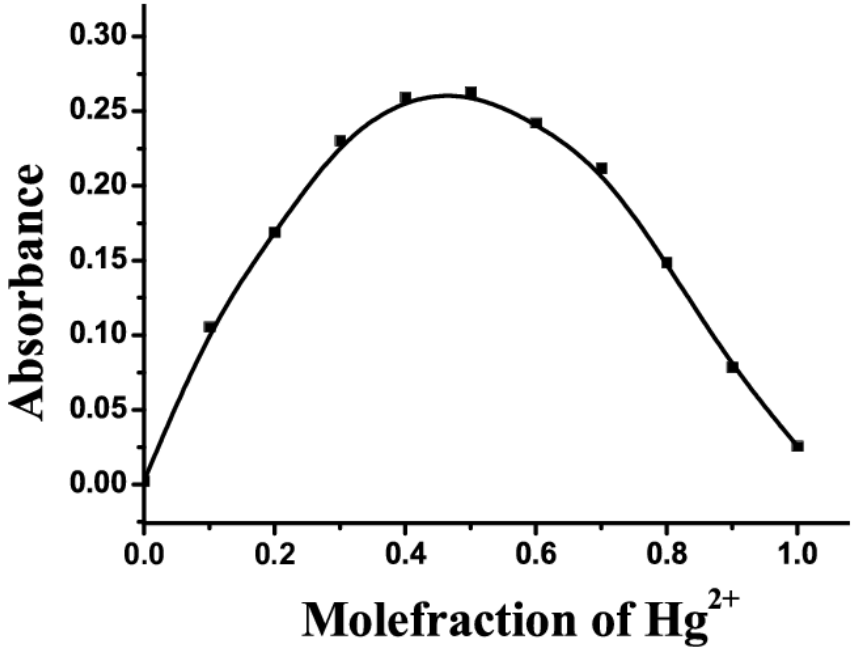

Figure 6: An example of a Job plot from a 1:1 binding stoichiometry complex[36]

1.1.2.3 Solvent effects

As stated above, the non-covalent interactions are reversible, weaker than the covalent counterparts and responsible for the sensitivity of supramolecular systems towards experimental conditions.[37] Particularly, the temperature and the solvent properties play a vital role in the thermodynamics and kinetics of such systems. This is profoundly correlated to changes in solubility, stability constant, reactivity, redox potential and some spectral parameters.[38] Host-guest systems in particular can be influenced significantly by solvent effects, as a partial desolvation of the host and the guest should occur before the complex formation. The desolvation energy, which is linked to the enthalpic term in the Gibbs-Helmholtz equation, is specific to the host-guest system and the solvent.[37] Especially in water is the desolvation energy high,[39] so in aqueous environments the K_a strongly affected by the solvent. An increase of entropy is related to the desolvation step, since it releases the regularly arranged solvent molecules on the surface of the host and guest molecules into the disorder bulk solvent. A fraction of this entropy gain is cancelled out by the loss of entropy that is

associated with the host-guest formation. This effect becomes much weaker if the host and guest molecules share small surfaces upon complexation in aprotic solvents.[37]

1.1.2.4 Pillar[n]arene hosts

The pillar[n]arene host molecules deserve a separate section, since this class of host molecules is used extensively in this thesis. Pillar[n]arenes are composed of para-dialkoxybenzene groups bridged together by methylene groups in a pillar-shaped macrocyclic structure (Figure 4). This relatively recent class of molecules was first reported in 2008 by the group of Tomoki Ogoshi[40] and is revolutionary in that it allows versatile functionalization of the aromatic units. Previously, paracyclophane macrocycles lacked functional groups on the phenyl units, which limited their solubility and processability. The versatile functionalization along with its unique pillar-shaped cavity, straight forward synthesis and excellent host–guest properties led to a rapid increase in its popularity.[41] Today, have pillar[n]arene macrocycles manifested themselves as key players in supramolecular host-guest chemistry.

1.1.2.4.1 The structure

Different sizes of pillar[n]arene can be obtained by varying the experimental conditions applied and subsequently the number of repeating units n composing the macrocycle. Each pillar[n]arene possesses a unique structure, as revelated by X-ray crystal analysis. For example, structural data of pillar[5]arene with 10 methoxy groups 1[5] revealed that it possesses a completely symmetric cylindrical form, when looked at it from the side, and a highly symmetrical regular pentagonal structure, when looked at it from the top.[42] The X-ray crystal structure data of pillar[6]arene 12 with propoxy groups 2[6] showed exactly the same features with the only difference being a hexagonal-like cyclic top view.[43] Studies done on larger pillar[n]arenes resulted in the same observations with regards to the side view, but revealed fundamental differences in the top view. Pillar[8]arene with 16 ethoxy groups 1[8] appeared to have two pentagonal cavities, pillar[9]arene with 18 ethoxy groups 1[9] consisted of one pentagonal and one hexagonal cavity and pillar[10]arene with 20 ethoxy groups 1[10] has two hexagonal cavities. An explanation for these double cavity structures is the fact that it reduces the ring strain.[44]

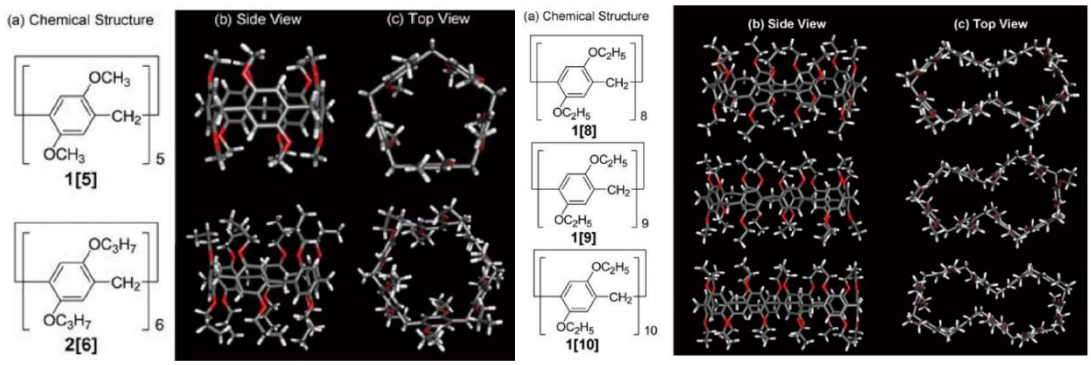

Figure 7: (a) Chemical structures and (b) side and (c) top views of per-methylated pillar[5]-,pillar[6]-, and per-ethylated pillar[8]-, pillar[9]-, and pillar[10]arenes (1[8], 1[9], and 1[10])[44]

1.1.2.4.2 Synthesis

Pillar[n]arenes are usually synthesized by combining 1,4 dialkoxybenzene with a Lewis acid (for example BF_3OEt_2) and paraformaldehyde.

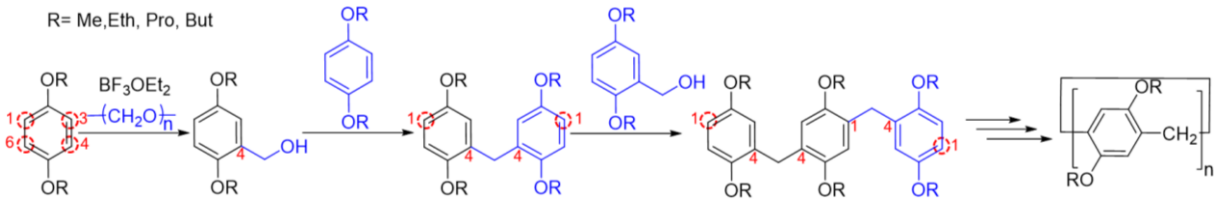

Figure 8: Steps of the synthesis of Pillar[n]arene with 1,4 dialkoxybenzene in the presence of paraformaldehyde and BF_3OEt_2

The addition of the paraformaldehyde can occur on four electronically equivalent reaction sites (positions -1, -3, -4 or -6). However, after the first reaction will the steric hindrance lead to a selective second addition step in the para-position (position 1) related to the first introduced group (in position 4).[44]

Pillar[n]arenes can be synthesized under kinetic and thermodynamic control. However, it is almost always desirable to work under thermodynamic control, and additives are generally added to the reaction to act as a template to favour cyclization. This cannot be done under kinetic control, where generally a wide range of cyclic homologues and/or linear structures as oligomers and polymers are formed.[44]

Thus, the selective synthesis of pillar[5]arenes can be done under thermodynamic control when using the right conditions. Key factors in the synthesis are the choice of the Lewis acid,[40] and the solvent used. Szumna et al. investigated these parameters and showed that yields up to 8 1% for the 5 member structure could be achieved when 1,2-dichloroethane was used as

a solvent.[45] In comparison, when chloroform, dichloromethane or 1,1,2,2-tetrachloroethane were used, the maximum yield obtained was 26 %. This is explained by the fact that pillar[5]arenes selectively form host–guest complexes with linear-shaped molecules, thus the linear dichloroethane can act as a template solvent.

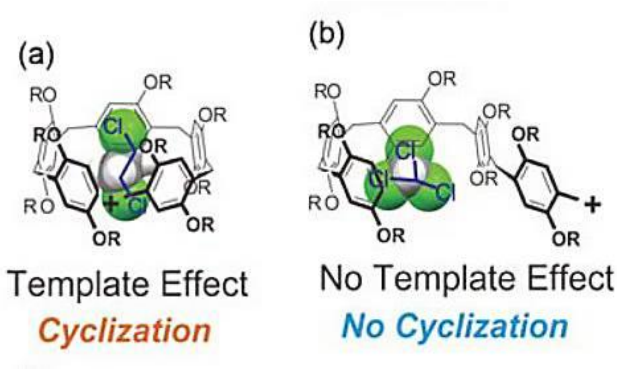

Figure 9: Linear 1,2-dichloroethane acts as a template for the formation of pillar[5]arenes, while (b) branched chloroform cannot act as a template fort the synthesis of pillar[5]arenes homologues[46]

Different groups attempted to selectively synthesize pillar[6]arene with high yield. The use of chlorocyclohexane as templating solvent was one of the most efficient ways.[47] The right synthetic conditions to have thermodynamic control over the formation of other pillar[n]arene homologues (n ≥ 7) have, however, not been found yet. These types of molecules have only been made under kinetic control and were obtained with low yield by separation of the mixture containing numerous other cyclic and linear structures.

From a synthesized pillar[n]arene macrocycle, modulation of the substituents on both rims is frequently used to modulate its physical properties, such as conformation, host-guest capability or solubility as well as to incorporate the pillar[n]arenes into larger polymeric structure and hydrogels. The most frequent way in doing so is to hydrolyze the methoxy groups from the methoxy substituted pillar[n]arene to produce a pillar[n]arene containing phenolic groups.[48] The further alkylation of the phenolic units allow the introduction of new functionalities, such as ionic functions to induce water solubility. Numerous homo-functionalized pillar[n]arenes have been prepared in this manner, and the selective synthesis of multifunctional pillar[n]arenes has also been achieved.[49,50] One strategies to create these more sophisticated pillar[n]arenes is to hydrolyze a certain number of methoxy groups or to oxidize one or more dialkoxybenzene rings to the quinone structures, followed by reduction and alkoxylation.[51] Another is to use a statistical co-condensation between two different dialkoxybenzenes[52] or the incorporation of different alkoxy substituents via asymmetrically

modified dialkoxybenzene precursors.[53] The creation of pillar[n]arenes that do not have two alkoxy substituents on all benzene rings has also been reported and three recently developed studies regarding this topic are highlighted in a recent report by our group.[41]

1.1.2.4.3 Host-guest properties of pillar[n]arenes

A broad range of interactions, such as, charge-transfer-, hydrophobic/hydrophilic-, cation-π-, hydrogen-bond- and electrostatic interactions can play a role in the host-guest complexation of pillar[n]arenes. This is also supported by the wide variety of functional groups that can be installed on the rim of the pillar[n]arenes to provide a suitable interaction site for the guest.[44] The favourable complexation is the result of a combination of these interactions.

Charge-transfer interactions

Pillar[n]arenes are usually composed of electron-donating units based on the hydroxyl or alkoxy-substituents on the benzene rings providing the ability to form host-guest complexes with neutral or cationic electron accepting molecules (Figure 10). For example, per-hydroxylated pillar[5]arene *(A)* can form host-guest complexes with viologen *(I)*,[42] alkyl pyridinium salt *(L),*[42] imidazolium ionic liquids *(J),*[54] and alkyl bis-pyridinium salts with various alkyl chain length *(M)*.[55] Similarly, the electron-rich per-alkoxylated pillar[n]arenes (C), can form host-guest complexes with tetracyanoethylene*(R),*[54] or tropylium cation (*O)*.[56]

Hydrophobic/hydrophilic interactions

Water soluble pillar[n]arenes are able to encapsulate hydrophobic guests within their hydrophobic cavity in aqueous media. The first water-soluble pillar[5]arene that was reported in the literature was described by T. Ogoshi in 2010 and contains 10 carboxylate groups *(E)*.[57] This host gives a high association constant with paraquat *(N),*[42] 1,4-bis(pyridinium)butane derivatives *(K),*[58] and is also able to selectively encapsulate lysine *(Z)*, arginine *(A2)* and histidine *(Y)* from a mixture of 20 basic amino acids.[59] The water soluble cationic pillar[5]arene bearing 10 ammonium groups *(F)*, can form strong host−guest complexes with anionic molecules such as sodium 1-octanesulfonate *(B2)*.[60] As a final example, the larger cavity of the cationic pillar[6]arene *(G)* is suitable to complex anionic naphthalene derivatives bearing sulfonate groups *(C2,D2)*.[61]

Cation-π interactions

Cation-π interactions can occur between electron-π rich pillar[n]arenes and cationic guests, such as between the decabutoxy-pillar[5]arene *(D)* and the n-octyltrimethylammonium hexafluorophosphate *(P)*,[62] or the decamethoxy-pillar[5]arene *(B)* and the n-octyltriethylammonium hexafluorophosphate *(Q)*.[63]

Hydrogen-Bond Interactions

The CH/π interaction is the weakest possible hydrogen-bond interaction. Its existence in pillar[n]arenes based host-guest systems was proven for the first time in 2010 by F. Huang, who reported its occurrence between n-hexane *(W)* and per-butylated pillar[5]arene *(D)*.[62] This discovery illustrated the existence of the recognition of alkyl chains by pillar[5]arene, which has been further explored by J. F. Stoddart who investigated the neutral guest recognition ability of the host *(B)* using 1,8-diaminooctane *(T)* and n-octylamine *(S)* as guests.[64] In addition hydrogen bonding, can also occur between pillar[n]arenes and nitrogen rich compounds such a bis-triazoles *(X)*,[65] or halogenated guests as dichlorobutane *(V)*.[66]

Electrostatic interactions

Cationic/anionic interactions can occur between pillar[n]arenes bearing ionic moieties and oppositely charged ionic guests. An illustrative example of this was reported in 2014 by G. Yu whom illustrated the formation of a host-guest complex between diaminopentane *(U)* and pillar[5]arene bearing dicarboxylic acid moieties *(H)*.[67]

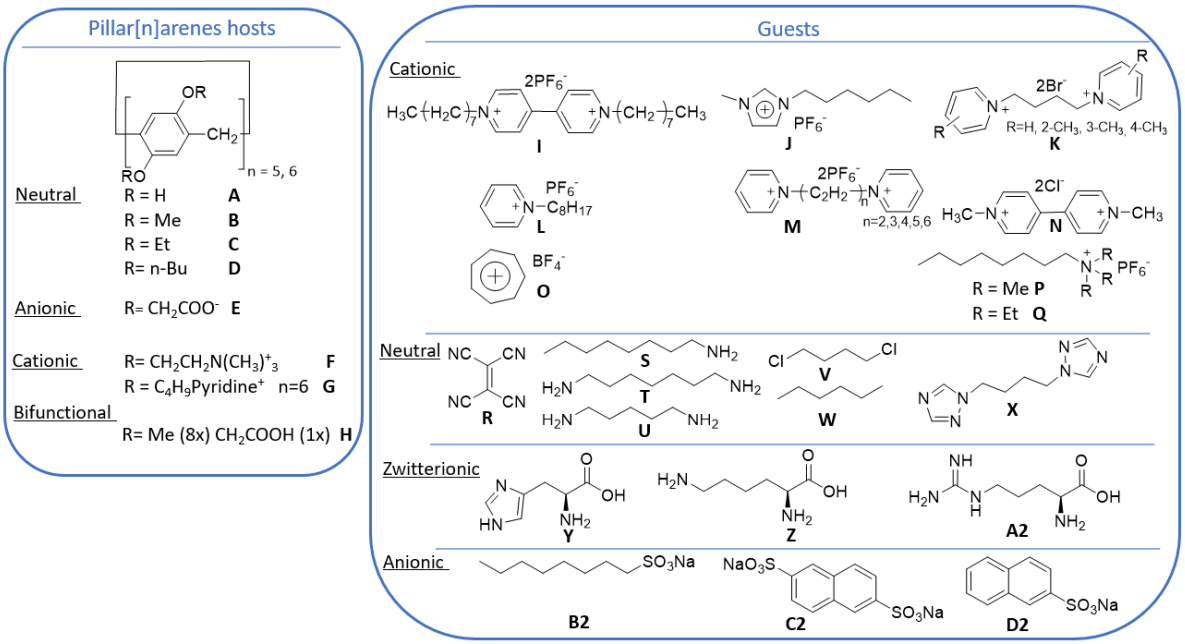

Figure 10: Molecular structures of the pillar[n] arenes and corresponding guest molecules to illustrate the host-guest properties of pillar[n]arenes

1.1.2.4.4 Applications of pillar [n]arenes

Despite their rather recent development, pillar[n]arenes have already found their way into a wide variety of applications falling in domains such as material chemistry, biomedicine, biomimetic, catalysis, robotic, and others. For example, pillar[n]arenes have been used for **supramolecular gel formation**, by L. Wang, who created polymeric supramolecular organo-gels including a redox-responsive host–guest systems based on ferrocene and pillar[6]arenes *(a)*.[68] The creation of **light-harvesting systems** is another type of application in which pillar[n]arenes are used. An illustrative example is the light-harvesting antennas made of a pillar[5]arene bearing ten photon accepting Zn^{II}-porphyrin moieties developed by the team of J-F. Nierengarten *(e)*.[69] The use of pillar[5]arene containing five hydroquinone units as a macrocyclic **reducing agent** *(b)*[70] and of a pillar[5]arene containing 10 tetra-alkyl phosphonium bromide groups as a **substrate-selective phase-transfer catalyst** *(f)*[71] highlight that pillar[n]arenes can also be used to promote or favour chemical reactions. Controlled **drug delivery systems** are another application in which these macrocycles are used. A recent example of this is the dual photo- and pH-responsive drug delivery system based on an hydrophobic azobenzene guest and an hydrophilic pillar[6]arene possessing 12 carboxylate anions host described by X. Hu and co-workers *(d)*.[72] A last example is the creation of **crystals with permanent porosity,** based on a pillar[5]arene possessing 10 phenolic groups, which is able to capture gases such as N_2, CO_2 and n-butane *(c)*.[73]

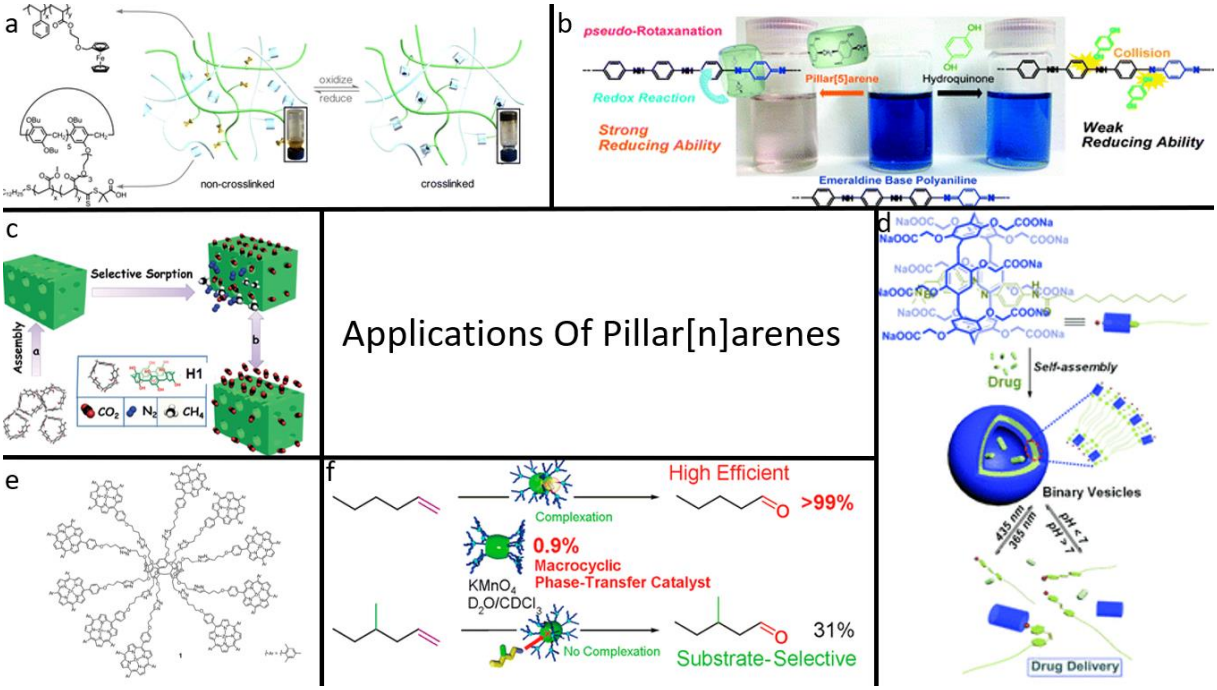

Figure 11: a) supramolecular gel formation[68] b) reducing agent[70] c) crystals with permanent porosity[73] d) drug delivery systems[72] e) light-harvesting systems[69] f) substrate-selective phase-transfer catalyst[71]

1.2 Polymers

1.2.1 General

The term polymer (which is based on the Greek words polus-,"many" and meros-,"part") refers to macromolecules whose molecular structure is composed of multiple repeating subunits, called monomers. They are defined by IUPAC as *"a molecule of high relative molecular mass, the structure of which essentially comprises the multiple repetition of units derived, actually or conceptually, from molecules of low relative molecular mass"*,[74] and can be classified in different ways. One way of doing so is by looking at the structure of the polymer, which result in the creation of three classes: the linear-, branch chain- and crosslinked polymers. They can also be classified based on their source, which can be natural (e.g. proteins), synthetic (e.g. polyethylene) or semi-synthetic (e.g. cellulose acetate). Classification based on mechanical and thermal properties results in the following diversification: elastomers (e.g. polyurethane), thermoplastics (e.g. polymethyl methacrylate), thermosets (e.g. Bakelite) and fibres (e.g. Nylon-66). Another popular way of classification is based on the polymerization techniques used to prepare them, e.g. polycondensation, radical polymerization, etc.. This is closely

related to a major way of classification, which considers the main chemical functional group which compose a polymer: polyester, polyamides, polyurethanes, polycarbonates, polyolefins, polyacrylates and others.

1.2.2 Polymerization techniques

The term polymerization is defined as "*the process of converting a monomer or a mixture of monomers into a polymer*".[75] There are many forms of polymerization and one way of categorizing them is through their reaction mechanism. Two different types of polymerization can accordingly be defined: chain-growth and stepwise polymerization. In a **chain-growth polymerization,** growth of the polymer chain taking places by repeated addition of the monomer to the growing chain. The monomers will not react with each other, but only with the active polymerization sites at the end of a growing chains. The active sites could be radical, anionic or cationic. In contrary, in the **step-growth polymerization** reactions can occur between monomers, polymers and oligomers. These fundamental differences between the two mechanisms results in different characteristic properties which are in listed in table 1.[76]

Chain-growth polymerization	Step-growth polymerization
The polymerization is subdivided in the initiation, the propagation (addition of the monomers to the active sites) and the termination step.	The termination step is absent. The end groups of the polymers/oligomers are reactive throughout the polymerization process.
Monomer concentration decreases steadily with reaction time.	Large quantities of the monomers are consumed in the early stage of the reaction to form oligomers.
High-molecular-weight polymers are formed immediately. The molecular weight will not chance much during the polymerization (Figure 12). In case of a living and controlled polymerization will the molecular weight grow at a constant rate.	The molecular weight increases slowly, and high-molecular-weight polymers are only attained at after prolonged reaction time (Figure 12).
The reaction speed depends on the concentration of the initiator.	The reaction proceeds rapidly at the beginning, then slow down.

The mixture consists mainly of polymer and monomer and only a small amount of growing chains.	Molecular species of different lengths are present throughout the reaction. The length distribution is broadening with increasing reaction time.

Table 1: Main differences between chain growth- and step growth polymerization

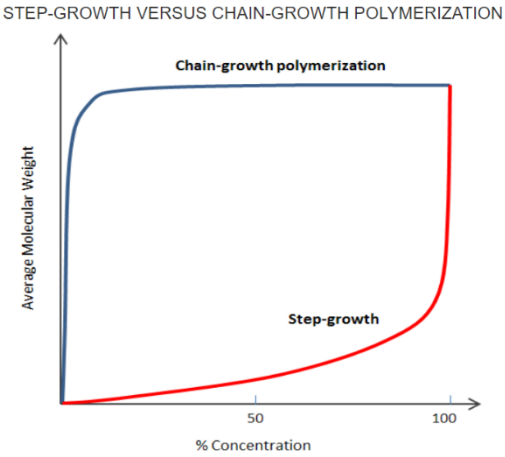

Figure 12: Molecular weight as a function of time for the two types of polymerization[76]

In this thesis, the polymers have been prepared using a chain growth polymerization technique, hence only this technique will be described in more detail.

1.2.2.1 Ring opening polymerization (ROP) and CROP of 2-alkyl-2-oxazolines

ROP is a specific type of chain-growth polymerization that is defined as " *a polymerization in which a cyclic monomer yields a monomeric unit which is acyclic or contains fewer cycles than the monomer".*[77] There are three main classes of ROP: the Anionic Ring-Opening Polymerization (AROP), the Cationic Ring-Opening Polymerization (CROP) and the Ring-Opening Metathesis Polymerization (ROMP), which differ from the nature of the propagating species. In this thesis, poly(2-alkyl-2-oxazolines) (PAOx) have been synthetized by CROP of 2-alkyl-2-oxazolines monomers and, therefore, a dedicated section on the CROP polymerization of this specific class of monomers is given.

The CROP of 2-alkyl-2-oxazoline is an enthalpic driven process. Its main driving force is the isomerization of the cyclic imino ether into a more stable tertiary amine resulting in a spontaneous polymerization after initiation (Figure 13).[78] There is some debate if the minor enthalpic contribution from the release of ring strain upon polymerization should also be taken into account or whether it is negligible.[79,80] The CROP of 2-oxazoline can proceed in a

living or quasi-living fashion if the right conditions are used, to avoid undesired termination or chain transfer side reactions, and allows control of the end group chemistry. Like every chain-growth polymerization, it consists of an initiation (electrophilic addition), a propagation (nucleophilic substitution) and a termination (with a nucleophile) step. Although often simplified to this, a broad range of extra or parallel steps can occur in reality. For instance, the equilibrium between cationic and covalent species is a phenomenon that has to be considered, as it impacts the polymerization speed and the termination. The chain transfer by β-elimination, a possible secondary reaction path, together with the premature termination by nucleophilic attack from impurities, can also influence the outcome of the polymerization. An in depth analysis of all these phenomena can be found in the review by Verbraeken et al.[78]

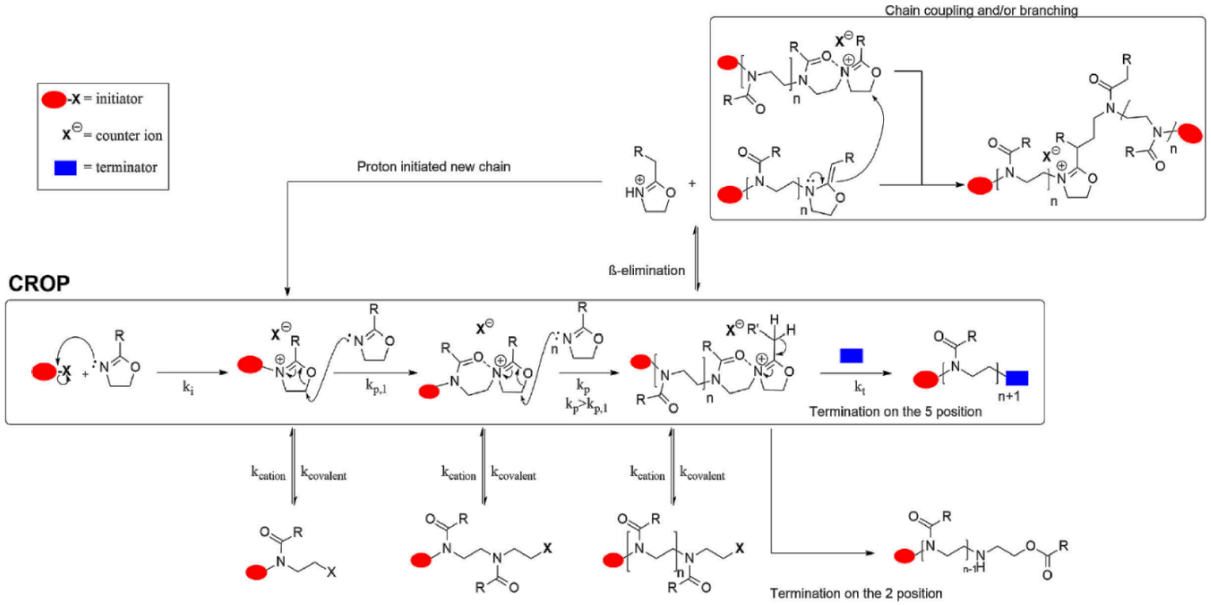

Figure 13: Detailed overview of the CROP 2-alkyl-oxazoline[78]

1.2.3 Stimuli-responsive polymers

Stimuli-responsive polymers (also known as smart polymers) are polymers that are capable of changing their physical and/or chemical properties, giving a detectable response, under the influence of an internal or an external stimulus. They exhibit great potential for a broad range of applications such as data storage,[81] highly sensitive sensors,[82] self-healing polymeric systems,[83] biotechnology[84] and drug delivery.[85] Stimuli that have been reported are, amongst other, temperature,[86] pH,[87] mechanical force,[88] biomolecules,[89] electric or magnetic fields,[90] photo,[91] inflammation,[92] and ultra sound.[93]

1.2.3.1 Thermo-responsive polymers

From the broad range of available stimuli, temperature has been most frequently studied. The main reasons for this is that temperature changes can be applied externally in a non-invasive manner.[86] There exist three main classes of thermo-responsive polymers; shape-memory materials, liquid crystalline materials and responsive polymer solutions.[86] This thesis focuses on thermo-responsive polymers in an aqueous solution, so a separate section to introduce this specific type of responsive polymers is given.

1.2.3.2 Thermo-responsive polymers in aqueous solution

Thermo-responsive polymers in aqueous solution exhibit a unique solubility phase transition property at a given temperature. Some of them show this phase transition near the physiological human body temperature, which is useful for biomedical applications. Thermo-responsive polymers are subdivided into three classes depending, on their response to temperature change. The classification is done by looking at the phase transition of the homopolymer solution as is schematically depicted in Figure 14.

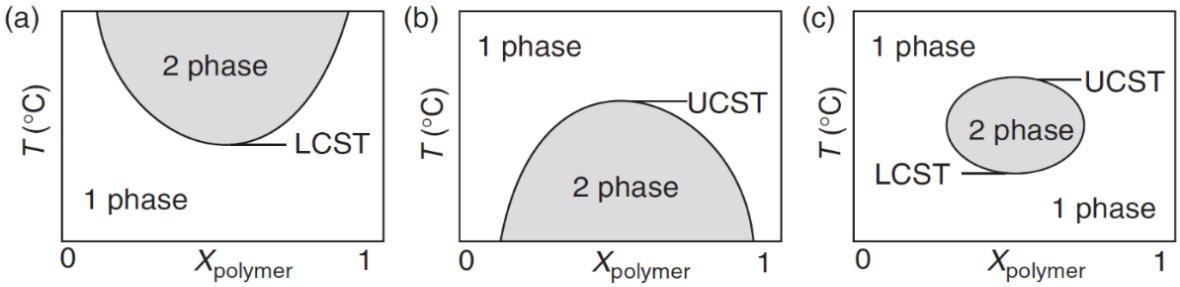

Figure 14: Schematic representation of the polymer phase diagrams (binodal or coexistence curves) for polymers exhibiting (a) LCST behaviour, (b) UCST behaviour and (c) closed loop coexistence[86]

These schematically drawn binodal or coexistence curves represent the equilibrium concentration of the two phases in the phase separated state.[86] The Lowest Critical Solution Temperature (LCST) is defined as the minimum of the binodal curve. The Upper Critical Solution Temperature (UCST) on the other hand is defined as the maximum of the binodal curve. The special case where a polymer exhibits a closed loop coexistence (LCST+UCST) has also been reported for a limited number of polymers. The most well-known examples of

polymers that manifest this dual behaviour are: poly(ethylene glycol),[94] acetylated poly(vinyl alcohol)[95] and poly(hydroxyethylmethacrylate).[96]

1.2.3.2.1 Polymers with LCST behaviour

Polymers undergoing a LCST transition in aqueous solution are soluble at low temperature and phase separate at elevated temperatures. From a thermodynamic perspective, the Gibbs free energy ($\Delta G = \Delta H - T\Delta S$) of the system at low temperature (dissolved polymer) is negative, the enthalpic term ΔH is negative (favourable hydrogen bonding between the water molecules and the polymer chains, i.e. hydration)[86], as well as a the entropic ($T\Delta S$) term (water loses entropy when it is hydrated to the polymer chains).[86] However, at elevated temperatures the Gibbs free energy of the system will become positive, if the polymer stays in solution, because the enthalpic hydrogen bonding interaction will become less while the loss of entropy (TΔS) will become higher and will dominate the system. As a consequence, the polymer drop out of solution to lower this energy giving to the system more degrees of freedom by releasing the hydrated water molecules back into the aqueous bulk phase. Well known examples of polymers that exhibit LCST behaviour are; Poly(*N*-isopropylacrylamide) (PNIPAM), poly(oligoethyleneglycol (meth)acrylate)s and poly(2-oxazoline)s (PAOx).

1.2.3.2.2 Polymers with UCST behaviour

Inversely, polymers undergoing a UCST transition in aqueous solution are soluble at high temperatures and phase separate at low temperatures. To explain this behaviour from a thermodynamic perspective, it is necessary to take in account an additional enthalpic term into the Gibbs free energy equation. This term is related to the beneficial enthalpy of the supramolecular association of the polymer chains.[86] If this term is dominant, the energy cost for breaking this supramolecular interaction is higher than the energy gain upon dissolving, resulting in a phase separation. However, at elevated temperatures the supramolecular associative interaction strength will decrease leading to dissolution of the polymer. Examples of polymers that exhibit UCST behaviour are; poly(N-acryloyl glycinamide) (PNAGA) and poly(sulfobetaine)s.

1.2.4 Host-guest-thermo-responsive polymers

The interplay between supramolecular chemistry and thermo-responsive polymers has led to the creation of a new class of adaptive and smart materials with remarkable properties. These

polymeric systems are for instance able to respond to multiple stimuli in a reversible manner, adapt their morphology on demand and store thermal information.[97]

This young field of research is all about the incorporation of a host and/or a guest in the polymeric side or end chain. Controlled polymerization techniques, including controlled radical polymerisation, but also CROP of 2-oxazolines, are appropriate tools to prepare such functional polymers. The resulting polymers are capable to fundamentally change their properties upon assembly/disassembly of the host-guest complex. An illustrative example of this was reported by Huang's group, who used carboxylate pillar[n] arenes to precisely control the LCST behaviour of PNIPAM, simply by changing the pH.[98] In a similar context, our group demonstrated the possibility to tune the cloud point temperature (T_{cp}) of poly(2-alkyl-2-oxazoline)s copolymers in a range of 30 K by using supramolecular host–guest interactions involving cyclodextrins or cucurbiturils (Figure 15).[99] In a more recent work, it was demonstrated that it is possible to form a double thermo-responsive block copolymer system with the assistance of the host-guest complexation between hydroxypropylated β-cyclodextrin (HPβCD) and hydrophobic alkyl-chains of an amphiphilic block copolymer.[100]

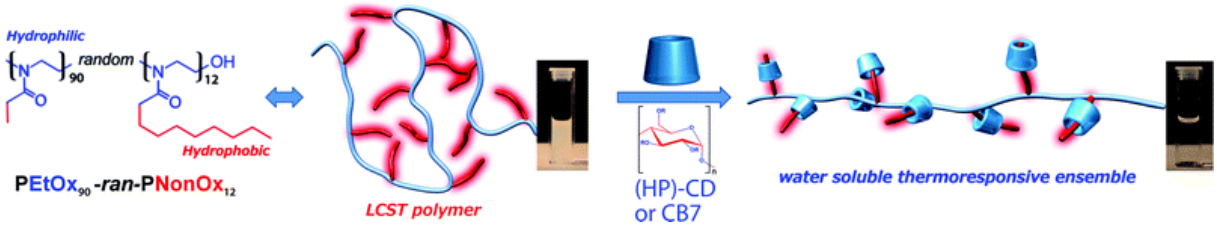

Figure 15: Tuning the cloud point of poly(2-alkyl-2-oxazoline)s by host-guest interactions[99]

An aqueous dual responsive host-guest synthetic system, in which the partial release of the host is regulated by the pH and temperature, has recently been developed in collaboration with the research group of P. Woisel. The system provided an orchestrated temperature and pH controlled regulation of the complexation between the cyclobis(paraquat-p-phenylene) host (BBox) and a 1,5-dialkyloxynaphthalene (DNP) guest attached to a well-defined dual responsive copolymer composed of PNIPAM N-isopropylacrylamide as thermo-responsive monomer and acrylic acid as pH-responsive monomer.[101] The system represents a basis to develop more complex systems with molecular communication.

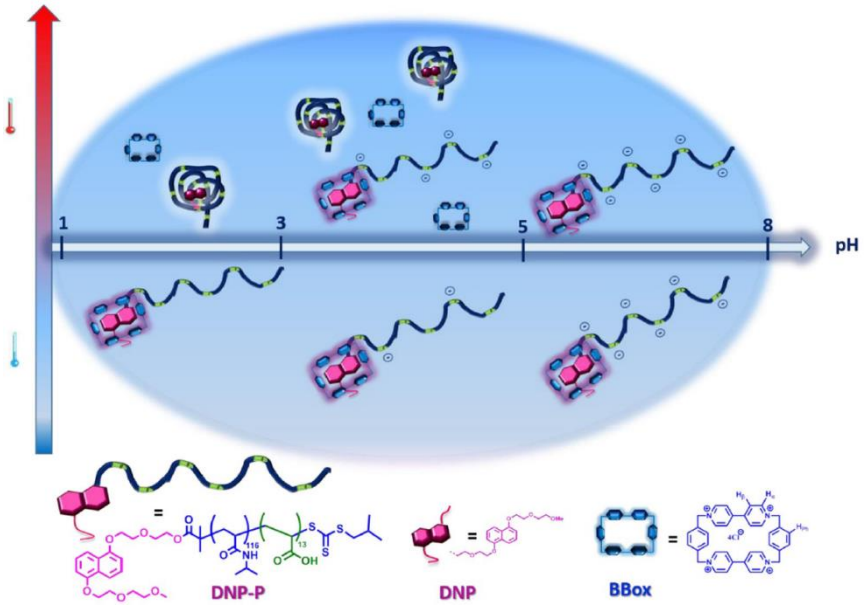

Figure 16: Regulation by pH and temperature of a host-guest complex to control the partial release of a host [101]

1.3 Hydrogels

Hydrogels are three-dimensional, insoluble, crosslinked polymer networks that are able to retain a large amount of water and biological fluids in their swollen state.[102] They were first reported by Wichterle and Lim in 1954,[103] and have evolved in a multidisciplinary field of research applied in a brought range of applications such as tissue engineering, disposable diapers, drug delivery, wound dressing, contact lenses and agriculture.[102] Forces that play a role in the interaction between the polymer chain network and water or biological fluids are capillary, osmotic and hydration forces.[102] These forces are counter-balanced, and the equilibrium depends on the magnitude of these opposing effects. Hydrogel properties such as diffusion characteristics, internal transport and mechanical strength are determined by this equilibrium.[104] From a structural point of view, this parameters will highly depend on the chemical structure of the polymer backbone as well as the crosslink nature and density in the hydrogel matrices.

1.3.1 Smart hydrogels

Just like stimuli stimuli-responsive are smart or stimulus-responsive hydrogels a new generation of hydrogels capable of changing their properties under a stimulus. In many cases, the hydrogels react with an abrupt reversible volume phase transition or sol-gel phase transition in response to an external stimuli in the environmental conditions.[105] These stimuli can be physical, chemical or biochemical. Physical stimuli, such as mechanical stress,

temperature, light, electrical or magnetic and ultrasound fields, affect the molecular interactions at critical onset points and affect various energy levels.[105] Chemical or biochemical stimuli, such as pH, ionic strength, solvent, electrochemical fields, antigen, and enzyme, change the interactions at the molecular level between polymer chains or between polymer chains and the solvent. Stimuli responsive hydrogels are generally constructed from stimuli responsive polymers, which are connected via a chemical (covalent bonds) or physical (non-covalent interactions) cross-linker.[106] Temperature-responsive hydrogels change their network structure, kinetics, permeability, mechanical strength, and surface properties in response to the temperature of their environment.[105] They can be "thermophobic" or negative volume-phase transition hydrogels, showing LCST behaviour or "thermophilic" or positive volume-phase transition hydrogels showing UCST behaviour. The area of thermo-responsive hydrogels is largely dominated by LCST behaving systems and especially PNIPAM-based hydrogels are used extensively, whilst UCST behaving thermo-responsive hydrogels are much less developed.[107] Temperature-responsive smart hydrogels show great potential in pharmaceutical and biomedical applications. This is due to the fact that the expansion or collapse that correlates with the critical shift in aqueous solubility has been utilized as a mechanism for drug delivery, membrane separation/cleaning and in situ gelling scaffolds for tissue regeneration.[108]

1.3.2 Host-guest-responsive-hydrogels

With similarity to the above mentioned host-guest-responsive polymers, the interplay between supramolecular chemistry and hydrogels is of growing interest, as it can offer numerous remarkable additional properties to the hydrogel. In this domain, host-guest chemistry is frequently employed,[109] and has been recently associated with a thermo-responsive polymer and guest-functionalized hydrogel by our group in collaboration with the research group of P. Woisel, to obtain one of the few hydrogel system that is able to show UCST-like behaviour.[107] The system is able to undergo an abrupt swelling upon heating while it remains hydrophilic in the contracted as well as the expanded state. It is based on a three-component supramolecular hydrogel system, a thermo-responsive PNIPAM end-functionalized with a tetrathiafulvalene guest unit (TTF-PNIPAM), which is complexed by the host BBox below the LCST phase transition. Heating of the system above the phase-transition temperature of the TTF-PNIPAM·BBox complex will lead to the collapse of TTF-PNIPAM and

induce dethreading of the host–guest complex and release of the free cyclophane unit into the aqueous solution. The released BBox will then diffuse towards the NaphtGel, a hydrogel system containing a non-thermo-responsive poly(N,N-dimethylacrylamide hydrogel functionalized with dialkoxynaphthalene guest groups, to form host–guest complexes with the naphthalene units, thus leading to the swelling of NaphtGel. Reversibly, upon cooling down the system, the return of the thermo-responsive TTF-PNIPAM in solution leads again to the transfer of the blue box to the polymer, as TTF is a more strongly binding guest, and the deswelling of the hydrogel. This communicating system between a thermo-responsive polymer guest in solution and a guest-bearing hydrogel, using a host as a chemical messenger, represents one step forward towards chemical communicating between hydrogels and forms the basis of this master thesis research.

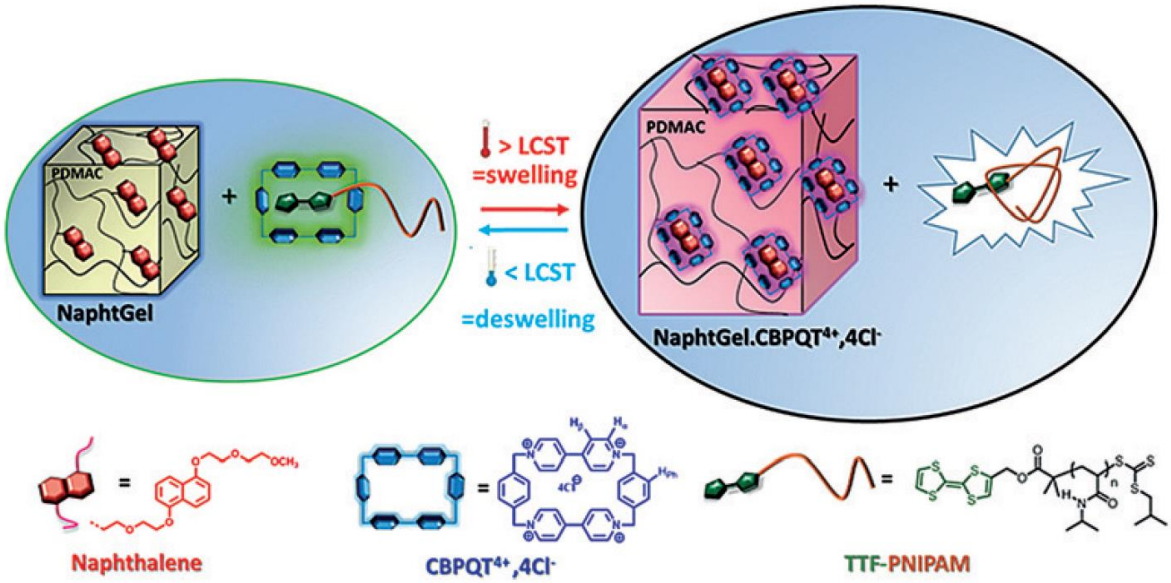

Figure 17: Illustration of the heating-induced swelling of the three-component supramolecular system based on NaphtGel, TTF-PNIPAM, and BBox [107]

2 Thesis goal and strategy

The overall **goal** of this project was to create *molecular communication between hydrogels* by combination of host-guest chemistry and thermo-responsive hydrogels. To achieve this goal, the objective was to use two thermo-responsive hydrogels which incorporate two different guest molecules in their molecular structure, and to let them interact with a water-soluble host. The difference in binding constant between the two host-guest complexes should be large enough to ideally only lead to complexation with the guest having the biggest binding affinity. This complexation would result in a swelling of the hydrogel due to host absorption. Decomplexation was envisioned to occur upon increasing the temperature above the cloud point temperature (T_{cp}) of the hydrogel with the strongest binding guest, as shrinking of the hydrogel would lead to the excretion of the host. This enables transfer to the host to the second hydrogel, creating a new complex involving the second guest, resulting in a swelling of the second hydrogel. Finally, once the temperature drops below the T_{cp} of the first hydrogel, it was postulated that the hydrogel would go back into solution and that a migration of the host molecule back into the first hydrogel would occur. In addition, the generality of the temperature induced guest release and transfer will be investigated by using functionalized poly(2-oxazoline)s as well as pillar[n]arene host-guest systems in contrast to the previously reported systems based on PNIPAM with BBox host-guest copmlexes.

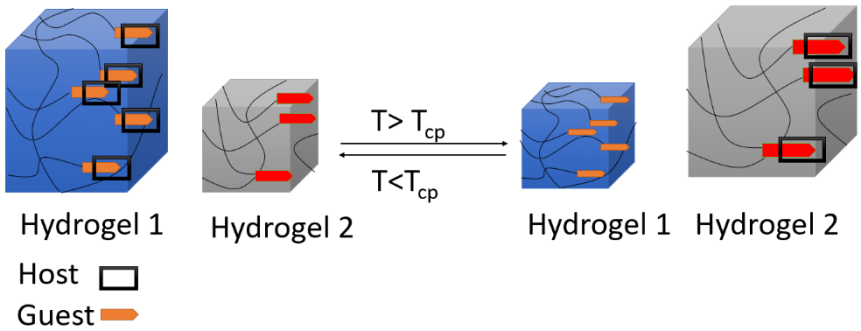

Figure 18: Illustration on the molecular communication between hydrogels

To achieve this ultimate goal, a general **strategy** was established with sub goals in order to validate the involved concepts step-by-step. Thus, this project was divided in three distinct tasks:

- Task 1: creation of a model system. This task requested:

- The synthesis, purification and characterisation of a thermo-responsive poly(2-n-propyl-2-oxazoline) (P*n*PrOx) end capped with a viologen guest unit
- The synthesis and characterisation of water-soluble pillar[n]arenes hosts
- The characterisation and thermal properties measurements of the corresponding host-guest complex

- Task2: the transposition to a 1 hydrogel system
- Task3: the creation of the ultimate 2 hydrogel system

However, due to COVID-19 and the restricted lab access, the experimental work has been seriously hampered, and only task 1 and part of task 2 were conducted. As alternative, a thorough literature study on the topic of "chemical communication between supramolecular systems" has been conducted, and the modelling of a system containing two hosts and one guest has also been performed to determine the required concentrations and difference in host-guest K_a of the host-guest complexes that are competing and form the basis for the host transfer. The results of these additional assignments are included at the end of the thesis after the description of the experimental work.

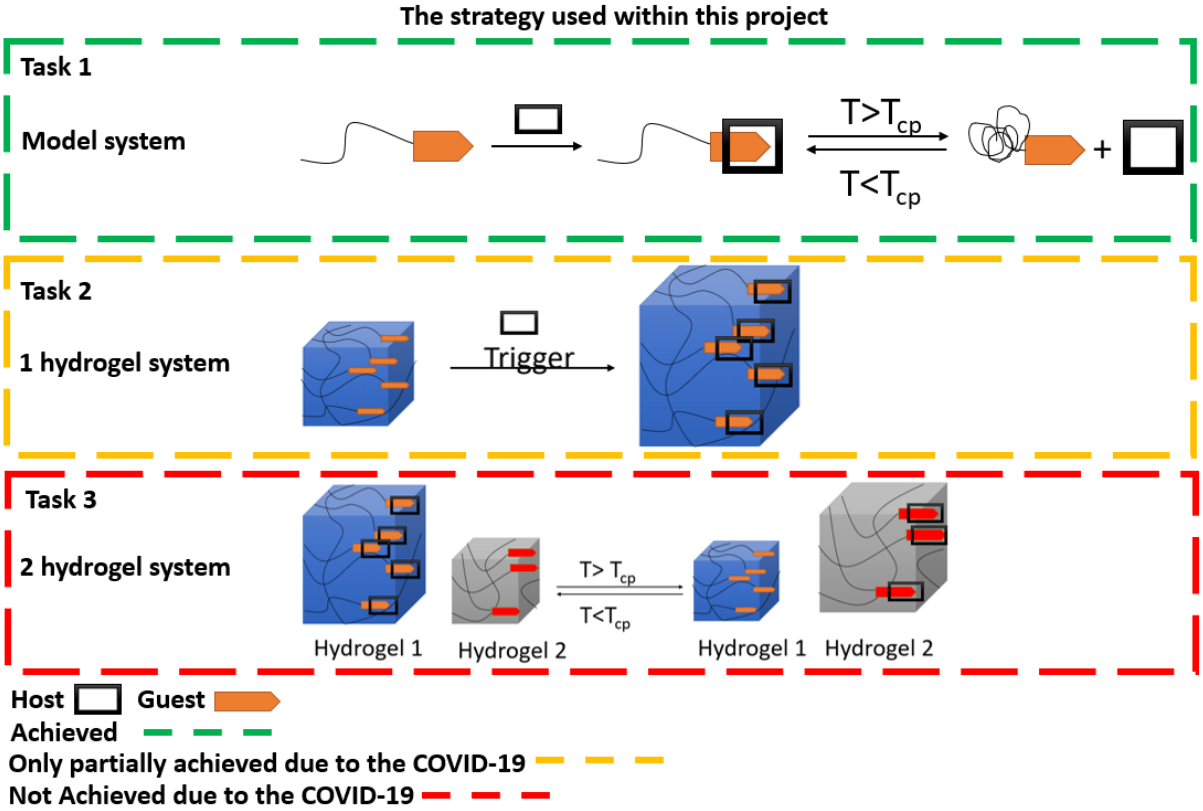

Figure 19: The strategy used within this project, the different tasks, and the influence of COVID-19 on the achievements

3 Results and discussion

3.1 Model system

The goal of this part was to prepare a suitable polymeric host guest model system containing a water-soluble pillar[n]arene and a thermo-responsive guest polymer that could be used at a later stage to create the hydrogels systems. The first objective was to synthetize the requested host and guests, and to explore their binding affinity. The second goal was to check the possibility to release the pillar[n]arene host in solution upon the application of a temperature higher than the LCST of the thermo-responsive polymer. Previous work revealed that using PNIPAM as temperature-responsive polymer with BBox as supramolecular host led to reversible dissociation of the host-guest complex and release of BBox in solution upon the LCST phase transition of PNIPAM during heating. To investigate the effect of the thermo-responsive polymer, this work will use poly(2-*n*-propyl-2-oxazoline) as thermo-responsive polymer, which has a T_{cp} around 25 °C.[52] In addition, the previously used BBox will be replaced by the pillar[n]arene host to investigate whether the previously observed host release is related to the BBox structure or whether it is more general. Two pillar[n]arenes will be investigated having neutral olgoethyleneglycol alkoxy-substituents or anionic carboxylic acid functionalized alkoxy-substituents (Figure 20). As guest molecule we have chosen viologen (dialkylated-4,4-bipyridine) as it is a well-known guest molecule for pillar[n]arenes.[42]

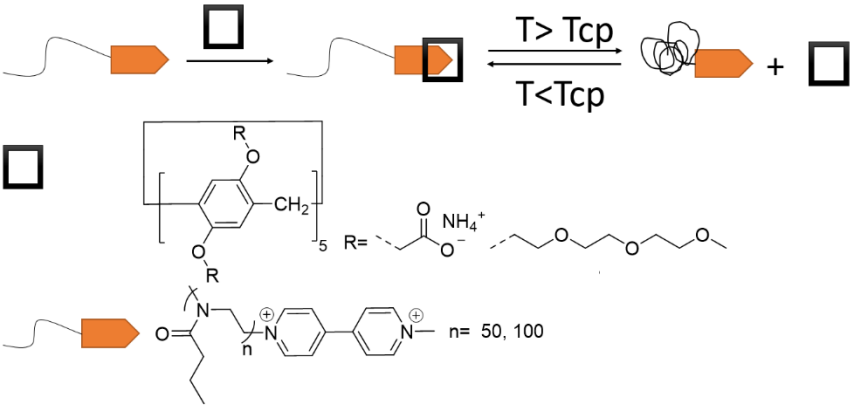

Figure 20: Strategy of the model system

3.1.1 Synthesis of the viologen end-capped 2-n-propyl-2-oxazoline (PropOx)

The practical work started with the methylation of the commercially available 4,4'-bipyridine **1**, using methyl iodide **2** as the methylating agent. The reaction, conducted in DCM, resulted in the single methylated product **3**, which precipitates from the reaction mixture, thus lowering the probability to obtain the double methylated product.[110] After simple filtration, the product was isolated with a yield of 82 % and the structure was confirmed by ^{1}H NMR.

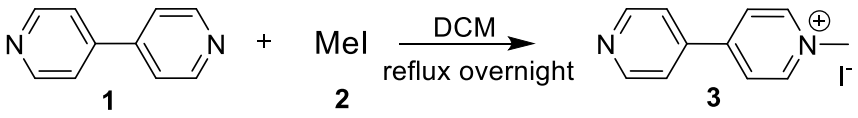

*Figure 21: Synthesis of **3***

In a second step, **3** was then used as the terminator during the CROP of the 2-propyl-2-oxazoline (PropOx), resulting in the polymer end-capped with a end-viologen group ([4,4']-

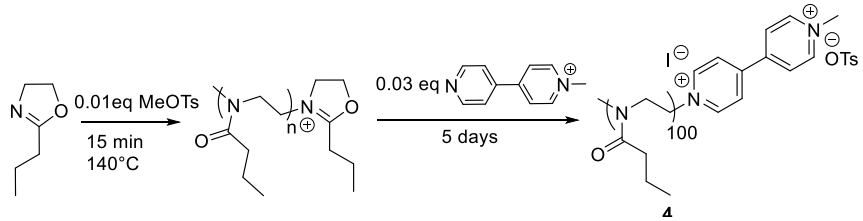

*Figure 22: The synthesis of **4***

bisalkylated bipyridinium group). The CROP was conducted using a procedure classically employed in the group. The PropOx monomer was heated at elevated temperature (140 °C) under microwaves irradiation in the presence of 0.01 equivalent of methyl tosylate (MeOTs) as initiator, aiming for a degree of polymerization (DP) of 100. After the polymerization, an excess of the terminator **3** was added to the mixture containing the living chains, to lead to the end-capped polymer **4** after a prolonged reaction time (3 days).

For the purification of **4**, which was needed to remove the unreacted excess of **3**, several techniques were explored. First, multiple attempts with size exclusion chromatography were conducted, using sephadex LH-20 as the stationary phase (hydroxypropylated beaded cross-linked dextran), and methanol (MeOH) as a mobile phase. The polymer was then analysed by size exclusion chromatography (SEC) (ultraviolet (UV) and refractive index (RI) as the detection system). After the first attempt, the chromatogram revealed that **3** was only partially removed, as the low molar mass peak on the chromatogram (RT≈ 39 min.) decreased in size compared to the polymer peak (RT≈ 29 min.), but it did not completely disappear (Figure 23.B). A second strategy, based on the use of dialysis bags in water, was then applied more

successfully. The use of semi-permeable membrane tubing with a cut-off of 1 kDa proved to be unsuccessful, but in the end it was possible to completely remove **3** via a dialysis membrane with a 3.5 kDa cut-off, the SEC-UV chromatogram confirmed complete disappearance of the excess of **3** (Figure 23 C,D). The polymer was then analysed by ^{1}H NMR spectroscopy, showing that all the signals corresponding to compound **3** were removed (Figure 24). Moreover, broad aromatic signals corresponding to the protons of the bis-pyrridium unit attached to the polymer (proton h,i,k,l) are well visible, proving the introduction of the viologen end-group. The end group fidelity, which correspond to the percentage of chain effectively terminated with this group, was thereafter determined by comparison of the integral of the -CH_3 signals of the polymer (proton d), stated for 300 protons for an ideal degree of polymerization (DP) of 100 attained, vs the integral of the signals of the bis-pyridinium (proton l). The latter was founded to be 1.38, giving an end group fidelity of 69 %. From the ^{1}H NMR, the actual DP and the corresponding number average molar mass (Mn) can also be calculated, by comparison of the signal of the initiator group (α-end-chain methyl group, proton a) with the signals of the polymer chain (protons b,c,d,e). Unfortunately, this signal (for proton a) is hidden by a solvent peak (water bounded to polymer, at 3 ppm) in the ^{1}H NMR of the pure polymer showed on figure 24, hampering the possibility to do the calculation. But in the ^{1}H NMR of the crude (before dialysis – full spectrum in Appendix; Illustration 1), this signal was well-visible, and stated for 3 protons, which allow to determine a DP at 102 from the integration of the polymer signal. Based on this DP together with the end group fidelity, the Mn could be determined and was found to be equal to 11.9 kDA before purification.

Thereafter were the polydispersity (*Đ)* and the Mn determined via SEC-LS (LS= Light Scattering detector) and the following value were obtained: Mn = 12.4 kDa and *Đ* = 1.061. These numbers confirmed that a well-defined polymer with a narrow dispersity was obtained via CROP. The Mn from SEC-LS is also consistent with the Mn value based on the ^{1}H NMR.

As a final technique was MALDI-TOF mass spectrometry used to confirm the DP, Mn, and to check the presence of the end group. In this method is the polymer ionised and detected using a TOF (Time of Flight) detector. The MALDI spectrum is depicted in Figure 25 A, showing one typical polymer mass distribution. The molar mass of the repeating unit is founded between each peak (± 113.1), and no other peaks were founded. The typical values (Mn, Mw, *Đ)* were determined by appropriate formula from the sum of value of each individual peak and their

respective intensities. The MALDI was also used to try to assign the end group. This was unfortunately not possible, as the right ion could not be found, whatever the charged form and the structure considered (mono-cation, di-cation, different counter anions, different ionised form,…).

Overall, three impended techniques yielded similar values for the Mn, and as one has to be chosen, the values from SEC-LS was ultimately used for the calculation in the following parts the project.

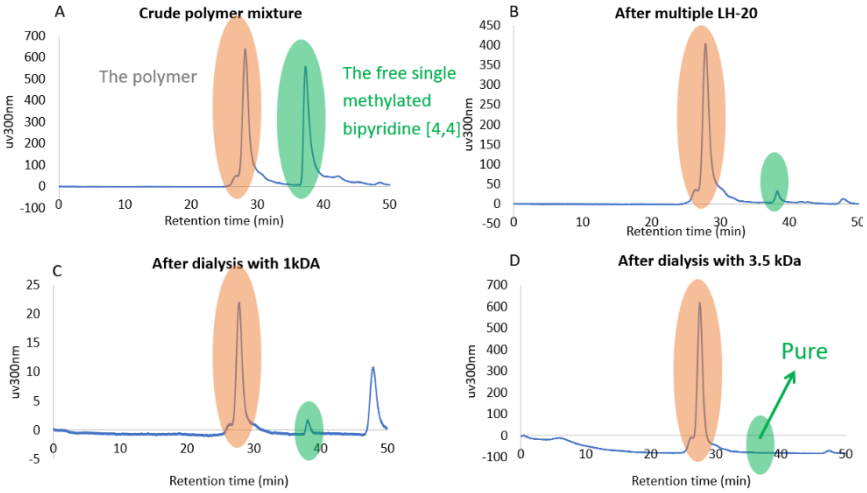

Figure 23: Sec-UV of the crude polymer (A) and after purification by LH20 (B) or dialysis (C,D)

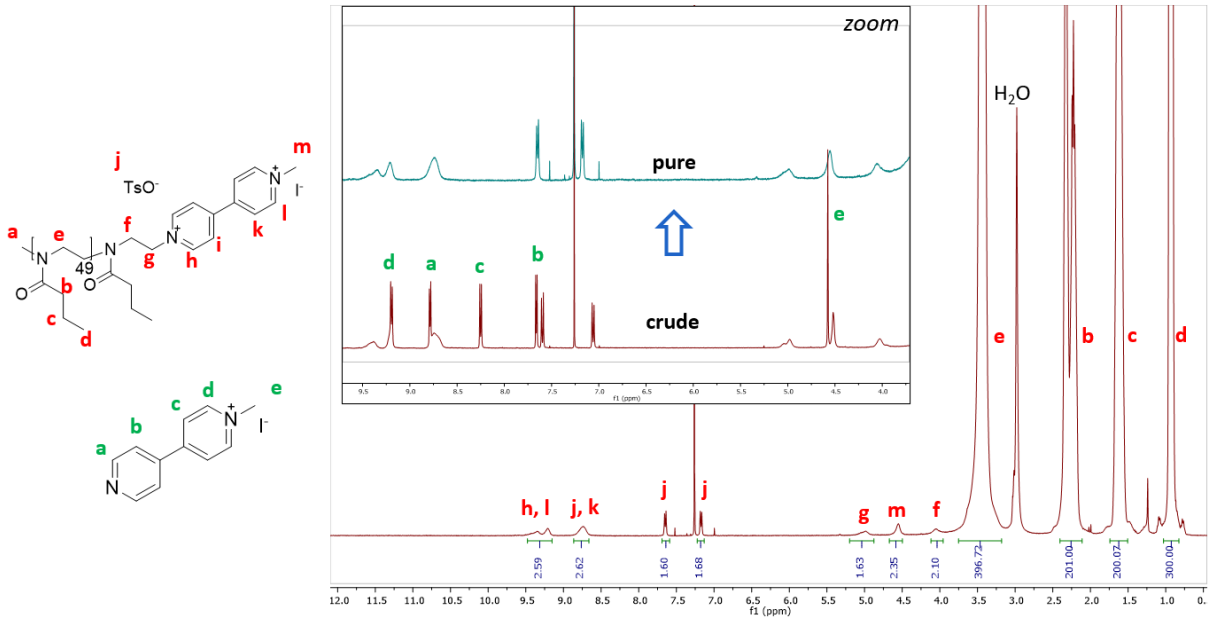

*Figure 24: The ^1H NMR of pure **4** and a comparison with the ^1H NMR of the crude of **4** (400 MHz, $CDCl_3$)*

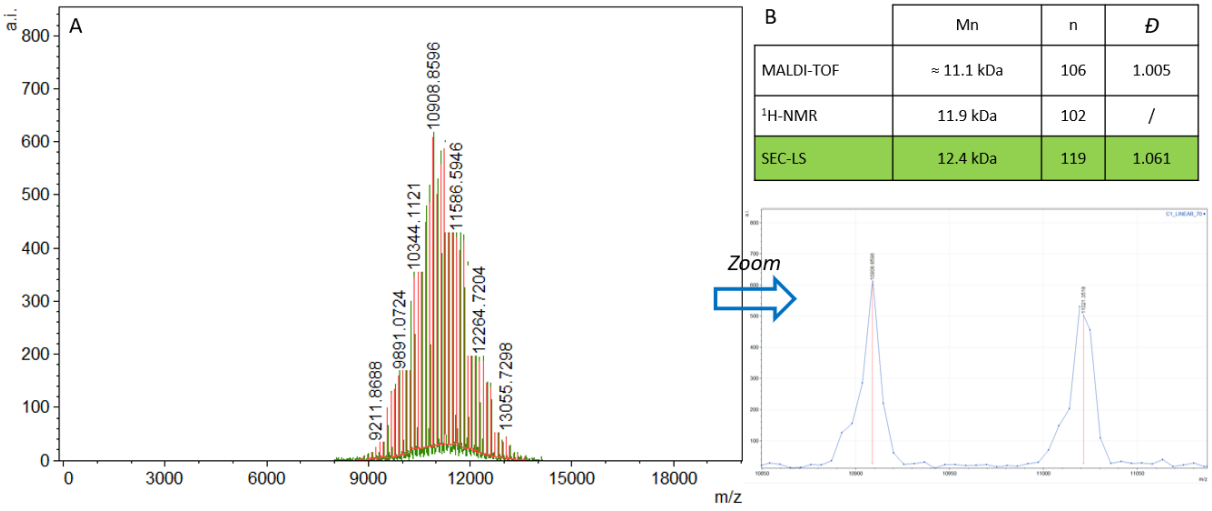

*Figure 25: A) MALDI-TOF of **4** B) Mn, Đ and n based on SEC-LS, MALDI-TOF and 1H-NMR measurements*

3.1.2 Synthesis of the water-soluble pillar[n]arenes

Two water-soluble pillar[n]arenes, namely the pillar[5]arene bearing ten carboxylate groups **6** and the pillar[5]arene with ten short glycol chains **7**, were identified as potential host molecules. Thus, the synthesis of **7** was conducted, while there was no need to synthesize **6** as this molecule was kindly provided by the lab of Prof. T. Ogoshi.

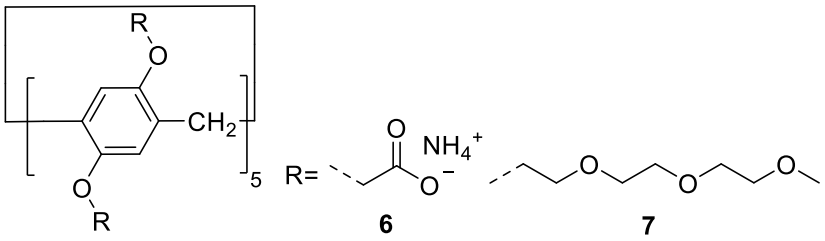

Figure 26: Structure of the water soluble pillar[5]arenes used in this project

3.1.2.1 The Synthesis from the dimethoxybenzene

The synthesis route of **7** is depicted in Figure 27 and consists out of three distinct steps. The first step is based on a procedure developed by T. Ogoshi [111] and leads to methoxy substituted pillar[5]arenes **9**. The second step,[112] is used to remove the methoxy groups and gives the pillar[5]arenes **10** with phenolic groups. This deprotection step allows to introduce new functionalities on both rims of the pillar[5]arenes by alkylation. The last step of the synthetic route is used to install the glycol units, employing the tri(ethylene glycol) monomethyl ether tosylate **12** as the electrophile to alkylate the pillar[5]arenes **10**. As this precursor is commercially available but rather expensive, it was synthesised from the triethylene glycol monomethyl ether **11** and p-toluenesulfonyl chloride.[113]

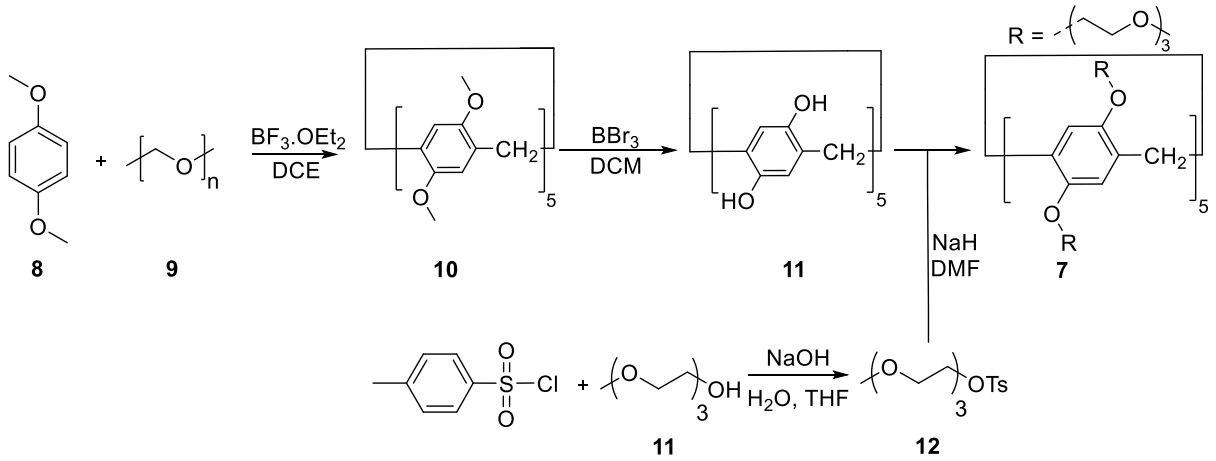

Figure 27: Synthesis route for the pillar[5]arene with triethylene glycol units 7

The first synthetic step was performed through the combination of 1,4-dimethoxybenzene **8** with paraformaldehyde in the presence of the Lewis acid $BF_3.OEt_2$ using dichloroethane as solvent and template, under inert conditions at 30 °C for 3 h. The product was purified by a series of precipitations using first methanol and then chloroform leading to an isolated yield of 23 % after drying. The pillar[5]arene structure **9** was confirmed by ^{1}H-NMR (Figure 28) and LC-MS analysis.

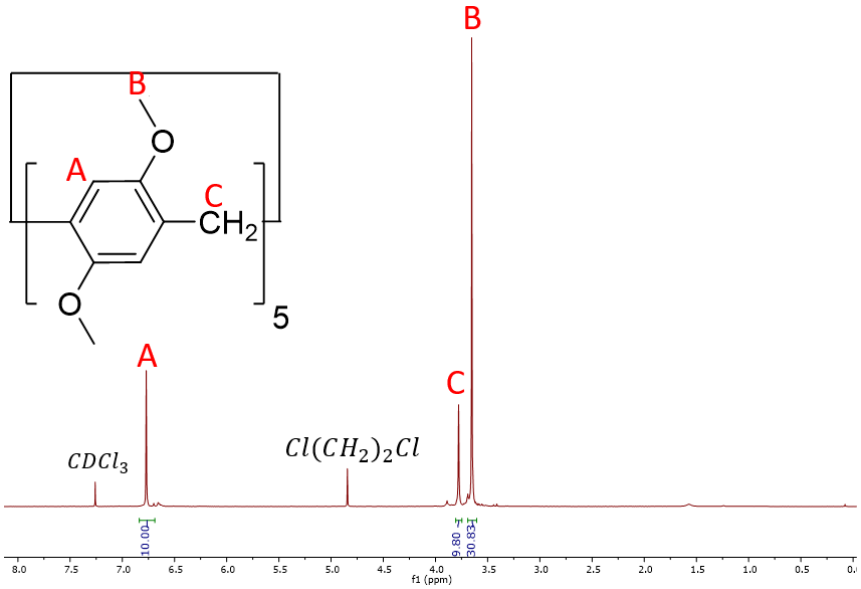

*Figure 28: ^{1}H NMR in chloroform of **9** (300 MHz, $CDCl_3$)*

Then the deprotection was performed by reacting **9** in anhydrous chloroform with boron tribromide for 3 days at 25 °C. The reaction was quenched upon the addition of water and the resulting precipitate was collected and washed with hydrochloric acid and water resulting in pure **10** with 90 % yield without the need of extra purification steps. The complete conversion

of the methoxylated starting product was confirmed by ^{1}H-NMR analysis, as no more methoxy peaks were found on the ^{1}H-NMR spectrum. The structure was also confirmed by LC-MS analysis, which gives only one peak on the chromatogram, having the mass corresponding to the targeted compound

The synthesis of the tosylate precursor requested for the final alkylation step started off by dissolving sodium hydroxide (NaOH) and triethylene glycol monomethyl ether in a water/tetrahydrofuran (THF) mixture under Ar atmosphere. Thereafter the solution of p-toluenesulfonyl chloride in THF was added slowly at 0°C and stirred for 3 hours, followed by another 2 hours of stirring at RT. The product **12** was obtained by evaporation of the THF followed by extraction from the water phase providing an isolated yield of 81 %. The ^{1}H-NMR analysis confirmed the expected structure.

The final step to obtain the targeted product **7** consists of the reaction of the decahydroxylated compound **10** with the tosylate precursor **12** in the presence of a base. This reaction has been reported multiple times in the literature using different procedures, and our first attempt was based on the procedure given by the group of F. Huang.[114] The authors used potassium carbonate as the base and acetonitrile as the solvent, under reflux for 3 days. However, it became clear upon the analysis of ^{1}H-NMR and LC-MS data from the mixture after 3 days of refluxing that the reaction was not successful in our case. The pillar[5]arenes aromatic signals were not present any more on the ^{1}H-NMR spectrum, and no peaks were visible on the LC chromatogram. A possible explanation for this could be the fact that the pillar[n]arene is degraded. Subsequently, another procedure adapted from a report of T.

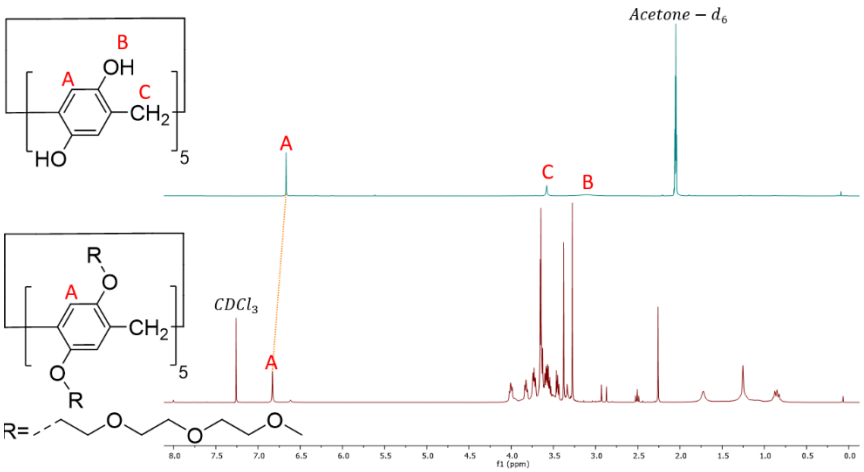

*Figure 29: ^{1}H NMR spectrum of the crude mixture of **7** stacked with the ^{1}H NMR spectrum of **10** (400 MHz, acetone-d_6)*

Ogoshi was used.[115] This method employed sodium hydride (NaH) as a stronger base to deprotonate the phenols, and dimethylformamide (DMF) as solvent. The analysis of the crude reaction mixture after 5 days of refluxing indicated the success of the method. This was visible from the ^{1}H-NMR spectrum, showing a clear chemical shift of the aromatic proton signals of the pillar[5]arene body, and from the LC-MS data, which shows the presence of the product in the mixture (API-ES : $[M+NH_4]^+$= 2087,1581). The purification by column chromatography which is desirable to obtain the pure product could unfortunately not be performed as a consequence of the COVID-19 crisis.

3.1.2.2 Alternative synthetic route

Because of the initial difficulties encountered during the last synthetic step of **7**, an alternative route has been explored in parallel, during this project. The two-step route is depicted in Figure 30 and consists first in the alkoxylation of the commercially available 1,4 hydroquinone **13** with the tosylated ethylene glycol, based on a procedure of M. Damavandi et al.[116] The second step aims to synthesize **7** by condensation of **14** with paraformaldehyde**,** using the procedure of T. Ogoshi which has already been employed in the first route described above.[111]

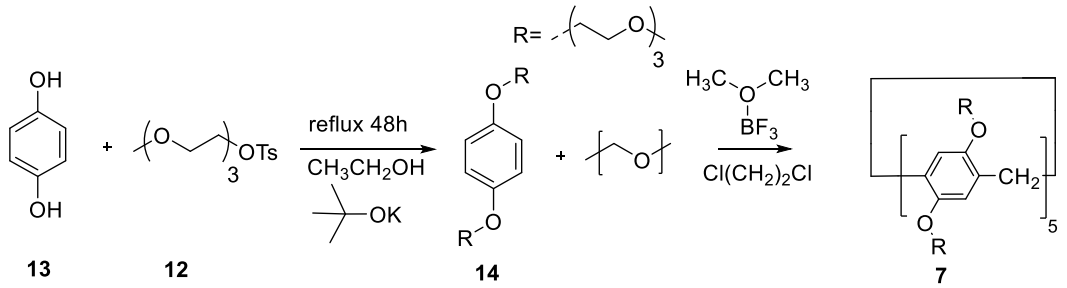

*Figure 30: An alternative route for the synthesis of **7***

An overall benefit of the alternative synthetic route is the fact that the number of synthetic steps is reduced, as the deprotection step is avoided.

The alkoxylation was first done by refluxing **13** in ethanol together with potassium tert-butoxide and **12** under an argon atmosphere for 48 h. The product **14** was isolated by extraction/washing, followed by flash silica gel column chromatography (hexane-ethyl acetate as the eluant). The reaction was confirmed by ^{1}H-NMR and yielded the product with a moderate yield of 17 %.

The procedure described above for the preparation of the pillar[n]arene was repeated using **14** instead of **8** as the starting material. Unfortunately, the ^{1}H-NMR spectrum of the crude mixture together with the LC-MS data revealed that no pillar[n]arene structures were formed. Only linear oligomers composed of two to five aromatic units were detected by mass analysis, as depicted in Figure 31. A possible explanation as to why this reaction failed could be that the glycol units give too much steric hindrance to form the macrocycle.

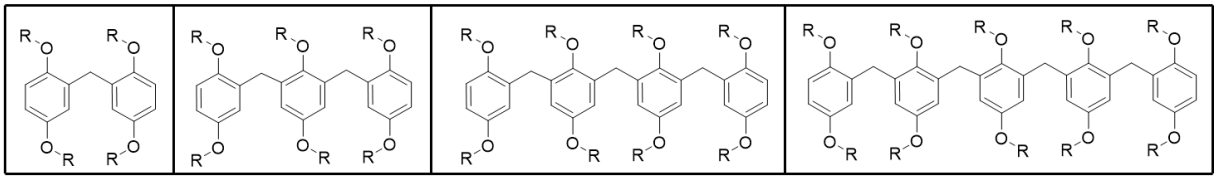

*Figure 31: Oligomers side products from the alternative synthesis route of **7***

3.1.3 Host guest complexation

Multiple analyses were conducted to study the host-guest complexation between the viologen end-capped Poly(*n*PropOx) **4** and the water-soluble pillar[5]arene **6**. This includes the determination of the binding constant in water, the exploration of the binding stroichiometry with the Job plot method, the influence of the complex on the LCST behaviour of the Poly(*n*PropOx), the analysis of the **[4-6]** complex by ^{1}H NMR spectroscopy, the monitoring of the release of **6** form the **[4-6]** complex under the influence of temperature by ^{1}H- and Diffusion-Ordered NMR Spectroscopy (DOSY) NMR spectroscopy, and its reversibility.

3.1.3.1 Determination of the association constant of the complexation in water

The procedure that was used for the determination of the association constant (K_a) is based on the method reported by the group of T. Ogoshi for the determination of the K_a for the similar [paraquat-**6**] complex.[57] It is based on recording steady-state fluorescence spectra at varying concentrations of **4** (C_{guest}) at 10 °C and plotting of the changing ratio of the fluorescence intensities ($\frac{I}{I_0}$) at 333 nm as a consequence of that variation (Figure 33). The fluorescence signal is decreasing upon complexation with **6** because the fluorescence active viologen goes inside the cavity of the slightly fluorescence active **6**. Upon fitting of the data by Eq. 1 (where α is a constant), it was possible to determine that the K_a 3.9 ± 0.6 x 10^4 M^{-1}. However the fit is not perfect, which could be due to the model not being right. The K_a value lays very much in line with the K_a of the [paraquat-**6**] complex, which is equal to 8.2 ± 1.7 x 10^4 M^{-1},[57] meaning that the polymer structure has no influence on the association constant.

$$\frac{I}{I_0} = \frac{(1 + \alpha K_a C_{guest})}{(1 + K_a C_{guest})} \quad (Eq. 1)$$

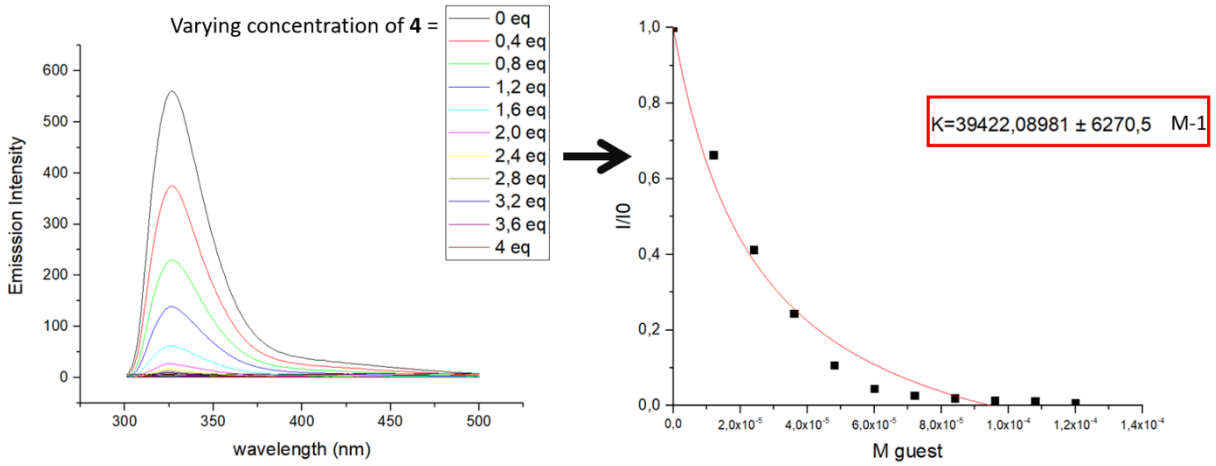

*Figure 33: Determination of the binding constant of the **[4-6]** complex by fluorescence at 10 °C*

*3.1.3.2 Influence of the complexation on the LCST behaviour of **4***

The determination of the T_{cp} of a solution of Poly(*n*PropOx) **4** on the one hand a 1 to 1 mixture of Poly(*n*PropOx) **4** and pillar[5]arene **6** on the other hand was done to determine if the **[4-6]** complex had an influence on the T_{cp} of **4**. Turbidimetry was the method used for this and the results shown in Figure 34 show that the T_{cp} of **4** is 23.5 °C, which is lowered to 20.1 °C as a consequence of the complexation with **6**. This is unexpected since **6** is very hydrophilic, meaning that the T_{cp} should increase. A possible explanation for this could be that the ionic interactions release the counterions, making the final complex less hydrophilic than the **4**.

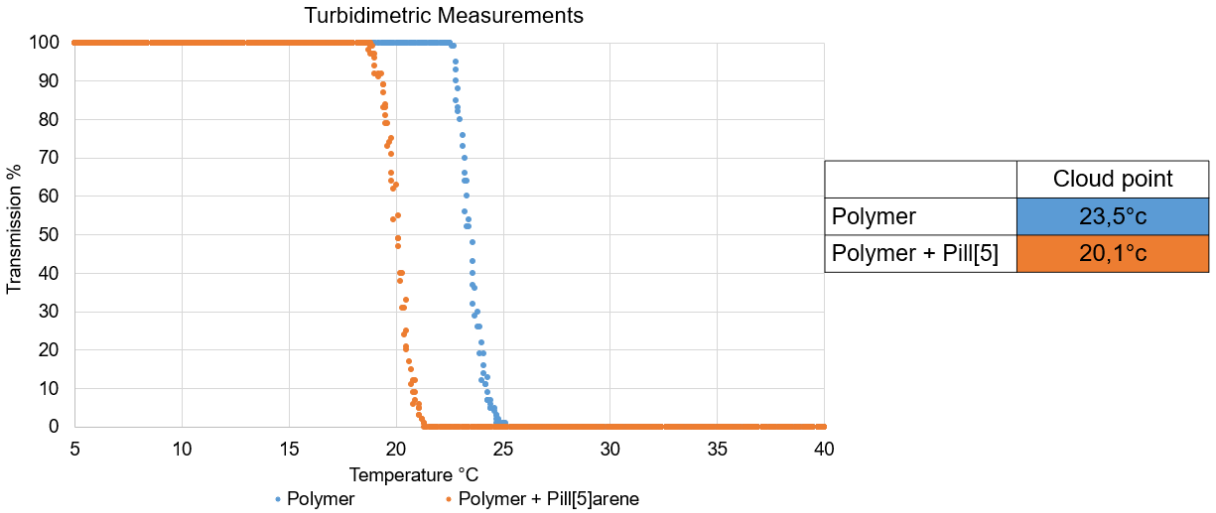

*Figure 34: Turbidimetry measurement of **4** and a 1 to 1 mixture of **4** and **6***

Observations on the decomplexation during the LCST transition were not done due COVID-19 crisis and this will be part of future work.

3.1.3.3 Job plot

The method of the Job plot was used to investigate the binding stoichiometry of the **[4-6]** complex. Equimolar solutions containing different molar ratios of **4** and **6** in water were prepared and the UV absorbance signal at 330 nm, which is proportional to the concentration of free **6**, was measured. It is important to mention that the polymer solution was prepared using the molar mass obtained by SEC-LS, and by taking in consideration the end-group fidelity, to obtain a precise molarity of the host. The response was then plotted against the mole fraction of **4**, resulting in the Job plot A depicted in Figure 35. The maximum of the curve lays at a mole fraction of **4** = 0,2 indicating that the stoichiometry of the **[4**-**6]** complex should be equal to 4:1. However this result seems pretty unlikely, since the binding stoichiometry of the very similar paraquat-**6** complex is equal to 1:1.[57] A second measurement was then made to obtain the Job plot, this time using fluorescence spectroscopy instead of UV spectroscopy as the detection mode. The Job plot derived from fluorescence spectroscopy is depicted in Figure 35.B resulting in the same conclusion. A possible explanation for this unexpected data could be that some polymer chains of **4** are coiled up in water (although the measurements were performed way below the cloud point, at 10 °C) leading to shielding of the methylated [4,4] bipyridinium guest molecule and resulting in a misleading Job plot. A method to investigate this hypothesis will be to redo the experiment in an organic solvent, which unfortunately was not possible because **6** was found to be insoluble in organic solvents. Alternatively, the organo-soluble pillar[5]arene **9** could be used, but this experiment was not possible due to limited time before the COVID-19 crisis. The measurements with the pegylated pillar[5]arene **7**, which may be soluble in some organic solvents, could also give extra information.

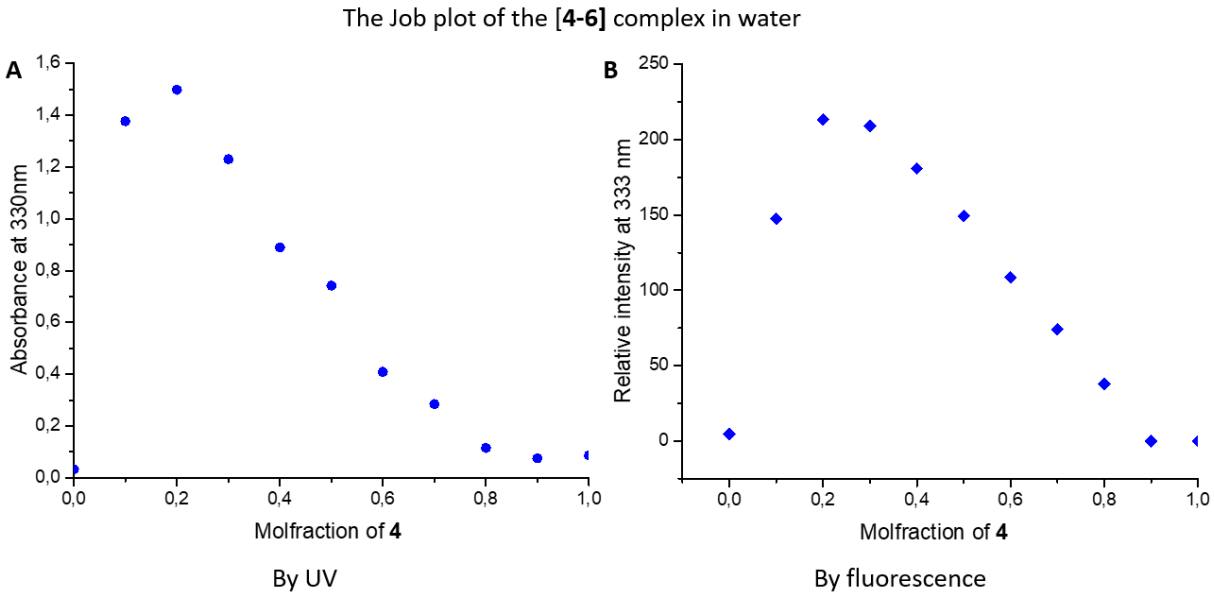

*Figure 35: A) Job plot of the **[4-6]** complex in H_2O A) by UV B) by fluorescence*

3.1.3.4 Observation of the complexation by ^{1}H NMR spectroscopy

The complexation between **4** and **6** was followed by measuring ^{1}H NMR spectra of multiple equimolar solutions with different equivalents of **4** in D_2O. The data generated from these measurements were then stacked together with a spectrum of **6** and **4**, part of which is depicted in Figure 36, and the following was observed:

- The aromatic proton peaks of **6** (A) are broadened and shifted in the presence of **4**, indicating that a new chemical environment is created, resulting from the complexation between **4** and **6**.
- A peak at 7.7 ppm (the red frame) , which is related to the aromatic protons B and C inside the cavity of **6**, is appearing upon the addition of **4**.
- There are always peaks related to free **4** (B and C) present, even with a high excess of **6**, i.e. 0.25 eq of 4, indicating that not all of **4** is forming a complex with **6**.
- The sharp doublets are coming from the TsO^- counter ion.

The first two points confirm the formation of the complex. However, the third point is surprisingly in line with the trend observed during the Job plot measurements indicating that some viologen units may indeed be shielded inside the polymer globules making them unavailable for complexation.

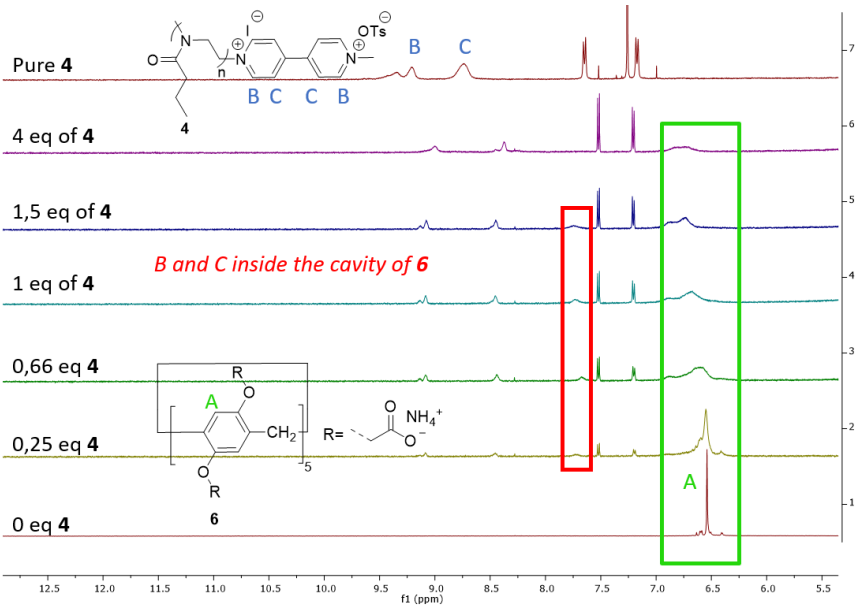

*Figure 36: Stacked ^{1}H NMR spectra of the **[4-6]** complex and **6***

*3.1.3.5 ^{1}H-NMR and DOSY monitoring of the release of **6** from the **[4-6]** complex*

The dissociation of the **[4-6]** complex due to the precipitation of **4** at elevated temperatures was investigated by recording ^{1}H NMR spectra of a 1:1 mixture of **4** and **6** in D_2O at different temperatures. The resulting spectra are illustrated in Figure 37. The signals related to the Poly (*n*PropOx) moiety are very broad at 35 °C, indicating that **4** is no longer in solution.

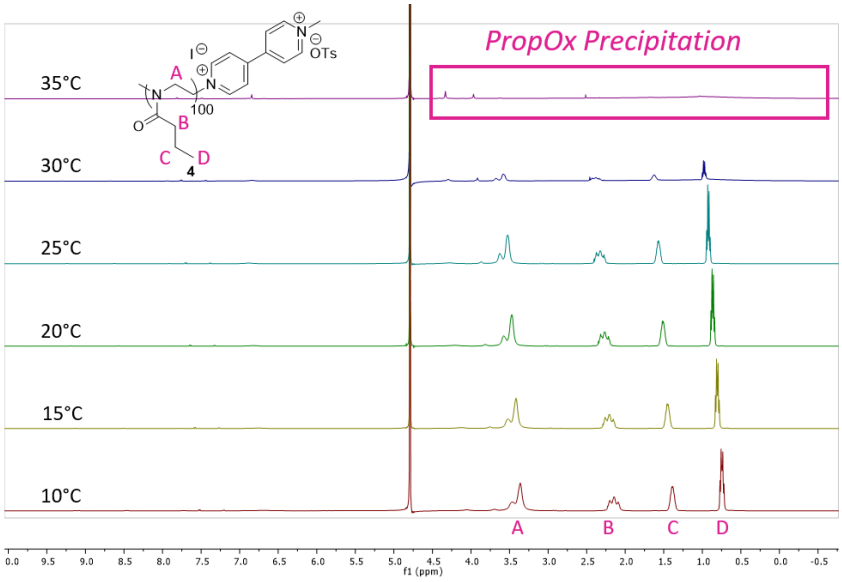

*Figure 37: ^{1}H NMR of the **[4-6]** complex in D_2O at different temperatures*

The release in solution of the host **6**, as a consequence of precipitation of its guest, is clearly visible in the zoomed in image of the ^{1}H-NMR spectra depicted below. The characteristic sharp proton signals of free **6** are absent in the ^{1}H NMR spectra at 10 °C (only the broad signals of **6**

in the complex are present), but appear as the temperature is increasing, and are well visible in the ^{1}H NMR spectra at 35 °C, proving that the precipitation of **4** results in a dissociation of the complex and the release of **6** in solution. The quantification of this release was calculated by integrating these signals and comparing them with the integrated signals of the TsO^- counter anion as an internal standard revealing that close to 100 % of **6** was released at 35 °C.

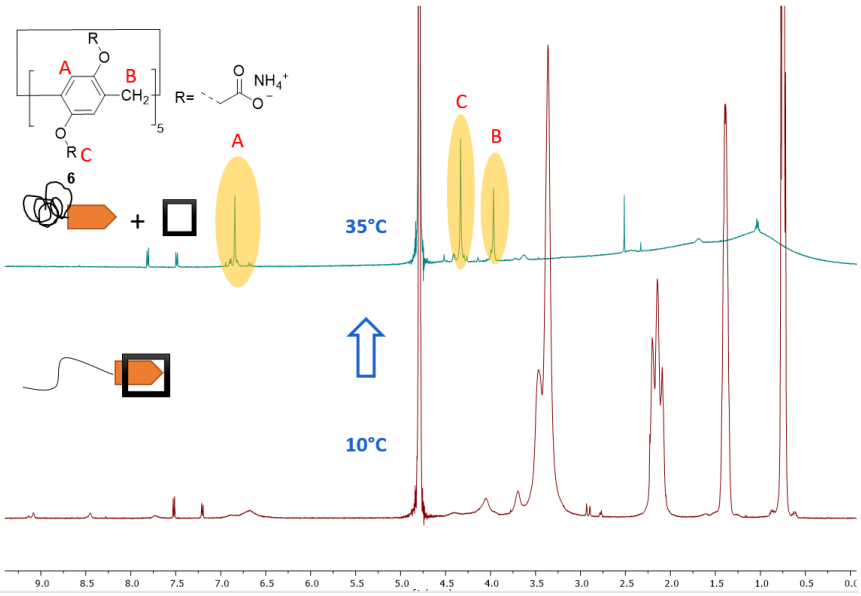

*Figure 38: Zoomed in ^{1}H NMR of the **4**-**6** complex in D_2O at 10 °C and 35 °C*

The collapse of the **[4-6]** complex at elevated temperature was also demonstrated via DOSY, which can be used to investigate the association and complexation behaviour of the **[4-6]** complex by measuring the diffusion coefficients via Brownian motion. The spectra of a 1:1 mixture of **4** and **6** in D_2O at 10 °C and 60 °C were recorded and resulted in the spectra depicted in Figure 39. At 10 °C are two lines visible. The line in the blue frame is related to free **4** and the line in the green frame comes from the **[4-6]** complex. At 60 °C, both lines are absent, indicating that **4** is no longer in solution. Two new lines are visible and one of them is related to free **6** (the yellow frame). The other is due to a combination of the fact that, together with the TsO^- counter ion, there is too much zooming in (red frame).

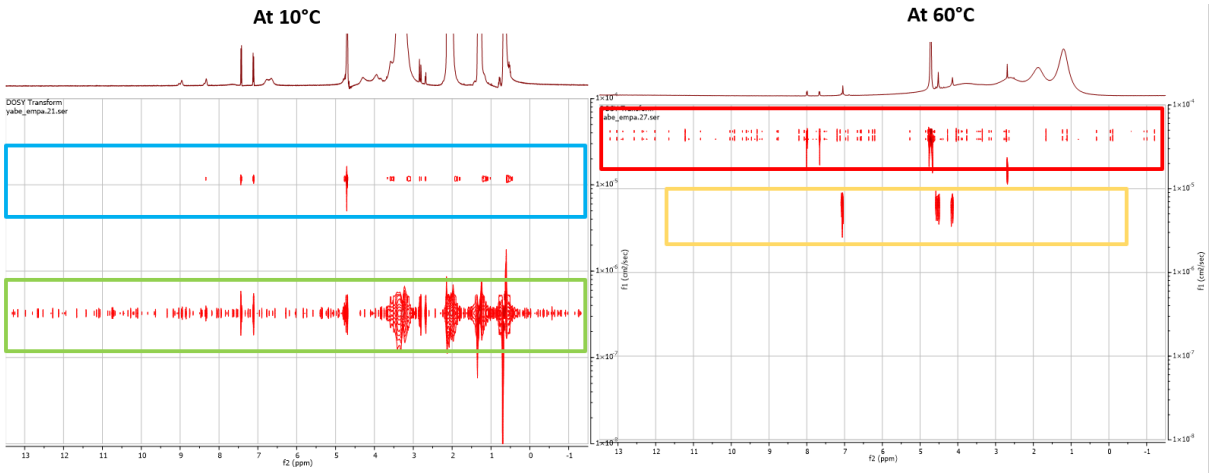

*Figure 39: DOSY-NMR of the **[4-6]** complex in D_2O at 10 °C and 60 °C*

3.1.3.6 Reversibility of the threading-dethreading process

T The last experiment conducted on the model system was done to visualize the reversibility of the release of **6** from the **[4-6]** complex and the cyclability of the process was assessed by recording the ^{1}H NMR spectra of a 1:1 mixture of **4** and **6** in D_2O at multiple cooling and heating cycles. The results are stacked on Figure 40 and show that the aromatic proton peaks of **6** alternate from broad at low temperature to sharp at high temperature due to the cyclic complexation-decomplexation process (highlighted in yellow). This result clearly demonstrates the reversible temperature controlled threading and dethreading of the host-guest complexation.

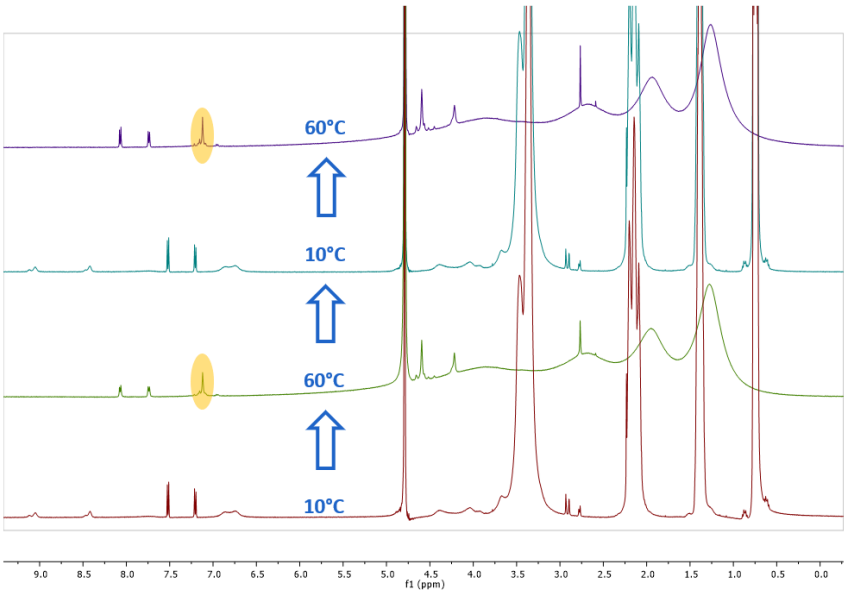

*Figure 40: ^{1}H NMR of multiple heating and cooling cycles of the **4-6** complex*

3.1.4 Conclusions

We successfully created and characterized the model system. The association constant was determined to be $K_a = 3.9 \pm 0.6 \times 10^4\ M^{-1}$ via fluorescence spectroscopy, the LCST behaviour was monitored via turbidimetry revealing a decrease upon complexation, the complex was observed with ^{1}H NMR, the temperature induced release of the host was confirmed with ^{1}H-NMR and DOSY and the reversibility of the system was illustrated. The targets set for the first task of the project were achieved, albeit only for one pillar[5]arene host, and subsequently the second task (the one hydrogel system) was initiated.

3.2 One Hydrogel system

Within this part, the aim was to synthesize a thermo-responsive hydrogel that contains viologen units in its molecular structure. The considered strategy consist in polymerizing a mixture of *N*-isopropylacrylamide (NIPAM) together with a viologen bearing monomers and a cross-linker, such as the *N*,*N*'-hexamethylenebis(acrylamide). For this part, polyacrylamide-based structures were preferred over the poly(2-oxazoline) for simplicity reasons as the hydrogels can be prepared in water using a radical polymerization mechanism. However, due to the COVID-19 lab interruption, only some preliminary results with regards to the synthesis of the viologen bearing monomer were achieved.

3.2.1 Synthesis of the viologen monomer

To covalently incorporate viologen units in the hydrogel structure, the synthesis of a methacrylamide monomer functionalized with a dialkylbispyridinium unit was explored. The synthetic route is depicted in Figure 41 and consists out of three steps. The first one is the methylation of the commercially available **1** and is based on the procedure described in 3.1.1.. The second step is used to introduce the aminoethyl linker and the third step to attach the methacrylate group.The procedure for the synthesis of **15** was inspired by the work of K. Jalani

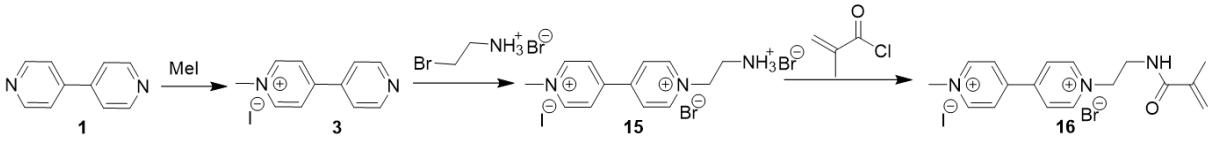

Figure 41: The first synthetic route for the synthesis of a viologen monomer 16

et al..[117] A mixture of 2-bromoethylamine hydrobromide and **1** were combined in dry MeCN and refluxed at 80 °C for 12 h under a controlled-atmosphere. As **15** is insoluble in MeCN, it

precipitated out as an orange solid, which was filtered and washed with copious amounts of solvent. Although the high purity of the product was confirmed by ^{1}H NMR (Figure 42), it was unfortunately obtained with a low yield (5 %). It became virtually impossible to obtain a workable amount of viologen monomer using this method. A first solution considered to counter this problem was to use ten equivalents of 2-bromoethylamine hydrobromide instead of two, but this failed to significantly improve the yield. A second, more successful, solution was to change the solvent from MeCN to THF resulting in a pure product after filtration and washing, obtained with a yield of 62 %.

The last step of the synthesis was not done due to COVID-19.

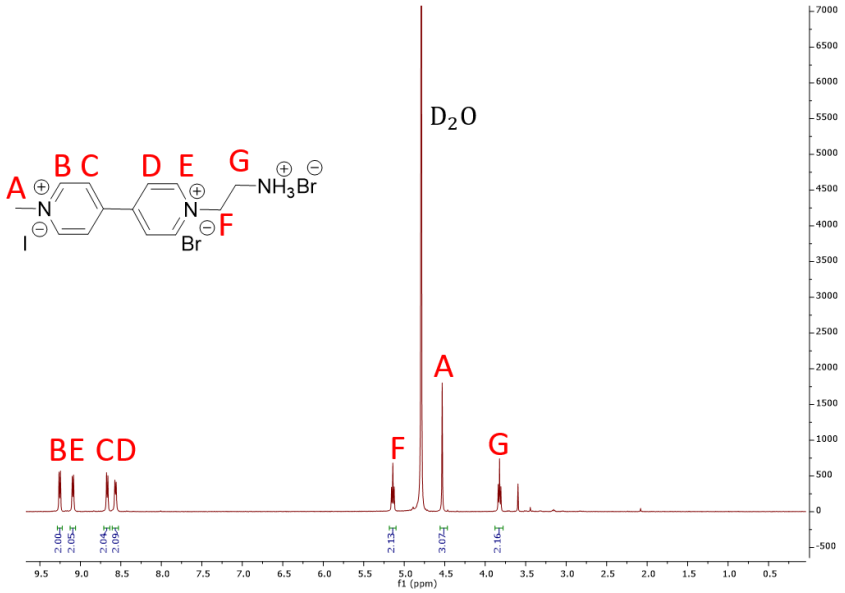

*Figure 42: ^{1}H NMR in water of **15** (300 MHz, D_2O)*

3.2.2 Alternative viologen monomer synthesis

In parallel of the previous methacrylamide monomer, a second synthetic route to obtain a viologen-styrene monomer was investigated during the project. The two-step synthetic pathway is depicted in Figure 43, and the first step is once again the methylation of the 4,4 dipyridine **1** as described in 3.1.1.. The second step is based on a procedure from a report of T. Ogoshi,[118] and is used to link **3** to a styrene unit.

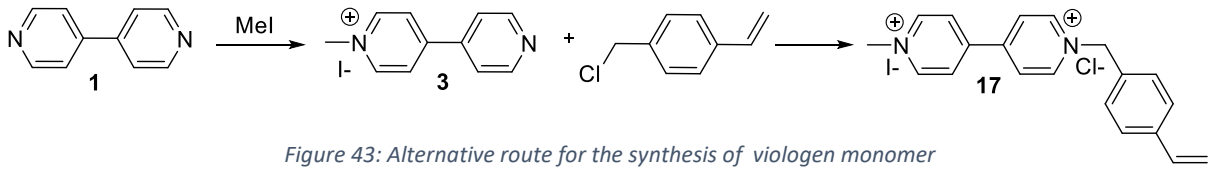

Figure 43: Alternative route for the synthesis of viologen monomer

Compound **3** was reacted with the 4-chloromethylstyrene in MeCN at 60 °C for 24 h. As the product **17** was insoluble in the reaction mixture, it could simply be isolated by filtration, with a yield of 55 %. The structure and purity were confirmed by ^{1}H NMR (Figure 44).

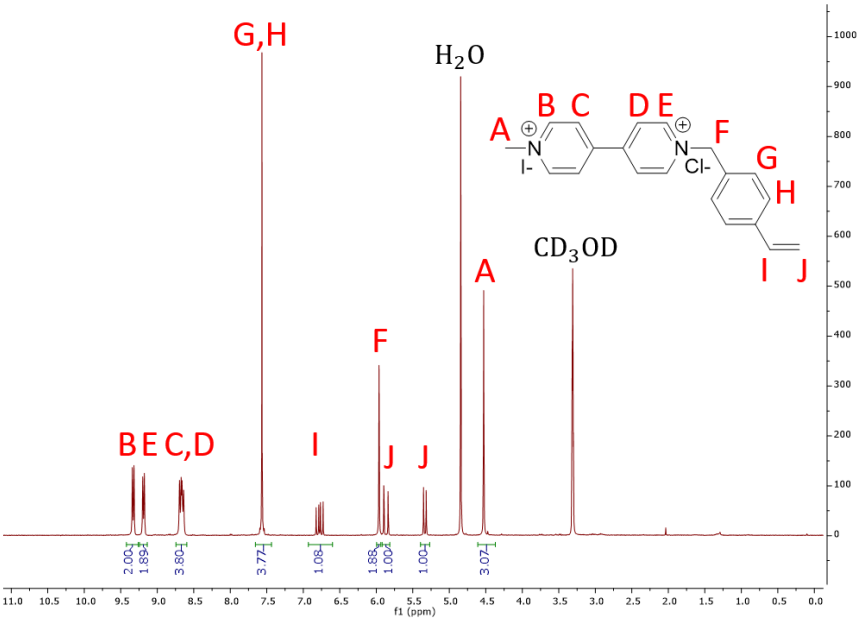

*Figure 44: ^{1}H NMR in methanol of **17** (300 MHz, CD_3OD)*

4 Conclusion and outlook

During this master project, we successfully synthetized and characterized a supramolecular polymeric host-guest system containing a water-soluble pillar[5]arene as the host and a thermo-responsive polymer end-capped with a viologen unit as the guest.

The synthesis of the poly(*n*PropOx) end-capped with the bis-bipyridinium guest was, apart from the purification, straightforward, and the protocol may be expanded to other guest molecule, which could be useful to expand the system to a two component system, a model for the two hydrogel system.

The synthesis of the water-soluble pillar[n]arenes was found to be more challenging than initially anticipated, and the creation of a robust protocol for the synthesis of the pillar[5]arene with triethylene glycol units on both rims was time consuming. The last step of alkylation appeared to be a bottle neck, although using NaH as a base appeared to be a reliable option. A final conclusion can only be given after work-up and subsequent characterization, which were unfortunately not done due to limited time. Although the synthesis of water- soluble pillar[6]arenes was only quickly explored, it would be useful to make it in further work, because it would allow for diversification of the model system and could potentially serve as an additional building block for the creation of molecular communication between hydrogels.

The supramolecular association of the viologen-functionalized poly(*n*PropOx) with the acid-functionalzied pillar[5]arene was characterized by multiple methods. The binding constant K_a was determined via the recording of steady-state fluorescence spectra at varying guest concentrations. It was found to be equal to $3.9 \pm 0.6 \times 10^4$ M^{-1} indicating that strong complexation was occurring. This host-guest complexation was also confirmed by ^{1}H NMR spectroscopy. The method of the Job plot was used to determine the binding stoichiometry, but UV/VIS- as well as fluorescence spectroscopy gave unlikely results. Further measurements, notably in organic solvents instead of water, could be done in the future to try to explain this result. Importantly, the ^{1}H-NMR technique was also used to monitor the influence of temperature on the release and uptake of the pillar[5]arene as a result of the collapse and redissolving of the P*n*PrOx. The quantification using the tosyl group as an internal standard showed that 100 % of the pillar[5]arene was released at elevated temperatures. The

reversibility was confirmed via the recording of multiple ^{1}H NMR spectra at different heating and cooling cycles.

Unfortunately, it was not possible to reach the final goal of creating molecular communication between hydrogels due to the COVID-19 crisis which considerably reduced the practical working time. Further work will be required to achieve it. But the supramolecular model system showed encouraging results that it should be possible to extend to hydrogels-based systems, enabling molecular communication between them. Additionally, a first step towards the synthesis of the thermo-responsive hydrogels was already done by preparing an intermediate in the synthesis of the viologen methacrylamide monomer.

5 Extra assignment

The translation of molecular communication, *i.e.* the use of a chemical signal as an information carrier, from biological systems, where chemical signals are for example used for intra- and inter-cellular communication,[119] to synthetic systems has been a long-standing challenge. These systems are expected to be deployable in many applications. Molecular computing, which is an alternative route to create computing devices using a bottom-up approach, [120] is a prime example of it. By allowing the interaction of different chemical systems with each other, it could lead to chemistry that will become alive, adaptive[121] and/or autonomous[122] due to smart interactions and communications within molecular networks.[122] It is also expected to be useful in drug delivery and smart materials. Even on the macroscopic level the use of chemical signals is evaluated to overcome the limitations that electrical and electromagnetic signals have.[123] Despite its large potential, the practical demonstration of molecular communication is still rather limited. However, numerous synthetic systems involving a single or multiple molecular communication process have been reported, although their performance lags far behind that what biological systems can achieve. The aim of this first extra assignment is to highlight the most prominent approaches from literature of chemical communications based on supramolecular systems

5.1 Chemical communication between supramolecular systems

Supramolecular systems that release a chemical signal (chemical messenger), such as a metal ion, a host or a guest, upon the application of a trigger such as light, temperature, pH, or another chemical, is a fruitful approach that has been used by various groups to create molecular communication. The section below discusses some of the most recent systems and is subdivided based on the type of supramolecular assemblies which is responsible of the signal.

5.1.1 Molecular communication based on metal coordination

Supramolecular systems which include metal to ligand coordination interactions display unique features that can be exploited to create molecular communication. The signal is generally transferred by the intermolecular metal-ion translocation, which is a well-known

phenomenon in biological signalling.[124] It gives highly directional interactions, which allow for a reliable design. Because the strength and the dynamics of the interactions can be modulated and fine-tuned through the choice of the right metal, redox-state or ligand,[125] the system is adaptable to need.

The group of M. Schmittle demonstrated possibility to use metal coordination to achieve chemical communication in a series of reports related to the metal-cation-mediated concatenation of nanoswitches, where the authors utilized competitive metal ion complexation to obtain communication between multiple molecular entities. As illustrated in a report from 2018, they showed that it is possible to establish a multifunctional chemical network of eight components which is able to control both the self-assembly of a three-component nanorotor and its catalytic action (Cu(I)-catalyzed azide-alkyne cycloaddition (CuAAC)[126]) through the addition/removal of zinc(II) ions (Scheme 1).[127] The system has been designed with the following constraints: (1) the components of the nanoswitch and the nanorotor should not interfere with each other (2) in the initial self-sorting should the copper(I) ions strongly bound towards the nanoswitch (3) The nanoswitch must have a higher binding affinity towards the external zinc(II) ions trigger so that the copper(I) ions will be liberated, resulting in the self-assembly of the catalytically active nanorotor, (5) there should be no interference between the eight-component system and the reactants and products of the catalytic reaction. The addition or removal of zinc(II) (the trigger) results in the transmission of copper(I) ion as a second chemical messenger, which conduce to the assembly or disassembly of the catalytically active nanorotor.

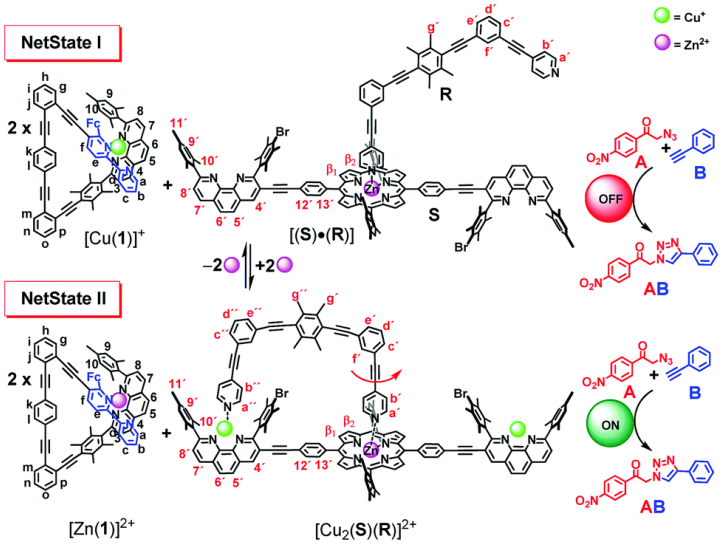

Scheme 1: Catalytically active nanorotor reversibly self-assembled by chemical signalling within an eight-component network[127]

Two years later, the Schmittle's group described the molecular communication between a molecular switch and loose building blocks, leading to supramolecular aggregates (Scheme 2).[128] The multi-component system reported shows a regulation of his assembly and disassembly into a prismal (P) or a rectanglulare (R) supramolecular architecture by a nonoswitch (**1**) and via ion translocation. In more detail, the addition of zinc(II) ions result in the release of copper(I) ions from the nanoswitch ([Cu(1)]$^+$)which act as a second chemical messenger to the free ligands in solution resulting in the self-assembly of supramolecular prism or rectangle aggregates. The addition of a strong complexation agent for zinc(II) ions (hexacyclen) result in the reset of the system and the disassembly of a supramolecular aggregates.

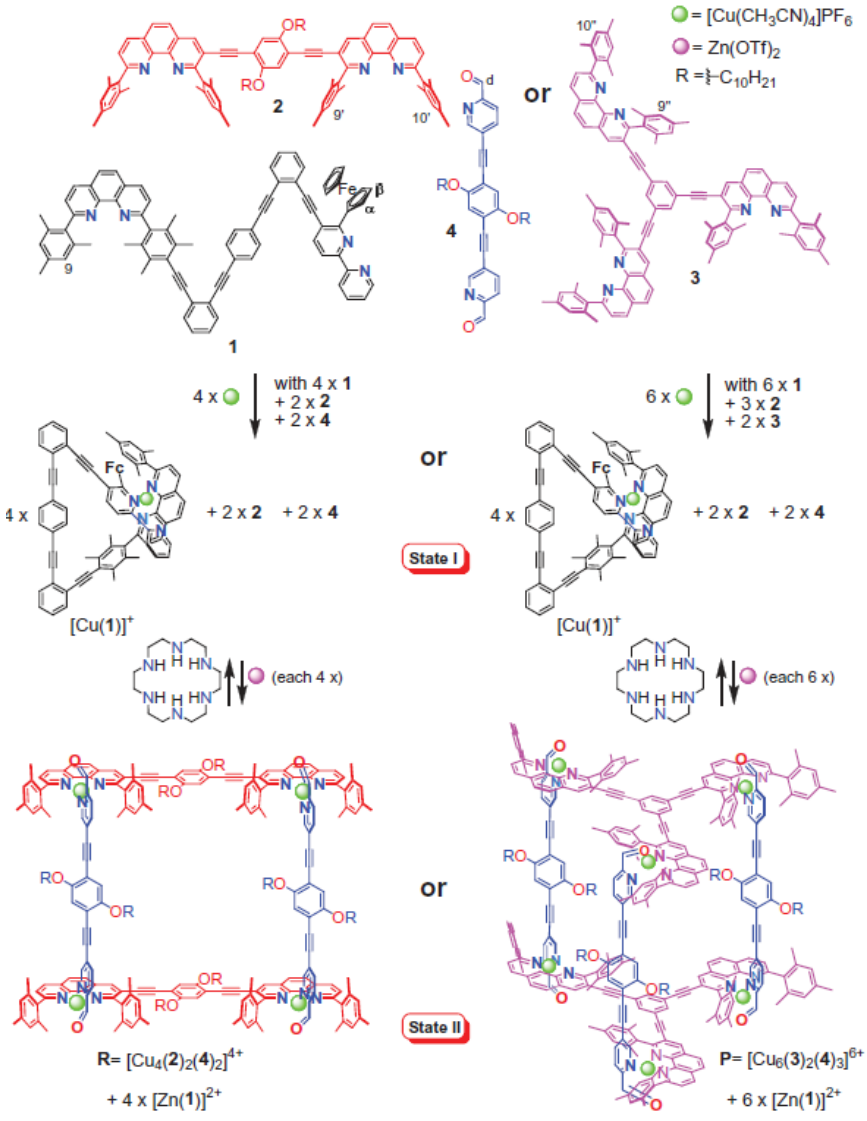

Scheme 2: Representation of the communication between nanoswitch [Cu(I)]$^+$ and the supramolecular architectures R or P.[128]

More recently, the same group reported a more advanced system, which is probably one of the most complex synthetic chemical-communication system known so far. The authors prepared a supramolecular AND logic gate that is able to control the construction of a catalytically active nanorotor via the molecular communication of two nanoswitches (Scheme 3 and 4).[129]

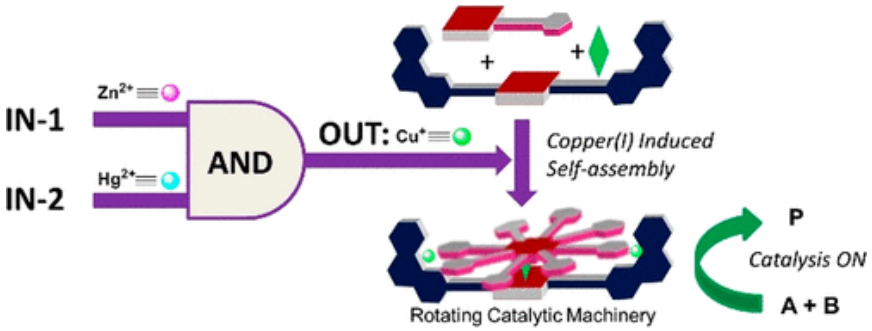

Scheme 3: Schmittle's supramolecular AND logic gate that is able to control the construction of a catalytically active nanorotor[129]

The system, based on competitive metal ion complexation, contains twelve distinct components: two nanoswitches, three metal ions, a stator, a rotator, an axle, a strong ligand (hexacyclen) to selectively remove the metal ions, and two reactants and products for the catalytical reaction. The supramolecular AND gate consists of two communicating molecular receptors that are activated by zinc(II) and mercury(II) ions and generates copper(I) ions as an output. As a consequence of the liberation of these copper(I) ions into solution, the self-assembly of the four-component rotor occurs, which is able to catalyse a click reaction.

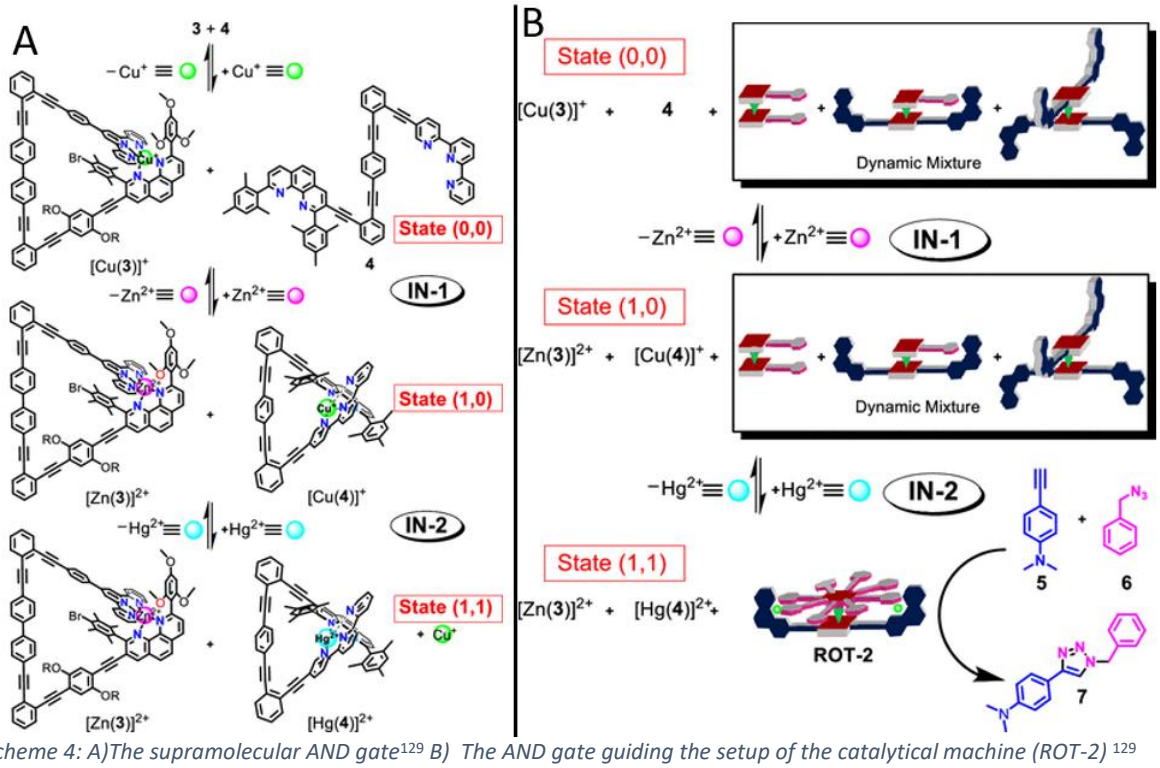

Scheme 4: A)The supramolecular AND gate[129] *B) The AND gate guiding the setup of the catalytical machine (ROT-2)* [129]

5.1.2 Molecular communication based on hydrogen bonding arrays

The use of hydrogen bonding arrays for the creation of molecular communication was demonstrated in 2017 by McClenaghan and Berna and co-workers, who used barbiturate as a chemical messenger to convert light into motion (Scheme 5).[130] The system is depicted in the Scheme 5 and works as follows: the release of barbiturate from the hydrogen-bonding acceptor (B⊂1) is triggered by the [4+4] photocycloaddition of anthracene moieties and results in the occupation of the hydrogen-bonding stations on the thread of the [2]rotaxane (2+2B), which modulate the wheel gliding. The photodimerization can be reverted upon the application of heat, which reset the system to its initial state.

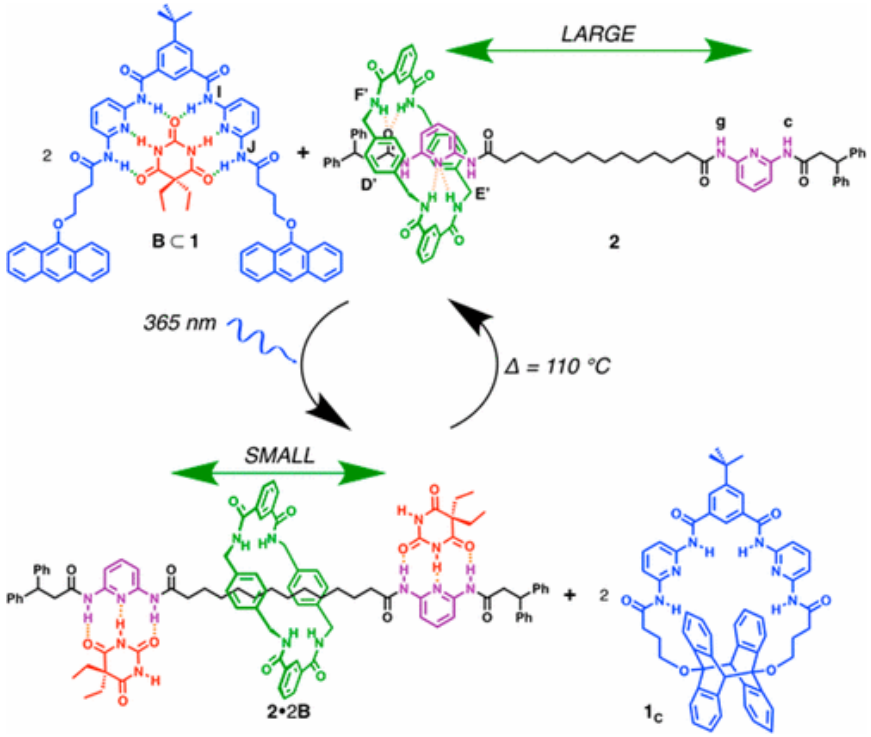

Scheme 5: Remote Photoregulated Ring Gliding in a [2]Rotaxane via a barbiturate[130]

5.1.3 Molecular communication based on host-guest chemistry

Host-guest complexes are another supramolecular platform that can be used for the creation of molecular communication. One of the strategies is based on the communication between two host molecules via the transformation of a guest A, initially bound preferentially to one of the hosts, into an electronically and/or structurally different guest B. If A binds stronger to one host and B has preference for the other host, then chemical communication by means of the transformed guest B is established.[131] Using light as stimulus to transform the guest is an attractive way to conduce such an approach, as is highlighted by Fedorova and Issacs and co-workers in 2015. The authors demonstrated the possibility to translocate a styryl dye (upon a

phototransformation) from a b-cyclodextrin derivative to a cucurbit[7]uril macrocycle (Scheme 6).[132]

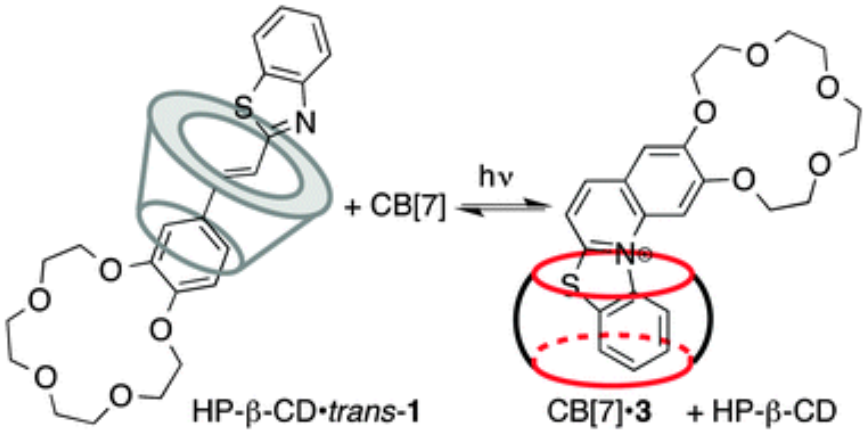

Scheme 6: Light-induced guest release from a b-cyclodextrin derivative to a cucurbit[7]uril macrocycle[132]

Many other groups have been attracted by this idea, leading to numerous examples. In this way, the group U. Pischel created a drug delivery system, by controlling a host–guest assembly with a reversible photo switch.[133] More specifically, they built a photoinduced switching system between the non-charged chalcone (the green dot in Scheme 7) and the charged flavylium (the yellow dot in Scheme 7) guest molecules, with the latter binding three orders of magnitude stronger toward CB7. Hence a competitive guest is formed upon irradiation, capable of releasing an initially complexed drug such as memantine. The chalcone/flavylium system acts as a chemical messenger, and is light used as a trigger for the release of a drug having a binding constant with CB7 between the ones of the chalcone and the flavylium. In a later report, the same authors used a similar system to create a pH-dependent and light-induced sequential logic gate capable of releasing a cargo (which is the tripeptide Phe-Gly-Gly) from a cucurbit[8]uril host molecule (Scheme 8).[134]

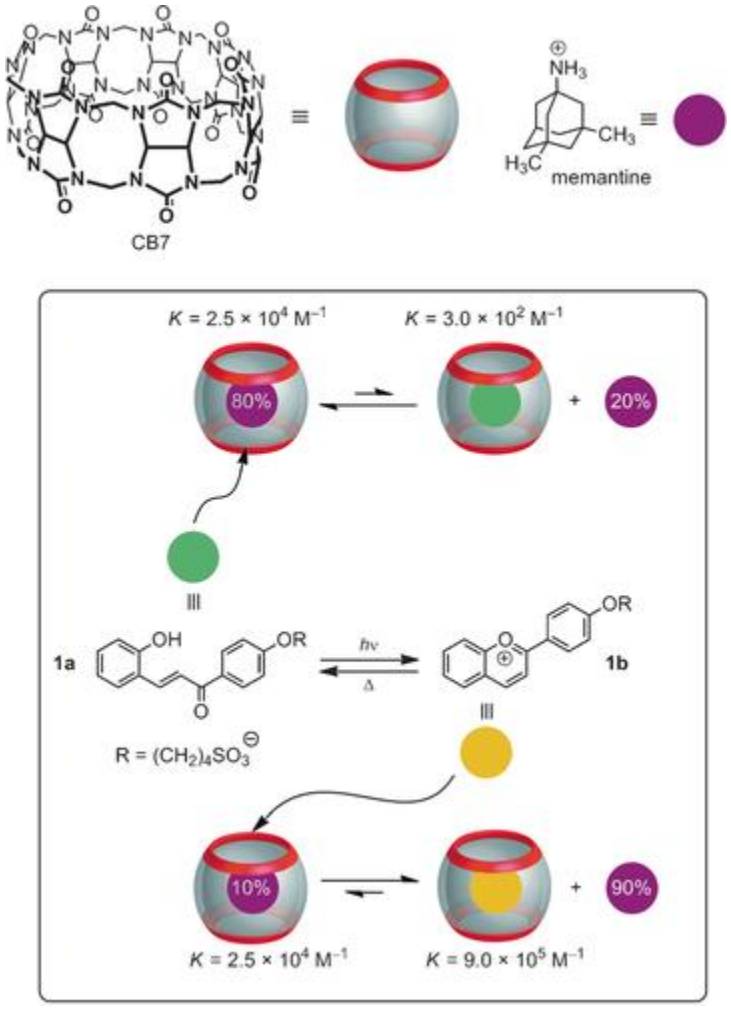

Scheme 7: A drug delivery system by controlling the host–guest assembly with a reversible photo switch[133]

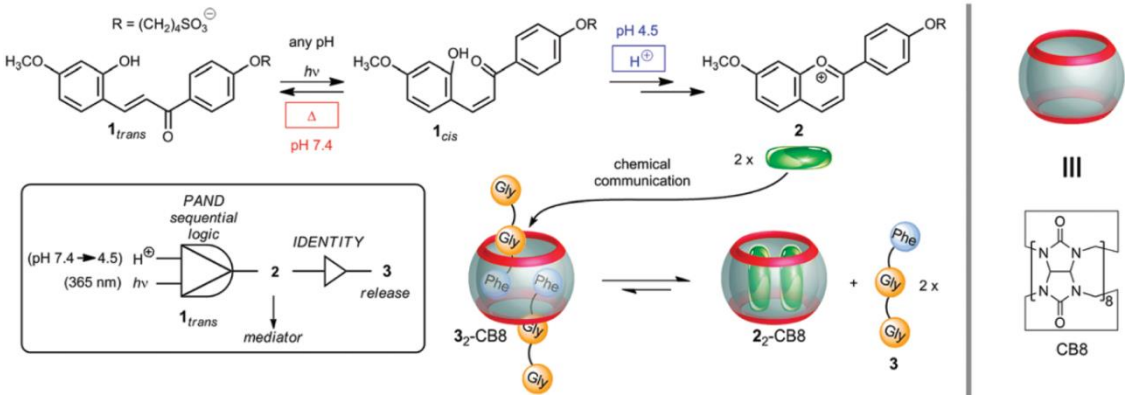

Scheme 8: Light-induced cargo release from a cucurbit[8]uril host by means of a sequential logic operation[134]

The use of temperature instead of light to induce the release of a guest and create molecular communication is another strategy explored by researchers. For example, the group of Zhang employed a temperature-induced reconfiguration between two metal-organic hosts to create a system capable of ejecting one guest and take up another in a reversible way.[135] The system (depicted in Scheme 9) consists of two thermally interconverting Zn_4L_4 tetrahedral diastereoisomers (T1 and T2) that act as a chemical messenger between different guest

molecules. At low temperature, T1 is favoured and is able to bind a small aliphatic guest (G1), whilst at higher temperatures, T2 predominates and bind larger aromatic molecules (G2). This system has great potential due to the versatility of guests that can be used. One guest molecule in particular, calix[4]arene, can be potentially used to achieve a higher level of communication, since it is also a host molecule.

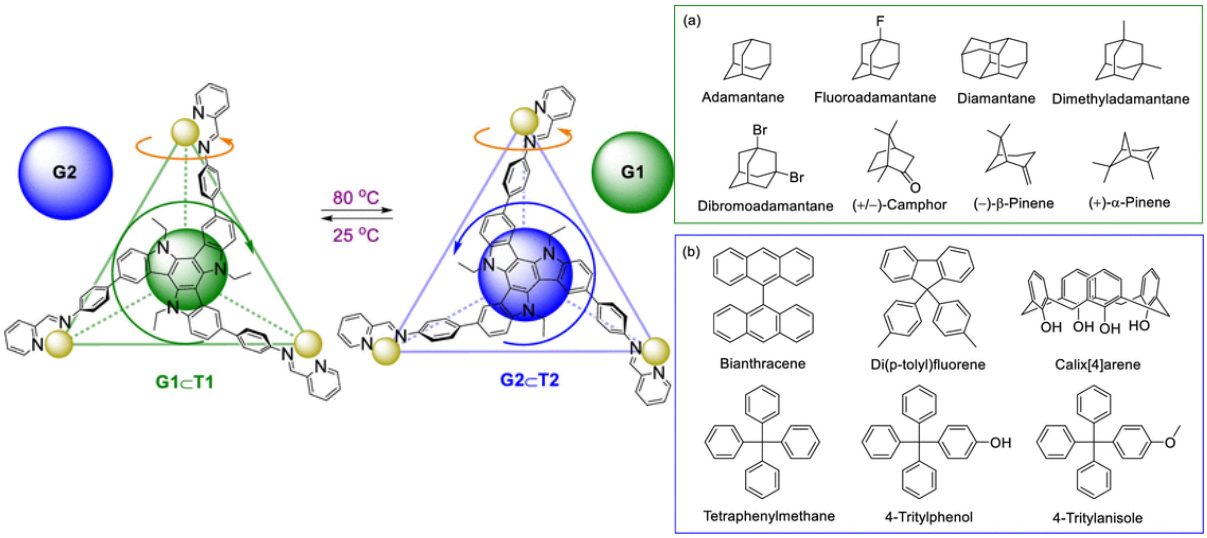

Scheme 9: Left hand side: Schematic representation of the reversible uptake and release of G1 and G2 The right hand side (a) G1 and (b) G2[135]

5.1.4 Molecular communication based on cascades

Signal transduction based on a cascade of biochemical reactions is a natural phenomenon used for molecular communication in cells.[136] The translation of such a system to a purely synthetic setting represent an important goal in system chemistry.[137] Supramolecular assemblies, which are reversible interactions that can adapt their equilibrium composition as a function of external stimuli,[138] proved to be ideal models for the demonstration of molecular communication based on cascades in synthetic systems. A prime example was recently given by the group of U.Pischel, who created a chemically-triggered signalling cascade between cucurbituril host– guest complexes by means of multi-step competitive displacements.[138] The four-component system is depicted in Scheme 10 and consists of two guest molecules (I and II) and two cucurbituril host molecules (CB7 and CB8). The chemical trigger used is memantine, whilst thioflavin (guest II), which is dislocated from CB8 to CB7 via competitive displacement, is used as a mediator, and tyrosine or dopamine (guest I) is the final released guest. As a last example, the use of metal–organic cages to create a chemically triggered signalling cascade was illustrated by S. Ma et al.. [139] The system created is depicted in Scheme 11 and consists of a larger (1) and a smaller (2) tetrahedral metal–organic capsules as hosts, PF_6^- as the chemical

trigger, ClO_4^-a mediator, by dislocating from (2) to (1) via competitive displacement, and NTf_2^- as the released guest.

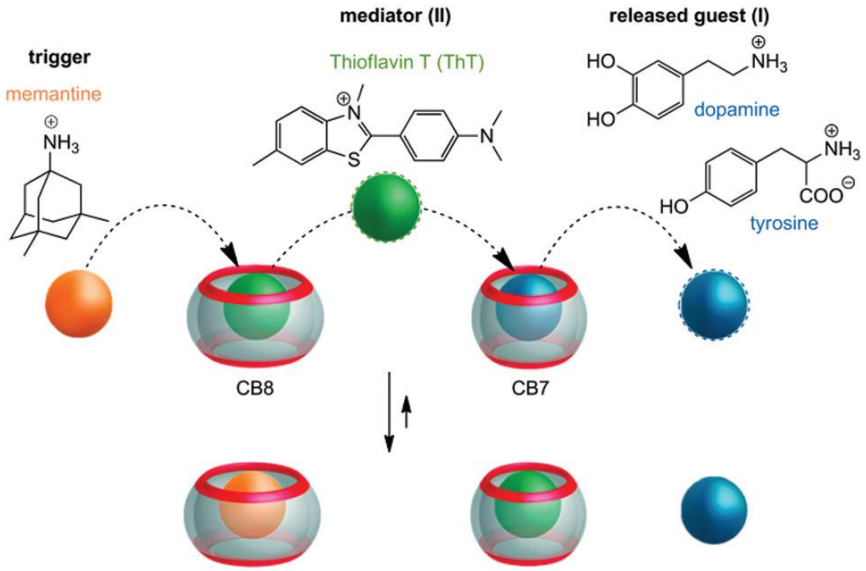

Scheme 10: Chemically-triggered signalling cascade with memantine as the trigger, Thioflavin as the mediator, and tyrosine or dopamine as released guest[138]

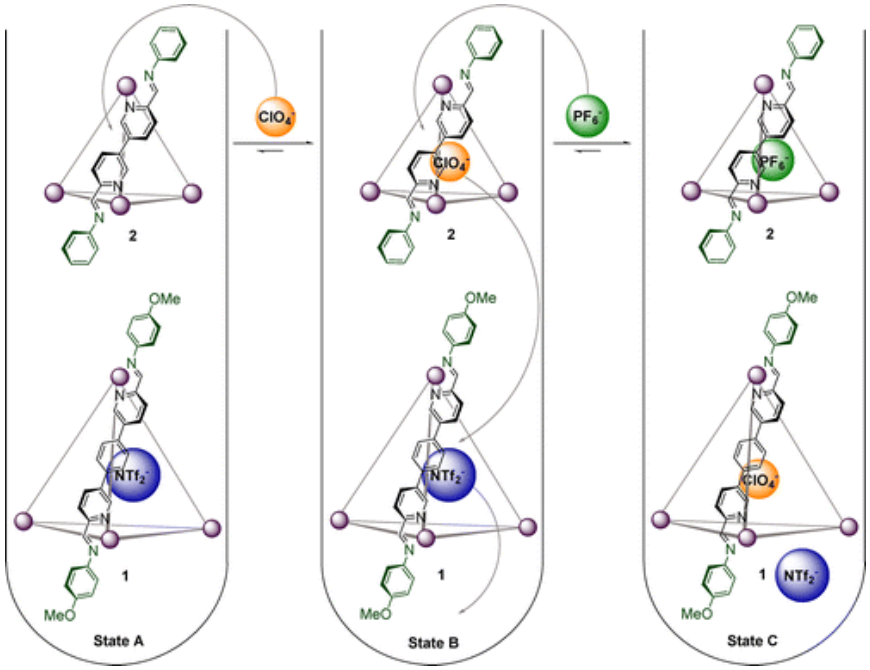

Scheme 11: Chemically triggered signalling cascade with PF_6^- as the trigger ClO_4^-as the mediator and NTf_2^- released guest[139]

5.1.4.1 Simulations on different multicomponent cascade systems

The above mentioned reports from U. Pischel's and S. Ma. highlight the possibility to create signalling cascades by carefully choosing host-guest complexes with binding constants that differ one or more orders of magnitude. A major challenge associated with this is the fact that the interplay of all these dynamic equilibria can lead to vague transitions and therefore result in only a partial release of the guest at the end of the cascade. To further examine and

highlight this problem, some simulations were done as a second extra assignment. The investigated system consists of a three component system containing two hosts and one guest. The binding equilibria that can be established in this multicomponent mixture (considering only the formation of 1:1 complexes is occurring) are depicted in Scheme 12 and the algorithm used for the simulation is based on a system of three equations constructed from the mass balance and equilibrium expressions. The system was solved using the Newton-Raphson algorithm and implemented in a spreadsheet to calculate the equilibrium concentrations of all the species, based on the relative binding constants and the initial concentrations.

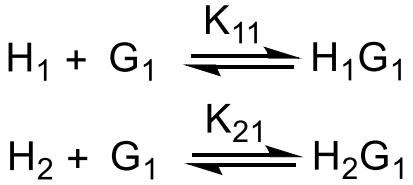

Scheme 12: The binding equilibria established in a mixture containing two hosts and one guest.

$$[H_1]_0 = [H_1] + [H_1G_2] \qquad \text{(eq. 2)}$$

$$[H_2]_0 = [H_2] + [H_2G_2] \qquad \text{(eq. 3)}$$

$$[G_1]_0 = [G_1] + [H_1G_2] + [H_2G_2] \qquad \text{(eq. 4)}$$

Substituting the concentrations of the complexes by the product of the respective binding constant with the equilibrium concentrations of the free hosts and guest (i.e., $[H_iG_j]=K_{ij}[H_i][G_j]$) result in a system of three equations and three unknown variables.

$$[H_1] + K_{11}\,[H_1][G_1] - [H_1]_0 = 0 \qquad \text{(eq. 5)}$$

$$[H_2] + K_{21}\,[H_2][G_1] - [H_2]_0 = 0 \qquad \text{(eq. 6)}$$

$$[G_1] + K_{11}\,[H_1][G_1] + K_{21}[H_2][G_1] - [G_0] = 0 \qquad \text{(eq. 7)}$$

The solutions of this system of equations leads to the equilibrium concentrations of all free species and can be inserted in the equilibrium equations (*i.e.* ., $[H_iG_j]=K_{ij}[H_i][G_j]$) to calculate the concentration of the complexes. Based on this, different plots based on the variable parameters were constructed, the results of which are given below.

First, the influence of the difference in orders of magnitude between the binding constants K_{11} and K_{21} on the selective binding was monitored. This was done because insight in how

much the Ka should vary is of great help for selecting the right host-guest system. Having A 10 and 100-fold difference in magnitude were used and resulted in two graphs (Graph 1 and 2). From these graphs it becomes clear that with a 100-fold difference in Ka, it is possible to work at 1:1:1 ratio while with at a 10-fold difference it is needed to work with a 2:1:1 (H_2-H_1-G_1) ratio to achieve a selective transfer (there is less than 5% [H_1G_1] left) of the guest from the [H_1G_1] complex to the [H_2G_1] complex.

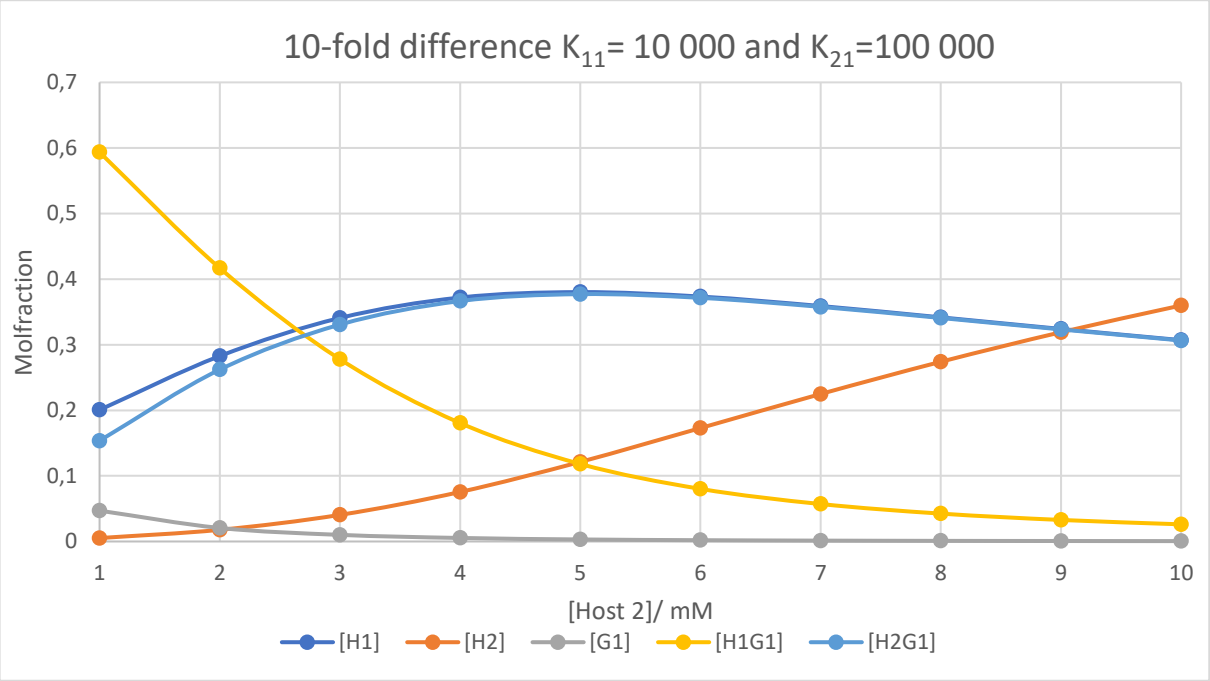

Graph 1: Addition of H_2 on a system containing H_1 and G_1, with K_{11}=10 000 and K_{21}=100 000, and the starting concentration of $H_1$and G_1=5mM

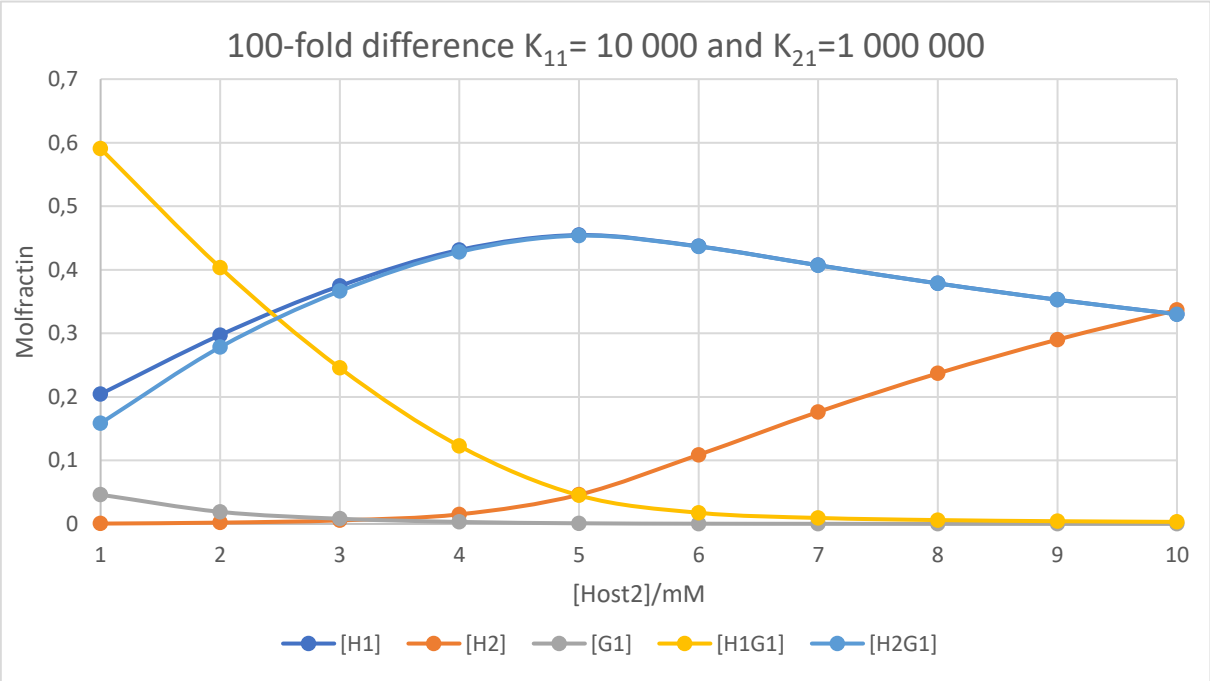

Graph 2: Addition of H_2 on a system containing H_1 and G_1, with K_{11}=10 000 and K_{21}=1 000 000, and the starting concentration of $H_1$and G_1=5mM

In a second step, the absolute numbers of K_{11} and K_{21} were varied, but the ratio between the two was not altered. This led to the two graphs illustrated below and show again that with a 100-fold difference in K_a, it is possible to work at a 1:1:1 ratio while with at a 10-fold difference you need to work with a 2:1:1 (H_2-H_1-G_1) ratio to get selective transfer of the guest to the added H_2. However, in both of these cases there is free G_1 left in the situation of a 1:1:1 ratio due to the lower K_a's. This is something that has not much impact in a three component system, but in more complex systems with multiple hosts and guest could this lead to significant interference in the cascade.

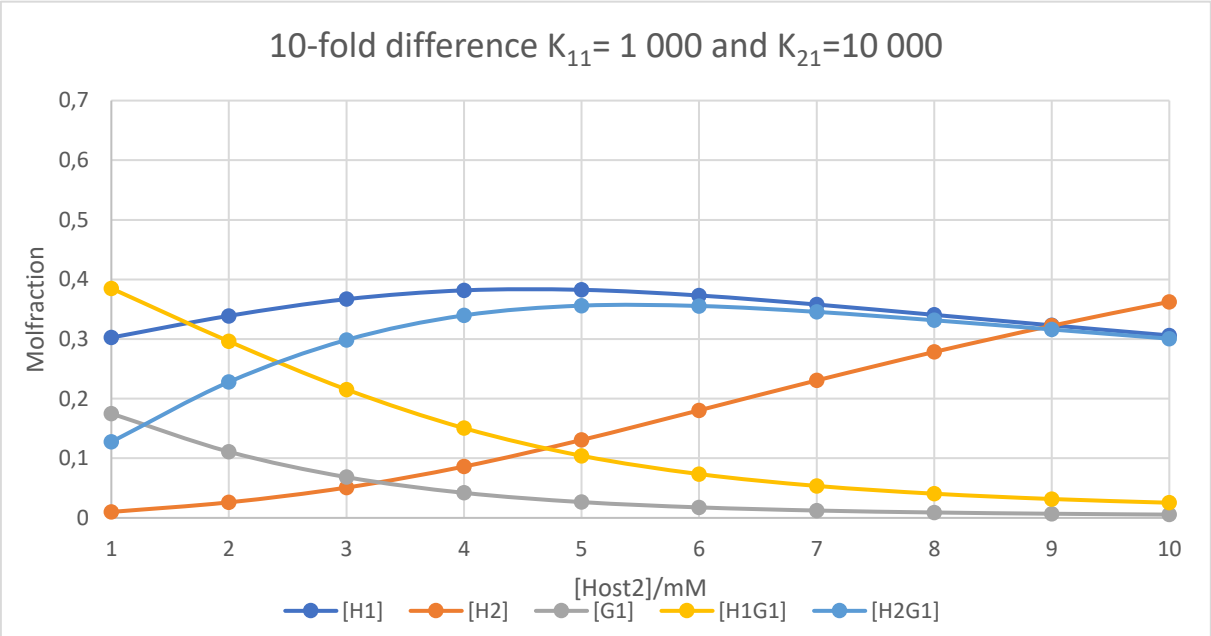

Graph 3: Addition of H_2 on a system containing H_1 and G_1, with K_{11}=1 000 and K_{21}=10 000, and the starting concentration of $H_1$and G_1=5mM

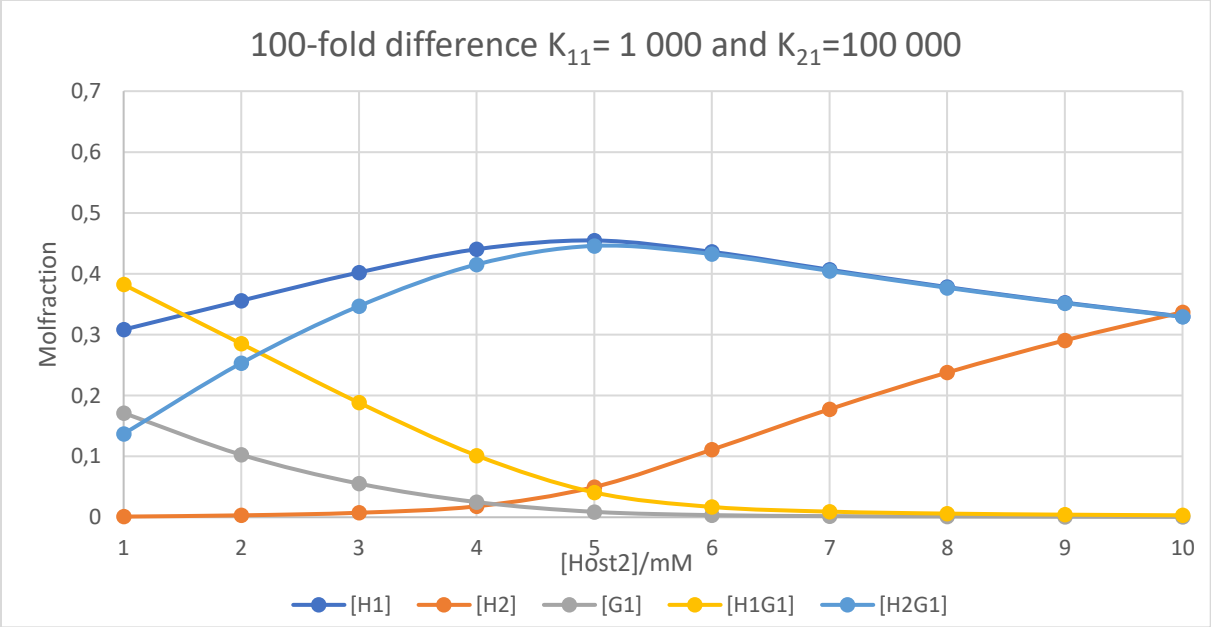

Graph 4: Addition of H_2 on a system containing H_1 and G_1, with K_{11}=1 000 and K_{21}=100 000, and the starting concentration of $H_1$and G_1=5mM

In a third step, the influence of varying equivalents (0.2 eq, 0.5 eq, 1 eq and 2eq) of the host molecules related to the amount of guest in solution was monitored while keeping an equimolar mixture of both hosts. The graphs are depicted below and show that in a 10-fold difference of K_a (K_{a1} = 10 000 ; K_{a2} = 100 000) a little more than a (2:2:1) (H_2-H_1-G_1) ratio is needed to get completely selective binding of the guest with H_2, while in a 100- fold difference of K_a (K_{a1} = 10 000 ; K_{a2} = 1 000 000) completely selective binding of the guest with H_2 is occurring at the (2:2:1) (H_2-H_1-G_1) ratio. This type of information is useful because the optimization of equivalents for efficient transfer can help in the decision and design for the exact experimental lay-out needed in future synthetic systems.

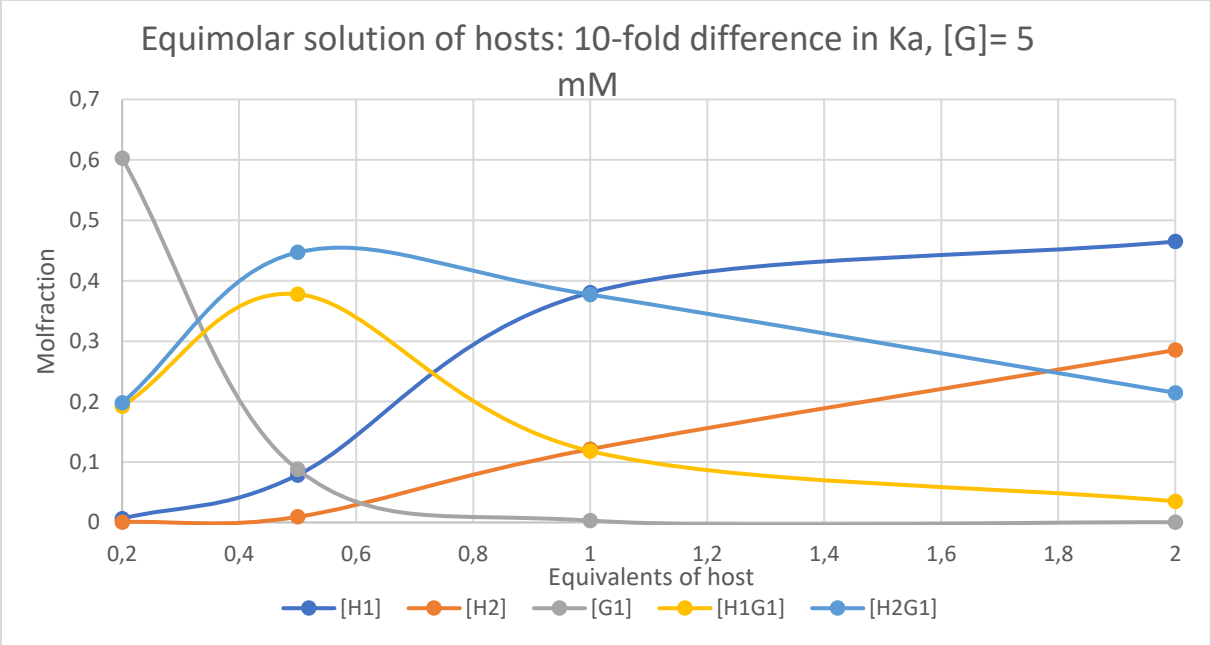

Graph5: Equimolar host (0.2, 0.5, 1 and 2 eq) mixture with G_1=5 mM and a 10-fold Ka difference

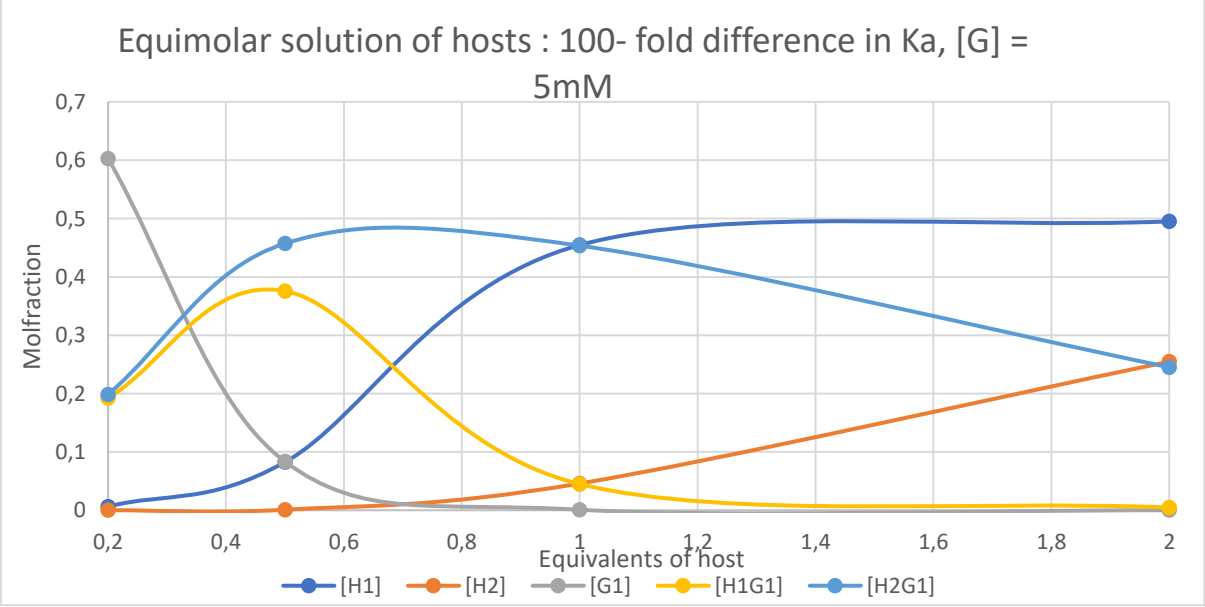

Graph 6: Equimolar host (0.2, 0.5, 1 and 2 eq) mixture with G_1=5 mM and a 100-fold Ka difference

Thereafter, the same situation was monitored but with varying the guest concentration from 5 mM to 10 mM. The resulting graphs reveal that this has no influence on the system, since the same graphs were generated. The graphs are depicted below and show that in a 10-fold difference of K_a (K_{a1} = 10 000 ; K_{a2} = 100 000).

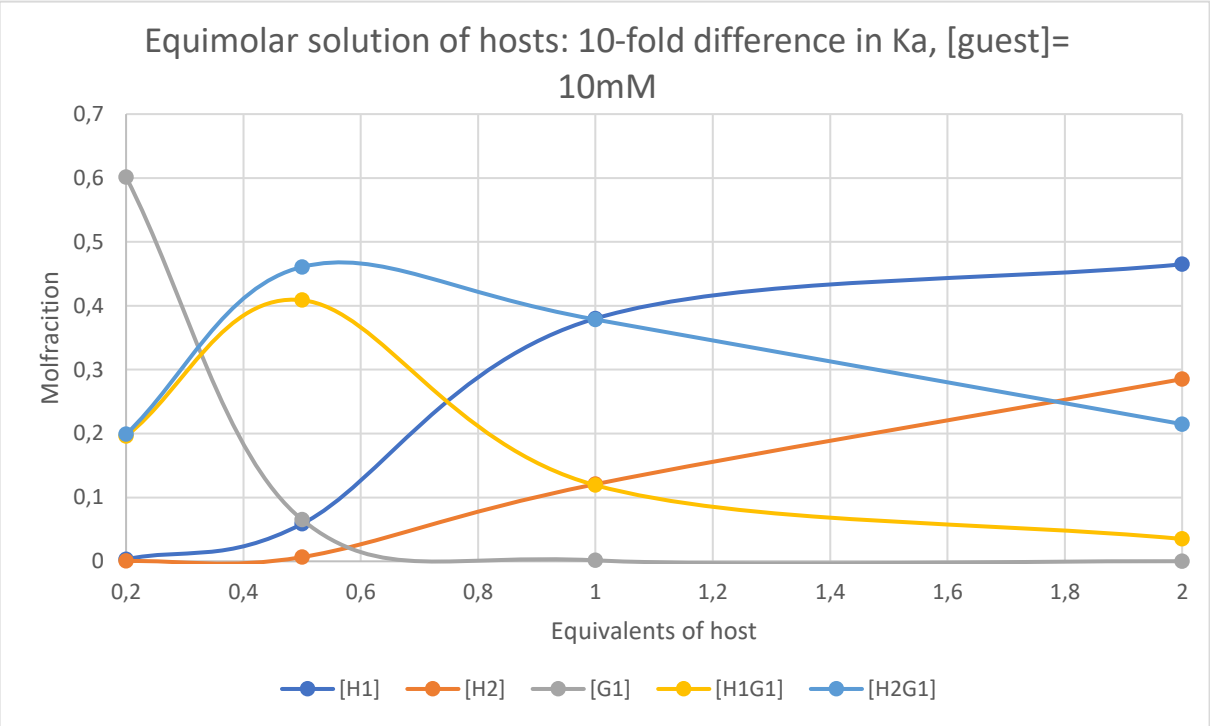

Graph 7: Equimolar host (0.2, 0.5, 1 and 2 eq) mixture with G_1=10 mM and a 10-fold Ka difference

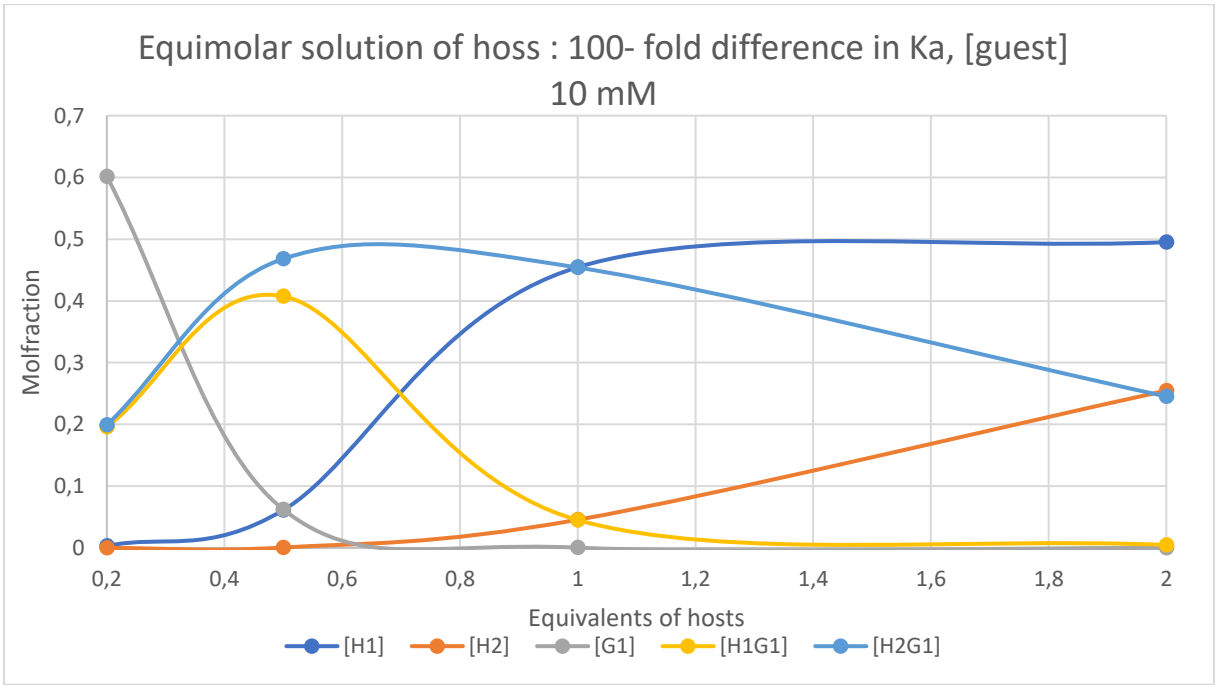

Graph 8: Equimolar host (0.2, 0.5, 1 and 2 eq) mixture with G_1=10 mM and a 100-fold Ka difference

In a final step an equimolar complexed mixture of H_2-G_1 was investigated with varying equivalents of the weakest binding host H_1. The graphs are depicted below and show that in a 10-fold (K_{a1} = 10 000 ; K_{a2} = 100 000) as well as in a 100-fold (K_{a1} = 10 000 ; K_{a2} = 1 000 000) difference in k_a a low amount of free H_2 is present independent of the number of H_1 equivalents. In the 10-fold difference is this amount higher than in the 100-fold difference , because K_{a1} is lower.

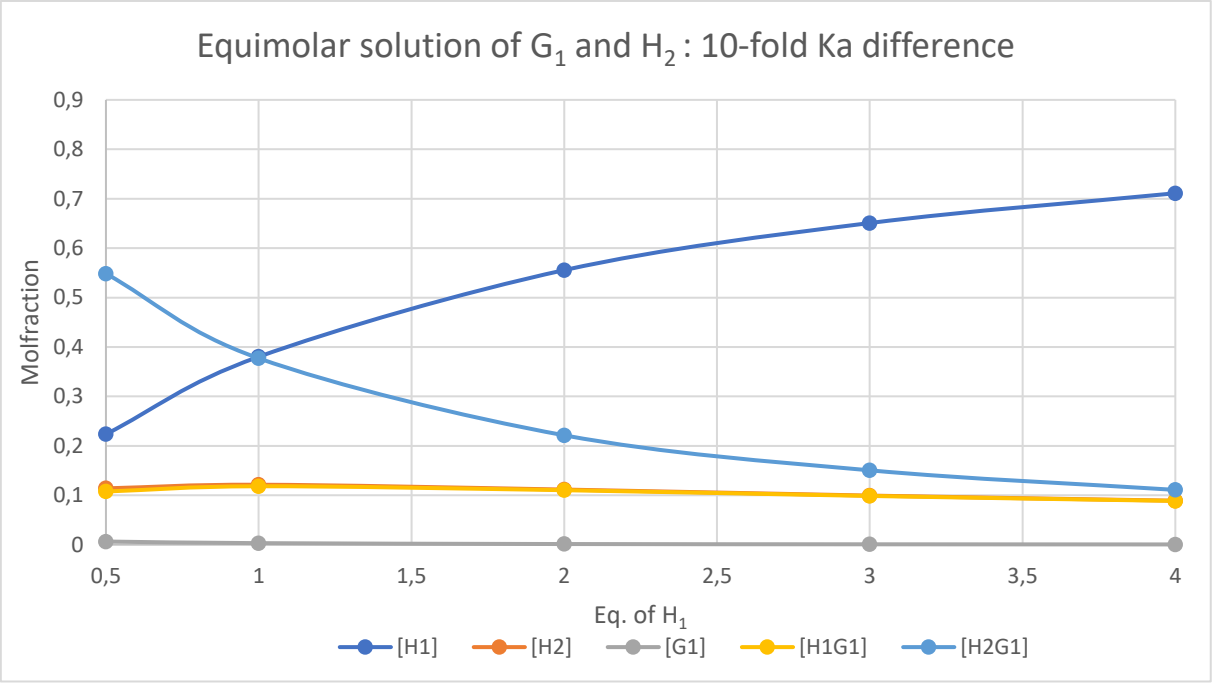

Graph 9: Equimolar H_2-G_1 mixture, [H2]=[G1]=5mM with variable eq of H1 and a10 -fold Ka difference

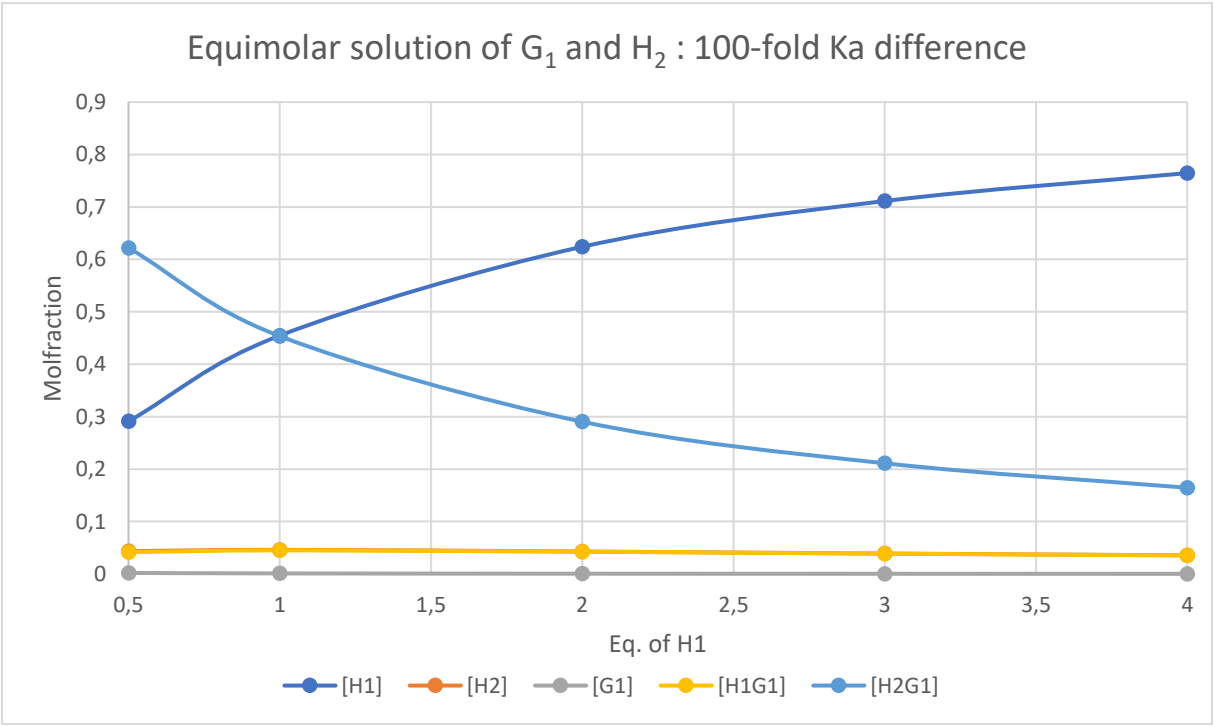

Graph 10: Equimolar H_2-G_1 mixture, [H2]=[G1]=5mM with variable eq of H1 and a 10 -fold Ka difference

5.2 Conclusion

Several supramolecular strategies for the creation of molecular communication have been highlighted. On the on hand is the use of metal coordination an attractive way, due to its highly directional interactions allowing for the creation of a reliable design. On the other hand, the use of host-guest chemistry also provided promising results for the creation of molecular communication. However, a wide range of available host and guest molecules have not been explored for molecular communication, meaning there is still much potential left. The use of cascades corresponds in a very visual way to the idea of molecular communication. By choosing the right supramolecular building blocks is it possible to simulate the biological phenomena of signal transduction. The simulations done in the assignment show that a lot of parameter should be taken into account when selecting a host-guest systems for signalling cascades. So is it important to have K_a values that are high enough so that there is as little as possible of free host or guest present in the system. The ratio between the different K_a should also be high enough to achieve selective transfer of the guest at low ratio's. Finally is it also important to have knowledge of the optimized equivalents and concentration for effective transfer, because it can help to decide and design the exact experimental lay-out for future synthetic systems. The use of supramolecular assemblies proved to be a valid strategy, but a lot of work lies ahead if these systems are to be used for real life applications. However, the progress in the past few years have been encouraging.

6 Bibliography

1. Desiraju, G. R. Chemistry beyond the molecule. **412**, 397–400 (2001).
2. Douglas, S. M. *et al.* Self-assembly of DNA into nanoscale three-dimensional shapes. *Nature* **459**, 414–418 (2009).
3. Senozan, N. M. & Hunt, R. L. Hemoglobin: Its occurrence, structure, and adaptation. *Journal of Chemical Education* **59**, 173–178 (1982).
4. Hoffman-Goetz, L. & Kluger, M. J. Protein deficiency: its effects on body temperature in health and disease states. *Am. J. Clin. Nutr.* **32**, 1423–27 (1979).
5. Betancourt, D. & Del Río, C. *Study of the Human Eye Working Principle: An impressive high angular resolution system with simple array detectors*.
6. Gonzalez, A. C. D. O., Andrade, Z. D. A., Costa, T. F. & Medrado, A. R. A. P. Wound healing - A literature review. *Anais Brasileiros de Dermatologia* **91**, 614–620 (2016).
7. Press release: The 1987 Nobel Prize in Chemistry. Available at: https://www.nobelprize.org/prizes/chemistry/1987/press-release/. (Accessed: 13th June 2020)
8. Lehn, J. -M. Supramolecular Chemistry—Scope and Perspectives Molecules, Supermolecules, and Molecular Devices (Nobel Lecture). *Angew. Chemie Int. Ed. English* **27**, 89–112 (1988).
9. Ariga K.; Kunitake T. *Supramolecular Chemistry – Fundamentals and Applications*. *Materials Science* (2006).
10. Ling, X. Y., Reinhoudt, D. N. & Huskens, J. From supramolecular chemistry to nanotechnology: Assembly of 3D nanostructures. in *Pure and Applied Chemistry* **81**, 2225–2233 (2009).
11. Supramolecular Material - an overview | ScienceDirect Topics. Available at: https://www.sciencedirect.com/topics/chemistry/supramolecular-material. (Accessed: 17th November 2019)
12. Chalmers Publication Library Storage and Processing of Information Using Molecules: The All-Photonic Approach with Simple and Multi-Photochromic Switches) 'Storage and Processing of Information Using Molecules: The All-Photonic Approach with Simple and Multi-Photochromic Switches'. doi:10.1002/ijch.201300014
13. Mann, J. L., Yu, A. C., Agmon, G. & Appel, E. A. Supramolecular polymeric biomaterials. *Biomaterials Science* **6**, 10–37 (2018).
14. Webber, M. J. & Langer, R. Drug delivery by supramolecular design. *Chemical Society Reviews* **46**, 6600–6620 (2017).
15. Wang, W., Zhang, Y. & Liu, W. Bioinspired fabrication of high strength hydrogels from non-covalent interactions. *Progress in Polymer Science* **71**, 1–25 (2017).
16. Allen, S. J. & Lumb, K. J. Protein-protein interactions: a structural view of inhibition strategies and the IL-23/IL-17 axis. *Adv. Protein Chem. Struct. Biol.* (2020). doi:10.1016/bs.apcsb.2019.12.006
17. Aoyama, Y. Hydrogen Bonding in Supramolecular Functions. in *Supramolecular Chemistry* 17–30 (Springer Netherlands, 1992). doi:10.1007/978-94-011-2492-8_2

18. Mauro, M. Dynamic Metal-Ligand Bonds as Scaffolds for Autonomously Healing Multi-Responsive Materials. *Eur. J. Inorg. Chem.* **2018**, 2090–2100 (2018).

19. Yuki, H., Tanaka, Y., Hata, M. & Ishikawa, H. Implementation of p - p Interactions in Molecular Dynamics Simulation. (2007). doi:10.1002/jcc

20. Steed, J. W., Turner, D. R., Wallace, K. J. & Wiley, J. No Title. **2009**, (2009).

21. Dougherty, D. A. The cation-π interaction. *Acc. Chem. Res.* **46**, 885–893 (2013).

22. Alberto, M. E., Mazzone, G., Russo, N. & Sicilia, E. The mutual influence of non-covalent interactions in π-electron deficient cavities: The case of anion recognition by tetraoxacalix[2]arene[2] triazine. *Chem. Commun.* **46**, 5894–5896 (2010).

23. Garau, C. *et al.* A Topological Analysis of the Electron Density in Anion - π Interactions. *ChemPhysChem* **4**, 1344–1348 (2003).

24. Robertazzi, A., Krull, F., Knapp, E. W. & Gamez, P. Recent advances in anion-π interactions. *CrystEngComm* **13**, 3293–3300 (2011).

25. Cram, D. J. THE DESIGN OF MOLECULAR HOSTS , GUESTS , with the aid of CPK molecular models [17]. Crystal structures of. (1987).

26. Lehn, jean-marie. Supramolecular chemistry – scope and perspectives molecules-molecular devices. (1987).

27. Pederen, C. J. the discovery of crown ethers. (1987).

28. inclusion compound (inclusion complex). **1077**, 2998 (2014).

29. Wittenberg, J. B. & Isaacs, L. Complementarity and Preorganization. in *Supramolecular Chemistry* (John Wiley & Sons, Ltd, 2012). doi:10.1002/9780470661345.smc004

30. Lucas, L. H. & Larive, C. K. Measuring Ligand-Protein Binding Using NMR Diffusion Experiments. 24–41 doi:10.1002/cmr.a.10094

31. Sohrabi, N. Binding And UV / Vis Spectral Investigation of Interaction of Ni (II) Piroxicam Complex With Calf Thymus Deoxyribonucleic Acid (Ct-DNA) : A Thermodynamic Approach. **7**, 533–537 (2015).

32. Leavitt, S. & Freire, E. Direct measurement of protein binding energetics by isothermal titration calorimetry. 560–566

33. Ward, B. L. D. Theory Dependence of Fluorescence of Ligand Binding Case (1): Perturbation of Ligand Fluorescence on Binding to Accep-. **48**, 400–414 (1985).

34. Ulatowski, F., Dabrowa, K., Bałakier, T. & Jurczak, J. Recognizing the Limited Applicability of Job Plots in Studying Host-Guest Interactions in Supramolecular Chemistry. *J. Org. Chem.* **81**, 1746–1756 (2016).

35. Hirose, K. A practical guide for the determination of binding constants. *J. Incl. Phenom.* **39**, 193–209 (2001).

36. Harsha, K. G., Appalanaidu, E., Chereddy, N. R., Baggi, T. R. & Rao, V. J. Pyrene tethered imidazole derivative for the qualitative and quantitative detection of mercury present in various matrices. *Sensors Actuators B Chem.* **256**, 528–534 (2018).

37. Kanagaraj, K. & Inoue, Y. *Solvation Effects in Supramolecular Chemistry Author ' s personal copy*. (2018). doi:10.1016/B978-0-12-409547-2.12481-3

38. Access, O. We are IntechOpen , the world ’ s leading publisher of Open Access books Built by scientists , for scientists TOP 1 % Solvent Effects in Supramolecular Systems.

39. Castellano, B. M. & Eggers, D. K. Experimental Support for a Desolvation Energy Term in Governing Equations for Binding Equilibria. (2013). doi:10.1021/jp402632a

40. Ogoshi, T., Kanai, S., Fujinami, S. & Yamagishi, T. para -Bridged Symmetrical Pillar [5] arenes : Their Lewis Acid Catalyzed Synthesis and Host – Guest Property. 5022–5023 (2008).

41. Xu, X., Jerca, V. V. & Hoogenboom, R. Structural Diversification of Pillar[n]arene Macrocycles. *Angew. Chemie - Int. Ed.* **59**, 6314–6316 (2020).

42. Ogoshi, T., Kanai, S., Fujinami, S., Yamagishi, T. A. & Nakamoto, Y. para-bridged symmetrical pillar[5]arenes: Their Lewis acid catalyzed synthesis and host-guest property. *J. Am. Chem. Soc.* **130**, 5022–5023 (2008).

43. Yu, G. *et al.* Pillar[6]arene-based photoresponsive host-guest complexation. *J. Am. Chem. Soc.* **134**, 8711–8717 (2012).

44. Ogoshi, T., Yamagishi, T. & Nakamoto, Y. Pillar-Shaped Macrocyclic Hosts Pillar [n] arenes : New Key Players for Supramolecular Chemistry. (2016). doi:10.1021/acs.chemrev.5b00765

45. Boinski, T. & Szumna, A. A facile , moisture-insensitive method for synthesis of pillar [5] arenes d the solvent templation by halogen bonds. *Tetrahedron* **68**, 9419–9422 (2012).

46. Boinski, T. & Szumna, A. A facile, moisture-insensitive method for synthesis of pillar[5]arenes - The solvent templation by halogen bonds. *Tetrahedron* **68**, 9419–9422 (2012).

47. Online, V. A. *et al.* The template effect of solvents on high yield synthesis, co-cyclization of pillar[6]arenes and interconversion between pillar[5]- and pillar[6]arenes †. 5774–5777 (2014). doi:10.1039/c4cc01968g

48. Han, J. *et al.* Activation-Enabled Syntheses of Functionalized Pillar[5]arene Derivatives. *Org. Lett.* **17**, 3260–3263 (2015).

49. Strutt, N. L., Zhang, H., Schneebeli, S. T. & Stoddart, J. F. Functionalizing pillar[n]arenes. *Acc. Chem. Res.* **47**, 2631–2642 (2014).

50. Ogoshi, T. & Yamagishi, T. Pillararenes: Versatile Synthetic Receptors for Supramolecular Chemistry. *European J. Org. Chem.* **2013**, 2961–2975 (2013).

51. Ogoshi, T. *et al.* Clickable Di-and tetrafunctionalized pillar[n]arenes (n = 5, 6) by oxidation-reduction of pillar[n]arene units. *J. Org. Chem.* **77**, 11146–11152 (2012).

52. Guo, M. *et al.* Rim-Differentiated C5-Symmetric Tiara-Pillar[5]arenes. *J. Am. Chem. Soc.* **140**, 74–77 (2018).

53. Yu, G. *et al.* A non-symmetric pillar[5]arene-based selective anion receptor for fluoride. *Chem. Commun.* **48**, 2958–2960 (2012).

54. Ogoshi, T., Ueshima, N., Yamagishi, T. A., Toyota, Y. & Matsumi, N. Ionic liquid pillar[5]arene: Its ionic conductivity and solvent-free complexation with a guest. *Chem. Commun.* **48**, 3536–3538 (2012).

55. Ogoshi, T., Kakuta, T. & Yamagishi, T. Applications of Pillar[*n*]arene-Based Supramolecular Assemblies. *Angew. Chemie Int. Ed.* **58**, 2197–2206 (2019).

56. Fan, J., Deng, H., Li, J., Jia, X. & Li, C. Charge-transfer inclusion complex formation of tropylium

cation with pillar[6]arenes. *Chem. Commun.* **49**, 6343–6345 (2013).

57. Ogoshi, T., Hashizume, M., Yamagishi, T. A. & Nakamoto, Y. Synthesis, conformational and host-guest properties of water-soluble pillar[5]arene. *Chem. Commun.* **46**, 3708–3710 (2010).

58. Li, C. *et al.* Complexation of 1,4-Bis(pyridinium)butanes by negatively charged carboxylatopillar[5]arene. *J. Org. Chem.* **76**, 8458–8465 (2011).

59. Li, C. *et al.* Molecular selective binding of basic amino acids by a water-soluble pillar[5]arene. *Chem. Commun.* **49**, 1924–1926 (2013).

60. Ma, Y. *et al.* A cationic water-soluble pillar[5]arene: Synthesis and host-guest complexation with sodium 1-octanesulfonate. *Chem. Commun.* **47**, 12340–12342 (2011).

61. Chen, W. *et al.* Synthesis of a cationic water-soluble pillar[6]arene and its effective complexation towards naphthalenesulfonate guests. *Chem. Commun.* **49**, 7956–7958 (2013).

62. Zhang, Z., Xia, B., Han, C., Yu, Y. & Huang, F. Syntheses of copillar[5]arenes by Co-oligomerization of different monomers. *Org. Lett.* **12**, 3285–3287 (2010).

63. Han, C., Yu, G., Zheng, B. & Huang, F. Complexation between Pillar[5]arenes and a secondary ammonium salt. *Org. Lett.* **14**, 1712–1715 (2012).

64. Strutt, N. L., Forgan, R. S., Spruell, J. M., Botros, Y. Y. & Stoddart, J. F. Monofunctionalized pillar[5]arene as a host for alkanediamines. *J. Am. Chem. Soc.* **133**, 5668–5671 (2011).

65. Han, K. *et al.* Binding Mechanisms and Driving Forces for the Selective Complexation between Pillar[5]arenes and Neutral Nitrogen Heterocyclic Compounds. *European J. Org. Chem.* **2013**, 2057–2060 (2013).

66. Shu, X. *et al.* Complexation of neutral 1,4-dihalobutanes with simple pillar[5]arenes that is dominated by dispersion forces. *Org. Biomol. Chem.* **10**, 3393–3397 (2012).

67. Yu, G., Hua, B. & Han, C. Proton transfer in host-guest complexation between a difunctional pillar[5]arene and alkyldiamines. *Org. Lett.* **16**, 2486–2489 (2014).

68. Xia, W. *et al.* Responsive Gel-like Supramolecular Network Based on Pillar[6]arene–Ferrocenium Recognition Motifs in Polymeric Matrix. *Macromolecules* **48**, 4403–4409 (2015).

69. Delavaux-Nicot, B. *et al.* A Rotaxane Scaffold for the Construction of Multiporphyrinic Light-Harvesting Devices. *Chem. - A Eur. J.* **24**, 133–140 (2018).

70. Ogoshi, T. *et al.* Reduction of emeraldine base form of polyaniline by pillar[5]arene based on formation of poly(pseudorotaxane) structure. *Macromolecules* **44**, 7639–7644 (2011).

71. Ogoshi, T., Ueshima, N. & Yamagishi, T. A. An amphiphilic pillar[5]arene as efficient and substrate-selective phase-transfer catalyst. *Org. Lett.* **15**, 3742–3745 (2013).

72. Hu, X.-Y. *et al.* Dual Photo- and pH-Responsive Supramolecular Nanocarriers Based on Water-Soluble Pillar[6]arene and Different Azobenzene Derivatives for Intracellular Anticancer Drug Delivery. *Chem. - A Eur. J.* **21**, 1208–1220 (2015).

73. Tan, L.-L. *et al.* Pillar[5]arene-Based Supramolecular Organic Frameworks for Highly Selective CO_2-Capture at Ambient Conditions. *Adv. Mater.* **26**, 7027–7031 (2014).

74. macromolecule (polymer molecule). in *IUPAC Compendium of Chemical Terminology* (IUPAC, 2008). doi:10.1351/goldbook.m03667

75. *Glossary of basic terms in polymer science (IUPAC Recommendations 1996)*.

76. Chain-Growth versus Step-Growth. Available at: https://polymerdatabase.com/polymer chemistry/Chain versus Step Growth.html. (Accessed: 11th April 2020)

77. ring-opening polymerization. in *IUPAC Compendium of Chemical Terminology* (IUPAC). doi:10.1351/goldbook.R05396

78. Verbraeken, B., Monnery, B. D., Lava, K. & Hoogenboom, R. The chemistry of poly(2-oxazoline)s. *European Polymer Journal* **88**, 451–469 (2017).

79. Levy, A. & Litt, M. Polymerization of cyclic imino ethers. II. Oxazines. *J. Polym. Sci. Part B Polym. Lett.* **5**, 881–886 (1967).

80. Hrkach, J. S. & Matyjaszewski, K. Reaction of 2-methyl-2-oxazoline with trimethylsilyl initiators: an unusual mode of ring opening. *Macromolecules* **25**, 2070–2075 (1992).

81. Blasco, E., Piñol, M., Berges, C., Sánchez-Somolinos, C. & Oriol, L. Smart Polymers for Optical Data Storage. in *Smart Polymers and their Applications* 567–606 (Elsevier, 2019). doi:10.1016/b978-0-08-102416-4.00016-8

82. Sanjuán, A. M., Reglero Ruiz, J. A., García, F. C. & García, J. M. Smart Polymers for Highly Sensitive Sensors and Devices: Micro- and Nanofabrication Alternatives. in *Smart Polymers and their Applications* 607–650 (Elsevier, 2019). doi:10.1016/b978-0-08-102416-4.00017-x

83. den Brabander, M., Fischer, H. R. & Garcia, S. J. Self-Healing Polymeric Systems: Concepts and Applications. in *Smart Polymers and their Applications* 379–409 (Elsevier, 2019). doi:10.1016/b978-0-08-102416-4.00011-9

84. Savina, I. N., Galaev, I. Y. & Mikhalovsky, S. V. Smart Polymers for Bioseparation and Other Biotechnological Applications. in *Smart Polymers and their Applications* 533–565 (Elsevier, 2019). doi:10.1016/b978-0-08-102416-4.00015-6

85. Duro-Castano, A., Talelli, M., Rodríguez-Escalona, G. & Vicent, M. J. Smart Polymeric Nanocarriers for Drug Delivery. in *Smart Polymers and their Applications* 439–479 (Elsevier, 2019). doi:10.1016/b978-0-08-102416-4.00013-2

86. Hoogenboom, R. Temperature-responsive polymers: Properties, synthesis and applications. in *Smart Polymers and their Applications* 15–44 (Elsevier Ltd, 2014). doi:10.1533/9780857097026.1.15

87. Kocak, G., Tuncer, C. & Bütün, V. PH-Responsive polymers. *Polymer Chemistry* **8**, 144–176 (2017).

88. Brighenti, R., Artoni, F. & Cosma, M. P. Mechanics of Active Mechano-Chemical Responsive Polymers. in *IOP Conference Series: Materials Science and Engineering* **416**, (Institute of Physics Publishing, 2018).

89. Colson, Y. L. & Grinstaff, M. W. Biologically responsive polymeric nanoparticles for drug delivery. *Adv. Mater.* **24**, 3878–3886 (2012).

90. Manouras, T. & Vamvakaki, M. Field responsive materials: Photo-, electro-, magnetic- and ultrasound-sensitive polymers. *Polymer Chemistry* **8**, 74–96 (2017).

91. Irie, M. Photoresponsive polymers. *Adv. Polym. Sci.* **94**, 26–67 (1990).

92. Espinosa-Cano, E., Aguilar, M. R., Vázquez, B. & San Román, J. Inflammation-Responsive Polymers. in *Smart Polymers and their Applications* 219–254 (Elsevier, 2019). doi:10.1016/b978-0-08-102416-4.00007-7

93. Wu, P. *et al.* Ultrasound-Responsive Polymeric Micelles for Sonoporation-Assisted Site-Specific Therapeutic Action. *ACS Appl. Mater. Interfaces* **9**, 25706–25716 (2017).

94. Saraiva, A., Persson, O. & Fredenslund, A. An experimental investigation of cloud-point curves for the poly(ethylene glycol)/water system at varying molecular weight distributions. *Fluid Phase Equilib.* **91**, 291–311 (1993).

95. Nord, F. F., Bier, M. & Timasheff, S. N. Investigations on Proteins and Polymers. IV. [1] Critical Phenomena in Polyvinyl Alcohol-Acetate Copolymer Solutions. *J. Am. Chem. Soc.* **73**, 289–293 (1951).

96. Longenecker, R., Mu, T., Hanna, M., Burke, N. A. D. & Stöver, H. D. H. Thermally responsive 2-hydroxyethyl methacrylate polymers: Soluble-insoluble and soluble-insoluble-soluble transitions. *Macromolecules* **44**, 8962–8971 (2011).

97. De La Rosa, V. R., Woisel, P. & Hoogenboom, R. Supramolecular control over thermoresponsive polymers. *Mater. Today* **19**, 44–55 (2016).

98. Ji, X., Chen, J., Chi, X. & Huang, F. PH-responsive supramolecular control of polymer thermoresponsive behavior by pillararene-based host-guest interactions. *ACS Macro Lett.* **3**, 110–113 (2014).

99. De La Rosa, V. R., Nau, W. M. & Hoogenboom, R. Tuning temperature responsive poly(2-alkyl-2-oxazoline)s by supramolecular host-guest interactions. *Org. Biomol. Chem.* **13**, 3048–3057 (2015).

100. Wei, Y. *et al.* Supramolecular control over self-assembly and double thermoresponsive behavior of an amphiphilic block copolymer. *Eur. Polym. J.* **125**, 109537 (2020).

101. Guo, H. *et al.* Dual Responsive Regulation of Host–Guest Complexation in Aqueous Media to Control Partial Release of the Host. *Chem. - A Eur. J.* **26**, 1292–1297 (2020).

102. Varaprasad, K., Raghavendra, G. M., Jayaramudu, T., Yallapu, M. M. & Sadiku, R. A mini review on hydrogels classification and recent developments in miscellaneous applications. *Mater. Sci. Eng. C* **79**, 958–971 (2017).

103. Wichterle, O. & Lím, D. Hydrophilic Gels for Biological Use. *Nature* **185**, 117–118 (1960).

104. Buwalda, S. J. *et al.* Hydrogels in a historical perspective: From simple networks to smart materials. *Journal of Controlled Release* **190**, 254–273 (2014).

105. Montero, A., Valencia, L., Corrales, R., Jorcano, J. L. & Velasco, D. *Smart Polymer Gels: Properties, Synthesis, and Applications*. *Smart Polymers and their Applications* (Elsevier Ltd., 2019). doi:10.1016/b978-0-08-102416-4.00009-0

106. Akhtar, M. F., Hanif, M. & Ranjha, N. M. Methods of synthesis of hydrogels … A review. *Saudi Pharmaceutical Journal* **24**, 554–559 (2016).

107. Belal, K. *et al.* Recognition-Mediated Hydrogel Swelling Controlled by Interaction with a Negative Thermoresponsive LCST Polymer. *Angewandte Chemie - International Edition* **55**, 13974–13978 (2016).

108. Koetting, M. C., Peters, J. T., Steichen, S. D. & Peppas, N. A. Stimulus-responsive hydrogels: Theory, modern advances, and applications. *Mater. Sci. Eng. R Reports* **93**, 1–49 (2015).

109. Appel, E. A., del Barrio, J., Loh, X. J. & Scherman, O. A. Supramolecular polymeric hydrogels. *Chem. Soc. Rev.* **41**, 6195–6214 (2012).

110. Martinez, K., Stash, J., Benson, K. R., Paul, J. J. & Schmehl, R. H. Direct Observation of Sequential Electron and Proton Transfer in Excited-State ET/PT Reactions. *J. Phys. Chem. C* **123**, 2728–2735 (2019).

111. Ogoshi, T. *et al.* Synthesis and Conformational Characteristics of Alkyl-Substituted Pillar [5] arenes. 3268–3273 (2010). doi:10.1021/jo100273n

112. Li, Q. *et al.* Hyperfast Water Transport through Biomimetic Nanochannels from Peptide-Attached (pR)-pillar[5]arene. *Small* **15**, 1804678 (2019).

113. Wang, C. C. & Yu, C. Y. Synthesis, characterization and nanoaggregates of alkyl and triethylene glycol substituted 3,6-carbazolevinylenes homopolymers and block copolymers. *Polymer (Guildf).* **166**, 123–129 (2019).

114. Chi, X. *et al.* Redox-Responsive Amphiphilic Macromolecular [2]Pseudorotaxane Constructed from a Water-Soluble Pillar[5]arene and a Paraquat-Containing Homopolymer. *ACS Macro Lett.* **4**, 996–999 (2015).

115. Ogoshi, T., Shiga, R. & Yamagishi, T. A. Reversibly tunable lower critical solution temperature utilizing host-guest complexation of pillar[5]arene with triethylene oxide substituents. *J. Am. Chem. Soc.* **134**, 4577–4580 (2012).

116. Damavandi, M. *et al.* Synthesis of grafted poly(p-phenyleneethynylene) via ARGET ATRP: Towards nonaggregating and photoluminescence materials. *Eur. Polym. J.* **89**, 263–271 (2017).

117. Kumar, R., Jalani, K., George, S. J. & Rao, C. N. R. Non-Covalent Synthesis as a New Strategy for Generating Supramolecular Layered Heterostructures. *Chem. Mater.* **29**, 9751–9757 (2017).

118. Ogoshi, T., Masuda, K., Yamagishi, T.-A. & Nakamoto, Y. Side-Chain Polypseudorotaxanes with Heteromacrocyclic Receptors of Cyclodextrins (CDs) and Cucurbit[7]uril (CB7): Their Contrast Lower Critical Solution Temperature Behavior with R-CD, γ-CD, and CB7. (2009). doi:10.1021/ma901474b

119. BURNSTOCK, G. Recent Concepts of Chemical Communication between Excitable Cells. in *Dale's Principle and Communication Between Neurones* 7–35 (Elsevier, 1983). doi:10.1016/b978-0-08-029789-7.50007-7

120. Varghese, S., Elemans, J. A. A. W., Rowan, A. E. & Nolte, R. J. M. Molecular computing: paths to chemical Turing machines. *Chem. Sci.* **6**, 6050–6058 (2015).

121. Lehn, J.-M. Perspectives in Chemistry-Steps towards Complex Matter. *Angew. Chemie Int. Ed.* **52**, 2836–2850 (2013).

122. Merindol, R. & Walther, A. Materials learning from life: Concepts for active, adaptive and autonomous molecular systems. *Chemical Society Reviews* **46**, 5588–5619 (2017).

123. Farsad, N., Guo, W. & Eckford, A. W. Tabletop molecular communication: Text messages through chemical signals. *PLoS One* **8**, (2013).

124. Ackerman, C. M., Lee, S. & Chang, C. J. Analytical Methods for Imaging Metals in Biology: From Transition Metal Metabolism to Transition Metal Signaling. *Analytical Chemistry* **89**, 22–41 (2017).

125. Goswami, A., Saha, S., Biswas, P. K. & Schmittel, M. (Nano)mechanical Motion Triggered by Metal Coordination: From Functional Devices to Networked Multicomponent Catalytic Machinery. *Chem. Rev.* **120**, 125–199 (2020).

126. Ackermann, L., Potukuchi, H. K., Landsberg, D. & Vicente, R. Copper-catalyzed 'click' reaction/direct arylation sequence: Modular syntheses of 1,2,3-triazoles. *Org. Lett.* **10**, 3081–3084 (2008).

127. Goswami, A., Pramanik, S. & Schmittel, M. Catalytically active nanorotor reversibly self-assembled by chemical signaling within. **2**, 3955–3958 (2018).

128. Mittal, N., Paul, I., Pramanik, S. & Schmittel, M. Remote control of the reversible assembly/disassembly of supramolecular aggregates. *Supramol. Chem.* **32**, 133–138 (2020).

129. Biswas, P. K., Saha, S., Gaikwad, S. & Schmittel, M. Reversible Multicomponent AND Gate Triggered by Stoichiometric Chemical Pulses Commands the Self-Assembly and Actuation of Catalytic Machinery. *J. Am. Chem. Soc.* (2020). doi:10.1021/jacs.0c01315

130. Tron, A. *et al.* Remote photoregulated ring gliding in a [2]rotaxane via a molecular effector. *Org. Lett.* **19**, 154–157 (2017).

131. Remón, P. & Pischel, U. Chemical Communication between Molecules. *ChemPhysChem* **18**, 1667–1677 (2017).

132. Fedorov, Y. V. *et al.* Photoinduced guest transformation promotes translocation of guest from hydroxypropyl-β-cyclodextrin to cucurbit[7]uril. *Chem. Commun.* **51**, 1349–1352 (2015).

133. Basílio, N. & Pischel, U. Drug Delivery by Controlling a Supramolecular Host–Guest Assembly with a Reversible Photoswitch. *Chem. - A Eur. J.* **22**, 15208–15211 (2016).

134. Romero, M. A., Fernandes, R. J., Moro, A. J., Basílio, N. & Pischel, U. Light-induced cargo release from a cucurbit[8]uril host by means of a sequential logic operation. *Chem. Commun.* **54**, 13335–13338 (2018).

135. Zhang, D. *et al.* Temperature Controls Guest Uptake and Release from Zn4L4 Tetrahedra. *J. Am. Chem. Soc.* **141**, 14534–14538 (2019).

136. Poonia, S., Chawla, S., Kaushik, S. & Sengupta, D. Pathway informatics. in *Encyclopedia of Bioinformatics and Computational Biology: ABC of Bioinformatics* **1**–**3**, 796–804 (Elsevier, 2018).

137. Ashkenasy, G., Hermans, T. M., Otto, S. & Taylor, A. F. Systems chemistry. *Chem. Soc. Rev.* **46**, 2543–2554 (2017).

138. Remón, P., González, D., Romero, M. A., Basílio, N. & Pischel, U. Chemical signal cascading in a supramolecular network. *Chem. Commun.* (2020). doi:10.1039/D0CC00217H

139. Ma, S. *et al.* Chain-reaction anion exchange between metal-organic cages. *J. Am. Chem. Soc.* **135**, 5678–5684 (2013).

7 Appendix and Experimental section

7.1 Materials

All commonly used solvents were of HPLC grade and include: methanol (MeOH, ≥99.9%, Sigma Aldrich), ethanol (EtOH, ≥99.8%, Sigma Aldrich), dichloromethane (DCM, ≥99.8%, Sigma Aldrich), chloroform ($CHCl_3$, ≥99.8%, Fisher Chemical), diethyl ether (Et_2O, ≥99.9%, Sigma Aldrich), acetonitrile (CH_3CN, ≥99.9%, Sigma Aldrich), ethyl acetate (EtOAc, ≥99.7%, Sigma-Aldrich), acetone ($(CH_3)_2CO$, ≥99.7%), tetrahydrofuran, (THF, CHROMASOLV™ Plus, inhibitor-free ≥99.7%, Sigma-Aldrich), *N*,*N*-dimethylformamide (DMF, 99.8%, Sigma Aldrich) and 1.2-dichloroethane (DCE ≥99.9%, Sigma-Aldrich).

Deuterated solvents for ^{1}H-NMR spectroscopy used were purchased from Euriso-top and include: chloroform-*d* ($CDCl_3$, ≥99.9%), deuterium oxide (D_2O, ≥99.9%), acetonitrile-d_3 (CD_3CN, ≥99.9), dimethylsulfoxide-d_6 (DMSO-d_6, ≥99.8% D) and acetone-d_6 ($(CD_3)_2CO$≥99.8%).

Dry dichloromethane, acetonitrile, tetrahydrofuran and *N*,*N*-dimethylformamide were obtained from a custom made JW Meyer solvent purification system by drying over aluminium oxide columns.

The chemicals used in this study have been purchased from various suppliers (TCI, Sigma Aldrich, Acros organic) and used as received, without any extra purification.

7.2 Equipment

De-ionized water was prepared with a resistivity less than 18.2 MΩ x cm using an Arium 611 from Sartorius with the Sartopore 2 150 (0.45 + 0.2 µm poresize) cartridge filter.

The **glovebox system** used is a VIGOR Sci-Lab SG 1200/750 system with water and oxygen purity levels below 1 ppm, both for water and oxygen content.

The **polymerizations** were performed in capped vials in a single mode microwave Biotage initiator with robot sixty and IR temperature sensor (Biotage, Uppsala, Sweden)

Nuclear magnetic resonance (NMR) spectra were recorded on a Bruker Avance 300 MHz, 400 MHz and 500 MHz spectrometer operating at room temperature (500 MHz for variable temperature measurements). All given chemical shifts, δ, are given relative to the solvent peak of

$CDCl_3$ (7.26 ppm), D_2O (4.79 ppm), DMSO-*d6* (2.50 ppm), $(CD_3)_2CO$ (2.05 ppm) or CD_3CN (1.94 ppm) as indicated at each spectrum. The obtained spectra were analysed with MestReNova.

Size-exclusion chromatography (SEC) was performed on an Agilent 1260-series HPLC system equipped with a 1260 online degasser, a 1260 ISO-pump, a 1260 automatic liquid sampler (ALS), a thermostatted column compartment (TCC) at 50°C equipped with two PLgel 5 µm mixed-D columns and a precolumn in series, a 1260 diode array detector (DAD) a 1260 refractive index detector (RID) and a multi-angle light scattering detector (Wyatt Dawn Hellos II or miniDawn Treos II) (MALS). The used eluent was DMA containing 50mM of LiCl at a flow rate of 0.500 ml/min. The spectra were analysed using the Agilent Chemstation software with the GPC add on. Molar mass values and Đ values were calculated against PMMA standards from PSS or using d_p/d_c value of polymer (d_p/d_c poly(nProPox) = 0.047) in case of LS detection.

Turbidimetry measurements were performed on a Crystal 16^{TM} parallel crystallizer turbidimeter from Avantium Technologies. Samples with a concentration of 5 mg per mL in deionized water were analysed in a temperature range from 5°C to 40°C at a heating rate of 1°C/min. Cloud point temperatures were determined at 50% transmission during the second heating run.

Freeze drying was performed on a Martin Christ Alpha 2-4 LDPlus with an ice condenser capacity of 4 kg and temperature of -85°C and 4 kg/24 h performance.

UV-VIS spectra were recorded on a Varian Cary 100 Bio UV-VIS spectrophotometer equipped with a Cary temperature and stir control. Samples were measured in quartz cuvettes with a pathlength of 1.0 cm in the wavelength range of 300 to 800 nm.

Liquid chromatography mass spectrometry (LCMS) analysis was performed on an Agilent 1100 HPLC with quaternary pump and UV-DAD detection, coupled to an Agilent G1956B MSD. Ionization of the samples was achieved through electronspray ionization (ESI).

Fluorescence spectroscopy The fluorescence measurements were carried out on a Cary Eclipse fluorescence spectrophotometer (under stirring) equipped with a Varian Cary Temperature Controller. The emission spectra resulting from excitation by a 291 nm laser with photomultiplier tube voltage at 600 V were monitored from 300 to 500 nm, and the slit width of the excitation and emission were kept at 5 nm during the measurements.

7.3 Methods

7.3.1 Synthesis of 1-methyl-4,4'-bipyridin-1-ium iodide (**1**)[110]

Methyl Iodide(5,44 g, 0.03 mol) was added to a solution of 4,4'-Bypiyridine (5 g, 0.03 mol) in DCM (65, ml) and the yellow reaction mixture was refluxed overnight. Then the mixture was cooled down to room temperature, resulting in the precipitation of a yellow solid. The solid was collected by filtration and washed with copious amounts of DCM. The product was obtained with 82 % yield after drying under reduced pressure.

^{1}H NMR (300 MHz, D_2O) δ_H= 8.92 (d, 2H, C*H*$_{Ar}N^+$), 8.68 (d, 2H, C*H*$_{Ar}$N), 8.30 (d, 2H, C*H*$_{Ar}$-CH$_{Ar}$-N$^+$), 7.87(d, 2H, C*H*$_{Ar}$-CH$_{Ar}$-N$^+$), 4.37 (s, 3H, -CH_3).

7.3.2 Synthesis of the poly (2-*n*-propyl-2-oxazoline) end capped with the 1-methyl-4,4'-bipyridinium group (poly-(nPropOx-viologen)

Under inert atmosphere (Glovebox), 2-*n*-propyl-2-oxazoline (4.11 ml, 24 mmol) was pipetted into a dry 10 ml microwave vial. Subsequently, MeOTs (72µl, 0.48 mmol), 1.69 ml of dry ACN and a stirring bar were added. The vial was capped, transferred out of the Glove box, and placed in a microwave reactor, where the mixture was heated for 15 min at 140 °C while stirred. After cooling down and transfer of the vial to the glove box, compound **1** was added as a terminator and the mixture was stirred for 5 days at 50 °C. After precipitation in diethyl ether, the polymer was dialyzed 3 times against deionized water with 3.kDa semi-permeable membrane tubing. The polymer was analysed by ^{1}H-NMR spectroscopy and by SEC.

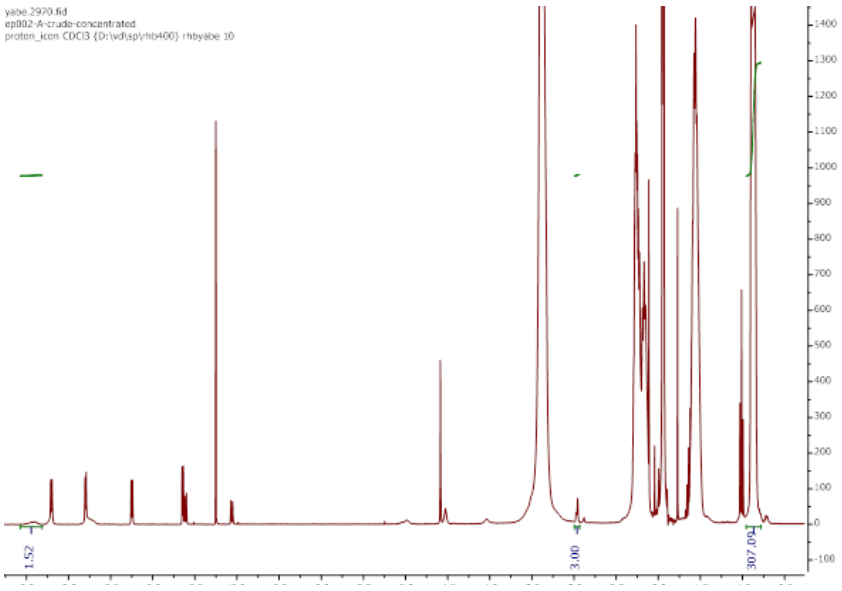

*Illustration 1: ^{1}H NMR of crude **4***

7.3.3 Synthesis of decamethoxy pillar[5]arenes (**9**)[111]

To a solution of 1,4-methoxybenzene (10 g, 10 mmol) in EDC (120 mL) was paraformaldehyde (2.16 g, 72.36 mmol) under a nitrogen atmosphere. Then, boron trifluoride diethyl etherate (8.88 mL, 72.36 mmol) was added to the solution and the green cloudy mixture was stirred at 30 °C for 3 h. The solution was poured into methanol and the precipitate was collected via filtration. The solid was dissolved in $CHCl_3$ and the insoluble part was filtered off. The $CHCl_3$ was removed in vacuo giving a yield of 23.2% (6g).

^{1}H NMR (300 MHz, Chloroform-d) δ_H= 6.80 (s, 10H,CH_{Ar}), 3.70 (s,10 H, CH_2), 3.66 (s, 30H, -CH_3).

ESI-LCMS: calculated for $C_{45}H_{54}NO_{10}^+$ $[M+NH_4]^+$, m/z, found 768,3742.

7.3.4 Synthesis of decahydroxypillar[5]arene (**10**)

To a solution of the methoxy substituted pillar[5]arenes (**10**) (2.00g, 2.67mmol) in DCM (150mL) was added boron tribromide(13.6 g, 54. 3 mmol). The mixture was stirred at 25 °C for 72 h. Then, water was added slowly into the cooled mixture. The resulting precipitate was collected and washed with 0.5M aqueous hydrochloric acid and chloroform to give 1.61g (2.64mmol) of the deprotected pillar[5]arenes (**10**).

^{1}H NMR (400 MHz, Acetone-d6) δ_h= 6.67 (s, 10H, CH_{Ar}), 3.75(s, 10 H, CH_2 3.58 (s, 10H, O*H*)

ESI-LCMS: calculated for $C_{35}H_{34}NO_{10}^+$ $[M+NH_4]^+$, m/z, found 628.2177

7.3.5 Synthesis of triethylene glycol monomethyl ether p-toluenesulfonate (**12**)[113]

Sodium hydroxide (10 g, 250 mmol) and triethylene glycol monomethyl ether (27.4 g, 177 mmol) were dissolved in THF (400 mL) and water (60 mL) under an argon atmosphere and cooled with an ice bath. A solution of p-toluenesulfonyl chloride (35 g, 184 mmol) in THF (60 mL) was slowly added and the resulting mixture was stirred for 3 hours at 0 ˚C. After stirring for another 2 hours at RT, the THF was removed by evaporation and the product was extracted three times with DCM. The combined organic layers were dried over anhydrous $MgSO_4$, filtered and concentrated. The product was obtained (**12**) as a colourless oils with 97 % yield.

^{1}H NMR (300 MHz, DCM-d_2) δ_H= 7.75 (d, J = 8.4 Hz, 2H, CH_{Ar}), 7.26 (d, J = 8.1 Hz, 2H, CH_{Ar}), 4.13 – 4.02 (m, 2H, CH_2), 3.66 – 3.38 (m, 6H, 3x CH_2), 3.49 (s, 4H, O-CH_2-CH_2-O), 3.27 (s, 3H, O-CH_3), 2.35 (s, 3H, , C_{Ar}-CH_3).

7.3.6 Synthesis of deca(2-(2-(2-methoxyethoxy)ethoxy)pillar[5]arenes (**7**) [115]

Per-Hydroxylated pillar[5]arene (**10**) (1.624 g, 2.644 mmol) was dissolved in DMF (66 mL). Sodium hydride (2.12 g, 52.9mmol) was added and the reaction mixture was stirred. triethylene glycol monomethyl ether *p*-toluenesulfonate (**12**) (18 g, 52.9 mmol) was added and the reaction mixture was heated at 80 °C for 48 h. The mixture was evaporated to dryness. The column chromatography was not conducted due to COVID-19.

7.3.7 Synthesis of 1,4-bis(2-(2-(2-methoxyethoxy)ethoxy)ethoxy)benzene (**14**)[116]

To a solution of 1,4 hydroquinone (0.43 g, 3.90 mmol) in ethanol (20 ml), was added potassium tert-butoxide (1.1 g, 9.80 mmol) and triethylene glycol monomethyl ether *p*-toluenesulfonate 3.07 g, 9.64 mmol) at room temperature. The reaction mixture was heated at reflux, under an atmosphere of nitrogen, for 48 h, and then diluted with water (20 mL). The aqueous layer was extracted with CH_2Cl_2 (35 mL), and the organic layer was washed with sodium hydroxide (2.5 M, 20 mL) and dried over sodium sulphate. The solvent was removed under vacuum to give the crude product which was purified using flash chromatography (Et2O-MeOH, 19:1) to give the product as a bright yellow oil (17% yield).

^{1}H NMR (400 MHz, Chloroform-d) δ_H 6.74 (s, 4H, CH_{Ar}), 4.07(t, 3H, OCH_2), 3.82 (t, J = 4.97 Hz, 4H, OCH_2), 3.72-3.74 (m, 4H, OCH_2)$_3$, 3.64 – 3.54 (m, 8H,OCH_2), 3.58(t, 4H, , OCH_2),3.38 (m, 6H,OCH_3))

7.3.8 Attempt at the synthesis of pillar[5]arenes (**7**) from the 1,4-bis(2-(2-(2-methoxyethoxy)ethoxy)ethoxy)benzene (**14**)[111]

To a solution of 1,4-bis(2-(2-(2-methoxyethoxy)ethoxy)ethoxy)benzene (10 g, 1.93mmol) in EDC (120 mL) was added paraformaldehyde (0.31 g, 1.93 mmol) under nitrogen atmosphere. Then, boron trifluoride diethyl etherate (0.173 mL, 1.93 mmol) was added to the solution and the mixture was stirred at 30 °C for 3 h. The solution was poured into methanol and the resulting precipitate was collected by filtration. The solid was dissolved in CHCl3 and the

insoluble part was filtered off. The LC-MS analysis of the mixture showed that the reaction failed to give the pillar[5]arene structure.

7.3.9 Synthesis of 1-(2-aminoethyl-)-1'-methyl-[4,4'-bipyridine]-1,1'-diium dibromide iodide (**15**)[117]

A mixture of *N*-methyl-4,4'-bipyridin-1-ium iodide (**1**) (0.5 , 1.6mmol) and 2-bromoethylamine hydrobromide (3.4g, 16mmol) was refluxed at 80 °C for 72h THF. After cooling, the product precipitated out as an orange solid and was filtered and washed with THF. Drying afforded the compound **15** with a yield of 62 %.

^{1}H NMR (300 MHz, D_2O) δ_H 9.48 – 9.40 (m, 2H, C*H*$_{Ar}N^+$), 9.28 (d, J = 6.5 Hz, 2H, C*H*$_{Ar}$N), 8.90 – 8.82 (m, 2H, C*H*$_{Ar}N^+$), 8.75 (d, J = 6.4 Hz, 2H, C*H*$_{Ar}$N), 5.33 (t, J = 6.6 Hz, 2H, N^+C*H*$_2$-CH_2), 4.72 (s, 3H, C*H*$_3N^+$).

7.3.10Synthesis of the 1-methyl-1'-(4-vinylbenzyl)-4,4'-bipyridinium salt (**17**)[118]

To a solution of *N*-methyl-4,4'-bipyridin-1-ium iodide (**1**) (328mg, 1.10mmol) in acetonitrile (10 mL) was added 4-chloromethylstyrene (265 mg, 1.73 mmol) added at room temperature under nitrogen atmosphere. Then, the mixture was stirred at 60°C for 24 h. After cooling, the precipitate was collected by filtration. The product was obtained a red powder with a 55 % yield.

^{1}H NMR (300 MHz, Methanol-d4) δ_H= 9.39 – 9.27 (m, 2H, C*H*$_{Ar}N^+$),), 9.24 – 9.15 (m, 2H, C*H*$_{Ar}N^+$), 8.67 (dd, J = 10.5, 6.5 Hz, 4H, C*H*$_{Ar}$), 7.57 (s, 4H), 6.78 (dd, J = 17.6, 11.0 Hz, 1H, C_{Ar}-C*H*=CH_2), 5.96 (s, 2H, C_{Ar}-C*H*$_2$- C_{Ar}), 5.87 (dd, J = 17.7, 0.9 Hz, 1H, C*H*$_2$=CH), 5.33 (dd, J = 11.0, 0.9 Hz, 1H,C*H*$_2$=CH), 4.53 (s, 3H, C*H*$_3N^+$).

7.4 Measurements

7.4.1 Measuring the binding constant in water by fluorescence spectroscopy[57]

To determine the association constant (K_a), steady-state fluorescence spectra were recorded at varying guest concentrations (C_{guest}). Changes in the ratios (I/I0) of the fluorescence intensities at 333 nm upon addition of guest were calculated and plotted. The K_a value was determined to be 3.94 ± 63 x 10^4 M^{-1} for the **[4-6]** complex by fitting data with Eq. 1, where α

is a constant (see section 3.1.3.1). The measurement was done at 10°C, with an excitation at 291 nm, and the emission was recorded in the range of 300-500nm.

7.4.2 Measuring the Job plot by fluorescence spectroscopy

The fluorescence emission of multiple equimolar solutions (6 x 10^{-5} M) containing different molar ratios of host and guest in water were measured. The measurement were done at 10°C, with an excited at 291 nm, and the emission was recorded in a range of 300-500nm.

7.4.3 Measuring the Job plot by UV-vis spectroscopy

The UV-vis emission of multiple equimolar solutions (6 x 10^{-5} M) containing different molar ratios of host and guest in water were measured. The measurement were done at 10°C, with a scanning rate = 200 nm/min, and the emission was recorded in a range between 200- 800 nm.

7.4.4 Turbidimetry

Two solutions were prepared in C-156 vails and measured; a solution 1 containing 5 mg of viologen-poly (2-*n*-propyl-2-oxazoline) **4** in 1 mL of water, and a solution 2 containing 5 mg of **4** + 1 eq of the pillar[5]arenes **6** in 1 mL water.

8 Scientific article

Temperature controlled uptake and release of water soluble pillar[5]arene

Emiel Pattyn[a], Yann Berhard [a], Debaditya Bera[a], Lieselot De Smet[a,b], Patrice Woisel*[b] and Richard Hoogenboom*[a]

[a] Supramolecular Chemistry Group, Centre of Macromolecular Chemistry (CMaC), Department of Organic and Macromolecular Chemistry, Ghent University, Krijgslaan 281-S4, 9000 Ghent, Belgium
[b] Unité des Matériaux et Transformations (UMET), UMR CNRS 8207ENSCL, Equipe Ingénierie des Systèmes Polymères (ISP) 59655 Villeneuve d'Ascq Cedex (France)
Richard.Hoogenboom@ugent.be

KEYWORDS: Host-guest chemistry, polyoxazolines, pillar[5]arenes, thermo-responsive polymers, molecular communication

The temperature controlled release and uptake of water soluble pillar[5]arenes was obtained by creating a supramolecular system which combines a thermo-responsive poly(*n*PropOx) end-capped with a viologen unit as a guest, and a percarboxylated pillar[5]arenes as a host. As the system exhibits LCST behavior, at temperature higher than its cloud point temperature, the collapse of the polymer leads to the dissociation of the host-guest complex and the release of the pillar[5]arenes in the aqueous environment. This LCST-induced threading-dethreading is completely reversible, and the free pillar[5]arenes is reforming the complex upon cooling the system below the Cp, as the polymer is back into solution. The system represents a first step towards the creation of temperature controlled molecular communication in aqueous environment, which could serve as a basis towards the creation of molecular communication between more complex polymeric/hydrogels systems.

Introduction

The translation of molecular communication, i.e. the use of a chemical signal as an information carrier, from biological systems, where chemical signals are for example used for intra- and inter-cellular communication,(1) to synthetic systems has been a long-standing challenge. The systems are expected to be deployable in many applications. Molecular computing, which is an alternative route to create computing devices using a bottom-up approach,(2) is a prime example of it. By allowing the interaction of different chemical systems with each other, which could lead to chemistry that will become alive, adaptive(3) and autonomous(4) due to smart interactions and communications within molecular networks.(4) It is also expected to be useful in drug delivery and smart materials. Even on the macroscopic level, the use of chemical signals is exploited to overcome the limitations that electrical and

electromagnetic signals have(5). Despite its large potential, the practical demonstrations of molecular communication has been limited. However, numerous synthetic involving a single or multiple molecular communication process have been reported, although their performances lags far behind that what biological systems can achieve.

The most complex communicating systems achieved so far are still far from mimicking the highly advanced systems found in nature. But it illustrates in an impressive manner the possibility to connect stand-alone chemical entities through molecular communication.(6) A promising strategy to do so is the use of supramolecular systems, and especially host-guest systems, in which a host or a guest can act as the communication carrier. Thus, in the pursuit of creating molecular communication between supramolecular assemblies in aqueous media. the macrocyclic artificial hosts cyclodextrins,(7) cucurbiturils(8) and cyclophanes(9) have emerged as relevant building blocks. However, the amount of reports remains very limited and the specific example of the use of the macrocyclic artificial host, pillar[n]arenes, as the information carrier has not been reported so far.

In this work, we report the temperature controlled uptake and release of the water-soluble pillar[5]arenes (**1**) in an aqueous environment through the use of the thermo-responsive poly(2-*n*-propyl-2-oxazoline) (P*n*PropOx) with a viologen end group (**2**) as a guest. The polymer was prepared by cationic ring opening polymerization (CROP) of *n*PrOx, which easily allowed for the introduction of the end-group by termination of the polymerization with 1-methyl-4,4'-bipyridinium iodide. This polymer is associated with a percarboxylated water-soluble pillar[5]arene, resulting in a responsive system that combines temperature-sensitive polymer and supramolecular host-guest chemistry.

Among the stimuli foundin smart polymeric systems, such as pH,(10) mechanical force, biomolecules,(11) electric or magnetic fields,(12) photo,(13) inflammation,(14) and ultra sounds(15), temperature is one of the most attractive since thermal changes can be applied externally in a non-invasive manner.(16) Thermo-responsive polymers in aqueous solution exhibit a unique sol-gel transition property at a certain temperature. Polymers which are soluble at low temperature and phase separate at elevated temperatures display Lower Critical Solution Temperature (LCST) behavior. Conversely, polymers that are soluble at high temperature and phase separate at low temperatures show Upper Critical Solution (UCST) behavior. The special case where polymers exhibit LCST as well as UCST in a closed loop coexistence can also be founded for some examples.

Poly(*n*-propyloxazoline) (P*n*PrOx) exhibits LCST behavior with a cloud point temperature (Tcp) around room temperature. This was exploited in our system to induce the release of the

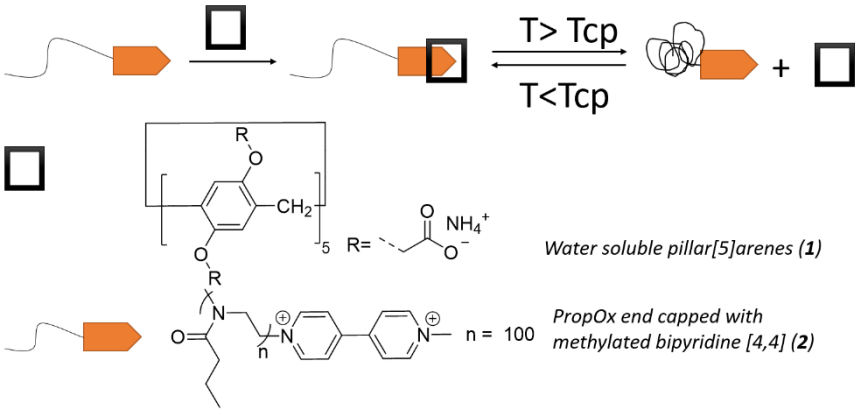

host **(1)** in the aqueous solution without changing its chemical structure but simply by elevating the temperature (T< Tcp). Upon cooling (T<Tcp), the polymer re-dissolves, making the viologen guest unit available again for the released pillar[5]arenes. The host-guest complex is then reformed, which result in the uptake of the released host (Figure 1).
Figure 1. The temperature controlled uptake and release of the water-soluble pillar[5]arene **1**, based on a supramolecular system containing the thermo-responsive viologen end-capped P*n*PropOx guest molecule

The reported system serves as a stepping-stone towards the creation of temperature controlled molecular communication in a supramolecular system containing multiple host and/or guests. It could potentially be expanded towards hydrogels, which could lead to the creation of molecular communication between hydrogels.

Experimental

The chemicals used in this study have been purchased from various suppliers (TCI, Sigma Aldrich, Acros organic) and used as received, without any extra purification.
De-ionized water was prepared with a resistivity less than 18.2 MΩ x cm using an Arium 611 from Sartorius with the Sartopore 2 150 (0.45 + 0.2 µm poresize) cartridge filter.
The **glovebox system** used is a VIGOR Sci-Lab SG 1200/750 system with water and oxygen purity levels below 1 ppm, both for water and oxygen content. .
The **polymerizations** were performed in capped vials in a single mode microwave Biotage initiator with robot sixty and IR temperature sensor (Biotage, Uppsala, Sweden)
Nuclear magnetic resonance (NMR) spectra were recorded on a Bruker Avance 300 MHz, 400 MHz and 500 MHz spectrometer operating at room temperature (500 MHz for variable temperature measurements). All given chemical shifts, δ, are given relative to the solvent peak of CDCl3 (7.26 ppm), D2O (4.79 ppm), DMSO-*d6* (2.50 ppm), $(CD_3)_2CO$ (2.05 ppm.
Size-exclusion chromatography (SEC) was performed on an Agilent 1260-series HPLC system equipped with a 1260 online degasser, a 1260 ISO-pump, a 1260 automatic liquid sampler (ALS), a thermostatted column compartment (TCC) at 50°C equipped with two PLgel 5 µm mixed-D columns and a precolumn in series, a 1260 diode array detector (DAD) a 1260 refractive index detector (RID) and a multi-angle light scattering detector (Wyatt Dawn Hellos II or miniDawn Treos II) (MALS). The used eluent was DMA containing 50mM of LiCl at a flow rate of 0.500 ml/min. The spectra were analysed using the Agilent Chemstation software with the GPC add on. Molar mass values and Đ values were calculated against PMMA standards from PSS or using d_p/d_c value of polymer (d_p/d_c poly(nProPox) = 0.047) in case of LS detection.
Turbidimetry measurements were performed on a Crystal 16^{TM} parallel crystallizer turbidimeter from Avantium Technologies. Samples with a concentration of 5 mg per mL in deionized water were analysed in a temperature range from 5°C to 40°C at a heating rate of 1°C/min. Cloud point temperatures were determined at 50% transmission during the second heating run.
Freeze drying was performed on a Martin Christ Alpha 2-4 LDPlus with an ice condenser capacity of 4 kg and temperature of -85°C and 4 kg/24 h performance.
UV-VIS spectra were recorded on a Varian Cary 100 Bio UV-VIS spectrophotometer equipped with a Cary temperature and stir control. Samples were measured in quartz cuvettes with a pathlength of 1.0 cm in the wavelength range of 300 to 800 nm.
Fluorescence The fluorescence measurements were carried out on a Cary Eclipse fluorescence spectrophotometer (under stirring) equipped with a Varian Cary Temperature Controller. The emission spectra resulting from excitation by a 291 nm laser with photomultiplier tube voltage

at 600 V were monitored from 300 to 500 nm, and the slit width of the excitation and emission were kept at 5 nm during the measurements.

Synthesis of 1-methyl-4,4'-bipyridin-1-ium iodide (17) Methyl Iodide(5,44 g, 0.03 mol) was added to a solution of 4,4'-Bypiyridine (5 g, 0.03mol) in DCM (65, ml) and the yellow reaction mixture was refluxed overnight. Then the mixture was cooled down to room temperature, resulting in the precipitation of a yellow solid. The solid was collected by filtration and washed with copious amounts of DCM. The product was obtained with 82 % yield after drying under reduced pressure. ^{1}H NMR (300 MHz, D_2O) δ_H= 8.92 (d, 2H, C$H_{Ar}N^+$), 8.68 (d, 2H, CH_{Ar}N), 8.30 (d, 2H, CH_{Ar}-CH_{Ar}-N^+), 7.87(d, 2H, CH_{Ar}-CH_{Ar}-N^+), 4.37 (s, 3H, -CH_3).

Synthesis of the poly (2-n-propyl-2-oxazoline) end capped with the 1-methyl-4,4'-bipyridinium group (poly-(nPropOx-viologen) (2) Under inert atmosphere (Glovebox), 2-n-Propyl-2-oxazoline (4.11 ml, 24 mmol) was pipetted into a dry 10 ml microwave vial. Subsequently, MeOTs (72µl, 0.48 mmol), 1.69 ml of dry ACN and a stirring bar were added. The vial was capped, transferred out the Glove box, and placed in a microwave reactor, where the mixture was heated for 15 min at 140 °C while stirred. After cooling down and transfer of the vail to the glove box, compound **1** was added as a terminator and the mixture was stirred for 5 days at 50 °C. After precipitation in diethyl ether, the polymer was dialyzed 3 times against eionized water with 3.kDa semi-permeable membrane tubing. The polymer was analysed by ^{1}H-NMR and by SEC.

The water soluble pillar[5]arenes **(1)** was a available in the lab, due to a collaboration with the group of T. Ogoshi. So there was no need in synthesizing this.

Measuring the binding constant in water by fluorescence spectroscopy(18)To determine To determine the association constant (K_a), steady-state fluorescence spectra were recorded at varying guest concentrations (C_{guest}). Changes in the ratios (I/I0) of the fluorescence intensities at 333 nm upon addition of guest were calculated and plotted. The K_a value was determined to be 3.94 ± 63 x 10^4 M^{-1} for the **[1-2]** complex by fitting data with Eq. 1, where α is a constant (see section 3.1.3.1). The measurement was done at 10°C, with an excitation at 291 nm, and the emission was recorded in the range of 300-500nm.

Measuring the job plot by fluorescence

The fluorescence emission of multiple equimolar solutions (6 x 10^{-5} M) containing different molar ratios of host and guest in water were measured. The measurement were done at 10°C, with an excited at 291 nm, and the emission was recorded in a range of 300-500nm.

Measuring the job plot by UV-vis

The UV-vis emission of multiple equimolar solutions (6 x 10^{-5} M) containing different molar ratios of host and guest in water were measured. The measurement were done at 10°C, with a scanning rate = 200 nm/min, and the emission was recorded in a range between 200- 800nm.

Turbidimetry

Two solutions were prepared in C-156 vails and measured; a solution 1 containing 5mg of viologen-poly (2-n-propyl-2-oxazoline) **2** in 1 mL of water, and a solution 2 containing 5mg of **2** + 1 eq of the pillar[5]arenes **1** in 1mL water.

Results and Discussion

a. Synthesis of the system

The practical work started with the methylation of the commercially available 4,4′-bipyridine, using methyl iodide as the methylation agent. The reaction, resulted in the single methylated product **3**, which precipitate in the reaction mixture, thus lowering the probability to obtain the

double methylated product. The product was isolated with a yield of 82 % and the structure was confirmed by ^{1}H NMR.

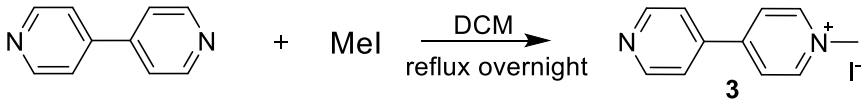

Figure 2. Synthesis of **3**

In a second step, **3** was then used as the terminator during the CROP of the 2-propyl-2-oxazoline (PropOx), resulting in the polymer end-capped with a viologen group ([4,4']-bisalkylated bipyridinium group). The PropOx monomer was heated at high temperature (140 °C) under microwaves irradiation in the presence of 0.01 equivalent of methyl tosylate (MeOTs) as initiator, aiming for a degree of polymerization (DP) of 100. After the polymerization, an excess of the terminator **3** was added to the mixture containing the living chains, to lead to the end-capped polymer **2** after a long reaction time (3 days).

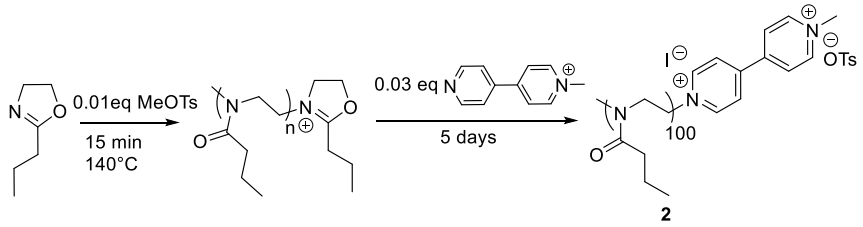

Figure 3. The synthesis of **2**

After precipitation in diethyl ether(once), the polymer was dialyzed 3 times against ionized water with 3.kDa semi-permeable membrane tubing. The polymer was then analyzed by ^{1}H NMR spectroscopy, by SEC-LS (LS= Light Scattering detector) and by MALDI-TOF mass spectrometry, and the determination of the number average molar mass (Mn) and polydispersity (*Đ)* was done. These three techniques yielded different values and ultimately were the values from SEC-LS used for the calculation in the following parts the project. The calculation of the end group fidelity was based on the ^{1}H NMR data and is equal to 69%.

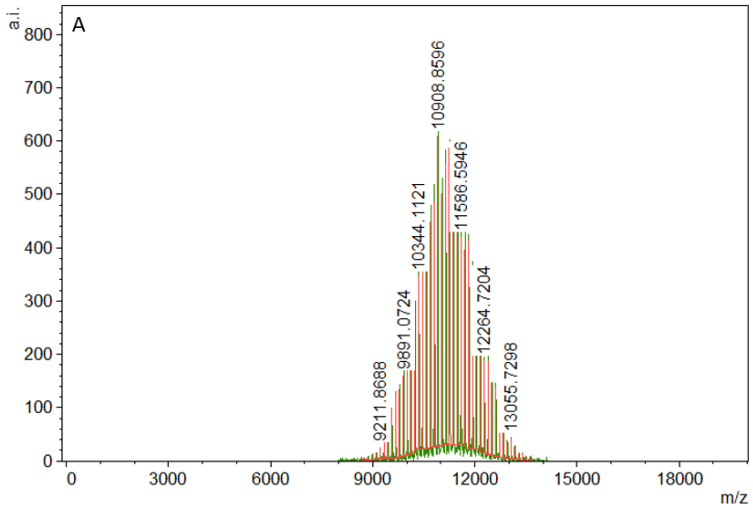

B	Mn	n	*Đ*
MALDI-TOF	≈ 11.1 kDa	106	1.005
^{1}H-NMR	11.9 kDa	102	/
SEC-LS	12.4 kDa	119	1.061

Figure 4. A) MALDI-TOF of **2** B) Mn, Đ and n based on SEC-LS, MALDI-TOF and ^{1}H-NMR measurements

The water-soluble pillar[n]arene was synthesized as described in literature and was provided by the lab of Prof. Ogoshi.(18)

b. <u>Properties of the system</u>

The properties and thermal behavior of the host-guest **(1)-(2)** complex and the overall system were explored. It includes the determination of the binding constant and the binding equivalence, the analysis of the complex, the LCST behavior, response to temperature and reversibility.

Association constant of the **(1)-(2)** complex in water

The procedure used for the determination of the K_a by fluorimetry is based on a report by group of T. Ogoshi, who determined the K_a for the similar paraquat-**(1)** complex.(18) It request the recording of steady-state fluorescence spectra at varying concentrations of **2** (C_{guest}) and the calculation and plotting of the changing ratio of the fluorescence intensities ($\frac{I}{I_0}$) at 333 nm as a consequence of that variation (Figure 5). The fluorescence signal is decreasing upon complexation with **1** because the fluorescence active viologen goes inside the cavity of the slightly fluorescence active **1**. Upon fitting of the data by Eq. 1 (where α is a constant), it was possible to determine that the K_a $3.9 \pm 0.6 \times 10^4$ M^{-1}. However the fit is not perfect, which could be due to the model not being right. The K_a value lays very much in line with the K_a of the [paraquat-**6**] complex, which is equal to $8.2 \pm 1.7 \times 10^4$ M^{-1},[57] meaning that the polymer structure has no influence on the association constant.

$$\frac{I}{I_0} = \frac{(1 + \alpha K_a C_{guest})}{(1 + K_a C_{guest})} \quad \text{(Eq. 1)}$$

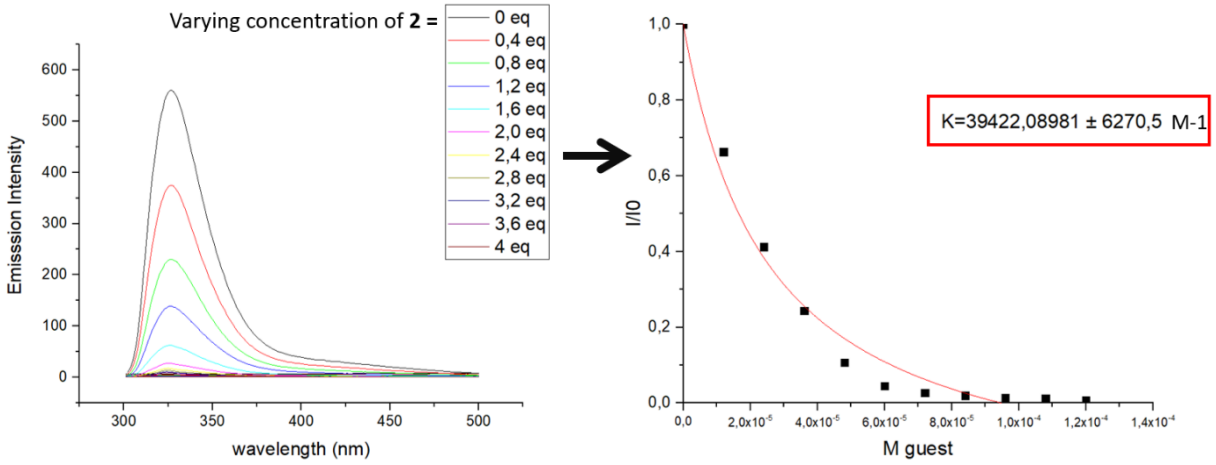

Figure 5. Determination of the binding constant of the **(1)-(2)** complex

Characterization of the **1-2** complex by ^{1}H NMR

The complexation between **1** and **2** was monitored by measuring ^{1}H NMR spectra of equimolar solutions containing different ratio of **1** and **2** in D_2O. The resulting spectra are stacked together with the spectra of pure **1** and **2** in figure 6, and the following was observed: The aromatic proton signals of **1** (A) are broadened and shifted in the presence of **2**, indicating that a new chemical environment is created, resulting from the complexation between **1** and **2**. A signal at 7.7 ppm (the red frame), which correspond to the aromatic protons B and C inside the cavity of **1**, is appearing upon the addition of **2**. However, there are always signals related to free **2** (B and C) present, even with a high excess of **1**, indicating that not all of **2** is forming a complex with **1**. The sharp doublets are coming from the TsO^- counter ion.

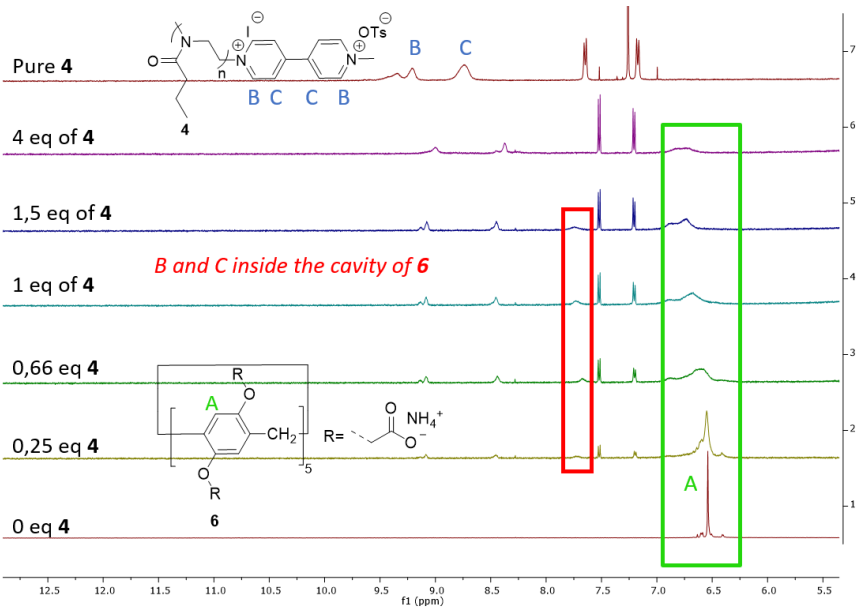

Figure 6. Stacked ^{1}H NMR spectra of the **1**-**2** complex and **1**

Job plot

The method of the Job plot was used to determine the binding stoichiometry of the **[1-2]** complex. Equimolar solutions containing different molar ratios of **2** and **1** in water were prepared and the UV absorbance signal at 330 nm, which is proportional to the concentration of free **1**, was measured. It is important to mention that the polymer solution was prepared using the molar mass obtained by SEC-LS, and by taking in consideration the end-group fidelity, to obtain a precise molarity of the host. The response was then plotted against the mole fraction of **2**, resulting in the Job plot A depicted in Figure 7. The maximum of the curve lays at a mole fraction of **2** = 0.2 indicating that the stoichiometry of the **[1-2]** complex should be equal to 4:1. However this result seems pretty unlikely, since the binding stoichiometry of the very similar paraquat-**1** complex is equal to 1:1.(18) A second measurement was then made to obtain the Job plot, this time using fluorescence spectroscopy instead of UV spectroscopy as the detection mode. The Job plot derived from fluorescence spectroscopy is depicted on the figure 7.B. However, it results in the same conclusion. A possible explanation for this unexpected data could be the fact that some polymer chains of **2** are coiled up in water (although the measurements were performed below the cloud point, at 10°C), shielding of the methylated bipyridine [4,4] guest molecule and resulting in a misleading Job plot. A considered solution to avoid this problem was to redo the experiment in an organic solvent. This was not possible because **1** was found to be insoluble in organic solvents. Alternatively, another organo-soluble pillar[5]arene could be used, but this experiment was not possible due to limited time before the COVID-19 crisis. The measurements with the pegylated pillar[5]arene **7**, which may be soluble in some organic solvents, could also give extra information

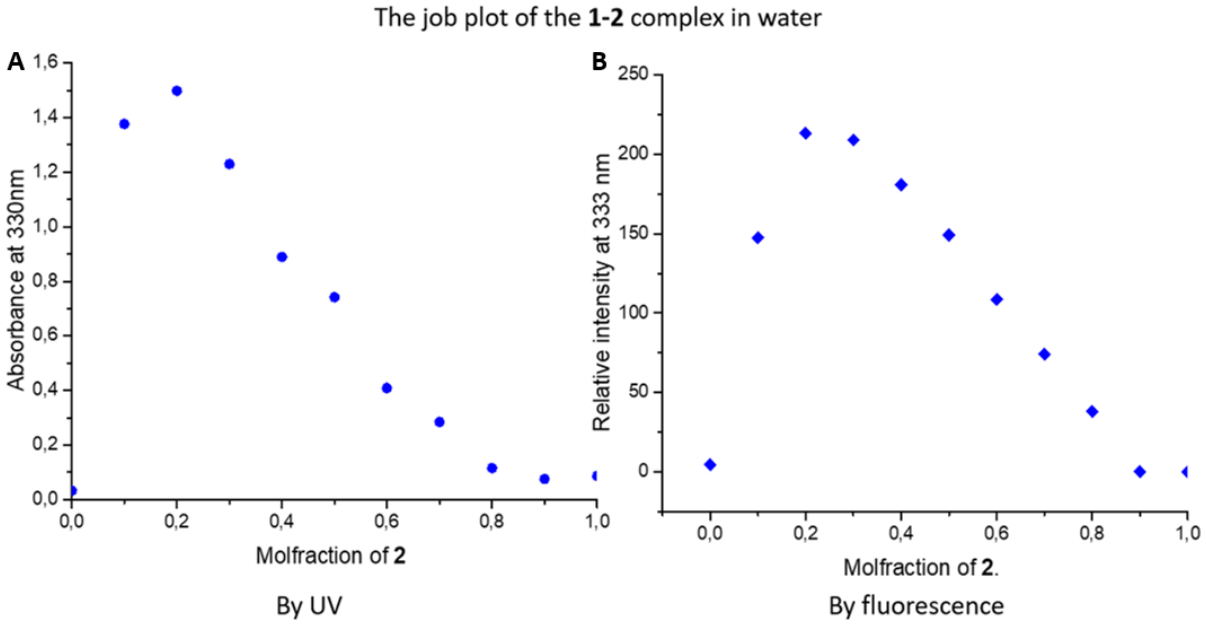

Figure 7. A) Job plot of the **[1-2]** complex in H_2O A) by UV B) by fluorescence

LCST property of the **(1)-(2)**

The elucidation of the cloud point of a pure solution of **2** on the one hand a 1 to 1 mixture of **2** and **1** on the other hand, was done by turbidimetry to determine if the complexation has an influence on the cloud point of **2**. The results, which are given in figure 8, show that the cloud point of **2** is slightly lowered when the show that the cloud point of **2**, initially measured at 23.5 °C, is lowered to 20.1 °C by the complexation with **1**. This is unexpected since **1** is very hydrophilic, meaning that the T_{cp} should increase. A possible explanation for this could be that the ionic interactions release the counterions, making the final complex less hydrophilic than the **2**.

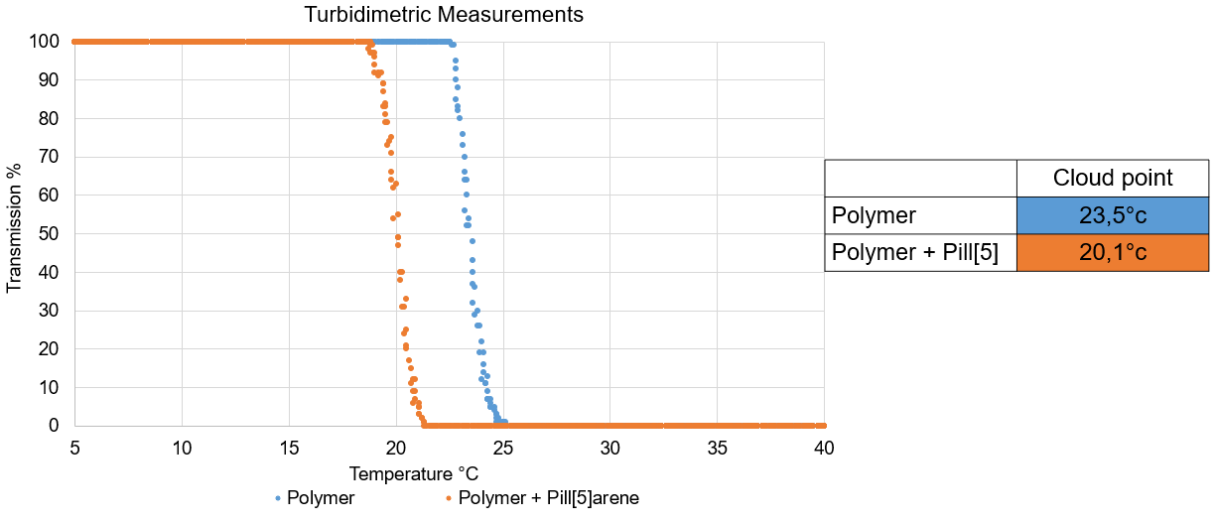

Figure 8. Turbidimetry measurement of **2** and a **1** to **1** mixture of **1** and **2**

^{1}H-NMR and DOSY monitoring of the release of **1** from the **[1-2]** complex The decomposition of the **[1-2]** complex due to the precipitation of **2** at elevated temperatures was explored and followed by recording ^{1}H NMR spectra of a 1:1 mixture of **2** and **1** in D_2O at different temperatures. The resulting spectra are on illustrated in figure 9. The signals related to the Poly (*n*PropOx) moiety are very broad at 35°C, indicating that **2** is no longer in solution.

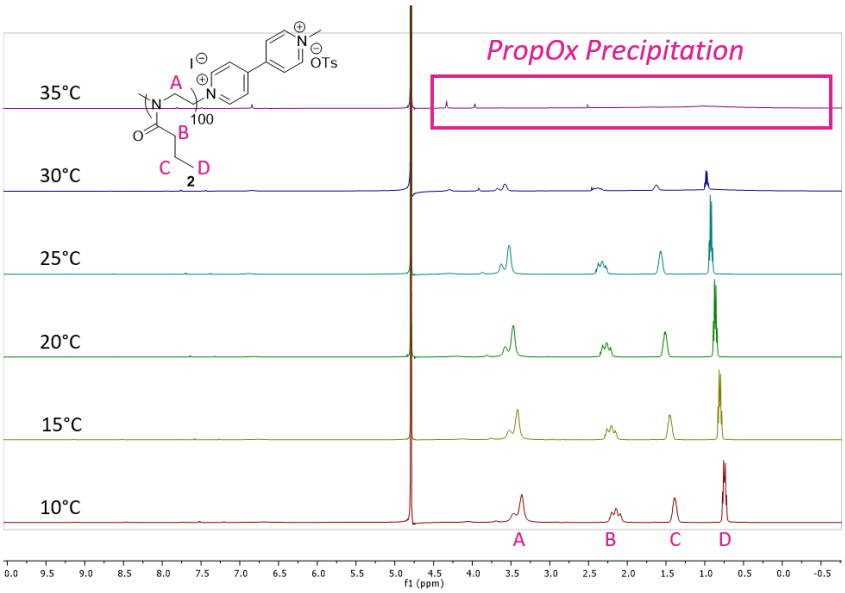

Figure 9. ^{1}H NMR of the **1-2** complex in D_2O at different temperatures

The release in solution of the host **1**, as a consequence of precipitation of the guest, is clearly visible in the zoomed in image of the ^{1}H-NMR spectra depicted below. The characteristic sharp proton signals of free **1** are absent in the ^{1}H NMR spectra at 10 °C (only the broad signals of **1** in the complex), but appear as the temperature is increasing, and are well visible in the ^{1}H NMR spectra at 35 °C, proving that the precipitation of **2** results in a dissociation of the complex and the release of **1** in solution. The quantification of this release was calculated by integrating these signals and comparing them with the integrated signals of the tosylate counter anion as an internal standard. It revealed that close to 100 % of **1** was released at 35 °C.

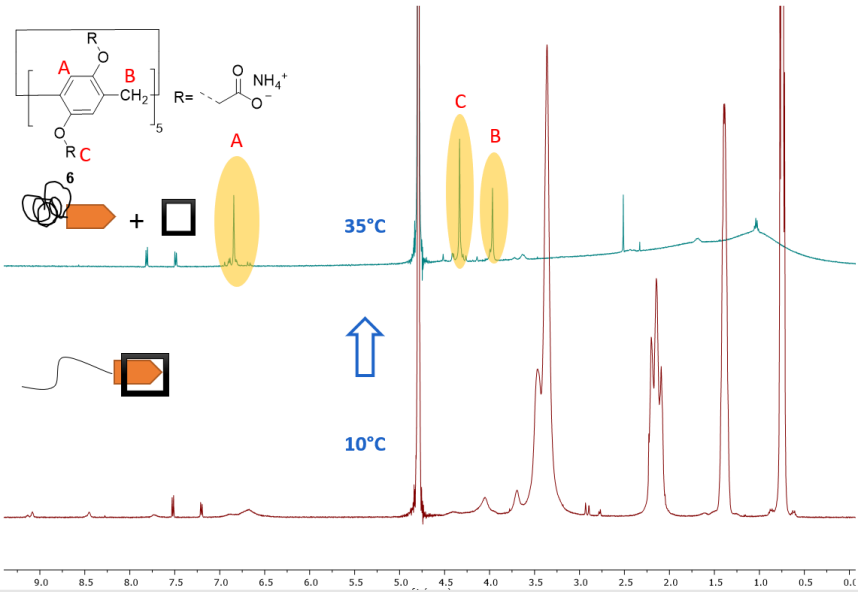

Figure 10. Zoomed in ^{1}H NMR of the **4-6** complex in D_2O at 10 °C and 35 °C

The collapse of the **[1-2]** complex at elevated temperature was also demonstrated via DOSY, which can be used to investigate the association and complexation behaviour of the **[1-2]** complex by measuring the diffusion coefficients via Brownian motion. The spectra of a 1:1 mixture of **1** and **2** in D_2O at 10 °C and 60 °C were recorded and resulted in the spectra depicted in Figure 39. At 10 °C are two lines visible. The line in the blue frame is related to free **2** and the line in the green frame comes from the **[1-2]** complex. At 60 °C, both lines are absent, indicating that **2** is no longer in solution. Two new lines are visible and one of them is related to free **1** (the yellow frame). The other is due to a combination of the fact that, together with the TsO^- counter ion, there is too much zooming in (red frame).

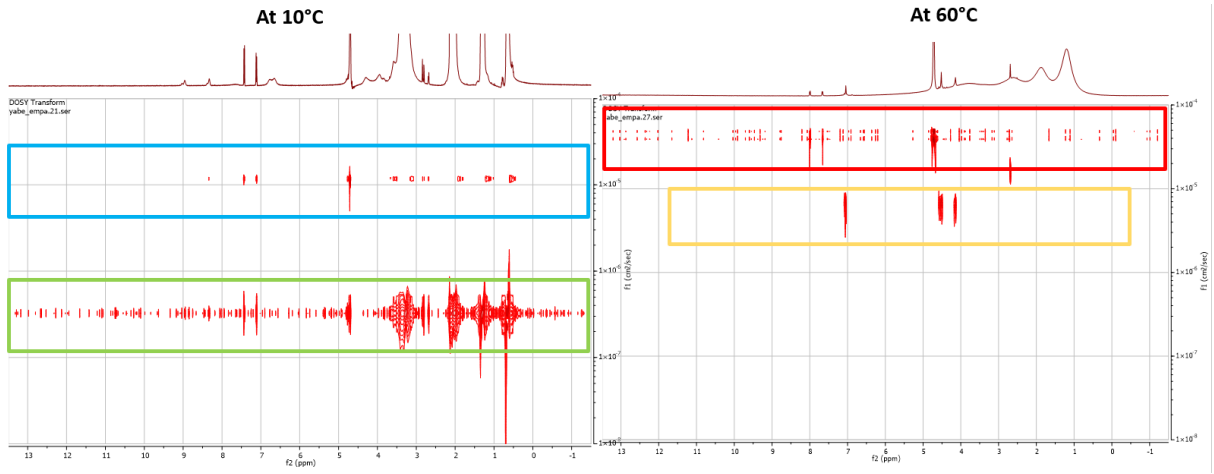

Figure 11. DOSY-NMR of the **[1-2]** complex in D_2O at 10 °C and 60 °C

<u>Reversibility of the threading-dethreading process</u>

The last experiment conducted was done to visualize the reversibility of the release of **2** from the **[1-2]** complex and the cyclability of the process was assessed by recording the ^1H NMR spectra of a 1:1 mixture of **2** and **1** in D_2O at multiple cooling and heating cycles. The results are stacked on Figure 12, and showed that the aromatic proton peaks of **1** alternate from broad at low temperature to sharped at high temperature due to the cyclic complexation-decomplexation process (highlighted in yellow)

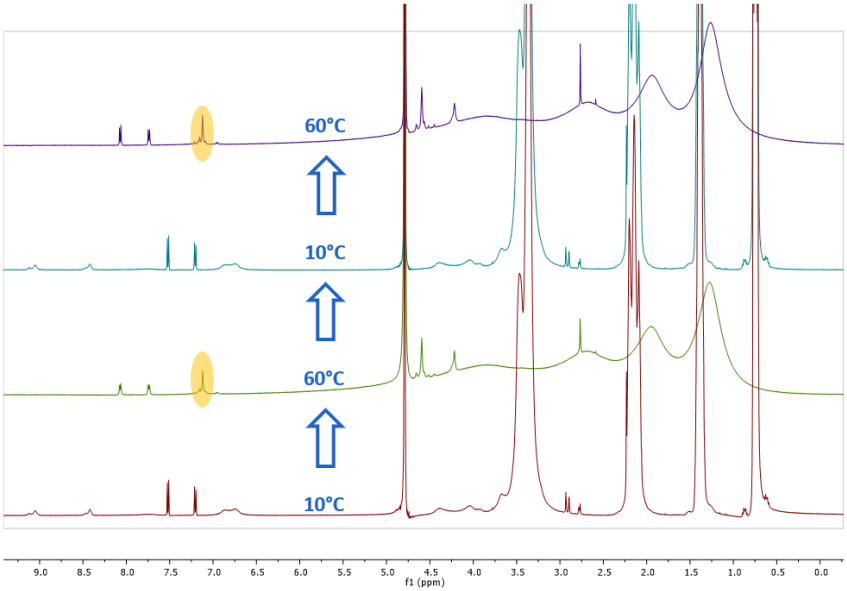

Figure 12. ^1H NMR of multiple heating and cooling cycles of the **1-2** complex

Summary

The aim of this study was to design a temperature controlled supramolecular system that can control the uptake and release of a water-soluble pillar[5]arenes. The system is based on the thermo-responsive polymer P***N***PropOx, which was end-capped with a viologen unit. The later serves as a guest for the water soluble pillar[5] host molecule and enables the connection between stimuli-responsive polymers and supramolecular host-guest chemistry. The binding constant of this host-guest complex was successfully determined via fluorescence spectroscopy, and its binding stoichiometry via the Job plot's method. The latter was not 1:1 as expected, and future work with further experiments, using an alternative pillar[5]arene host or another polymeric guest should give more insight. The complexation-decomplexation process at different temperature, as a result of the PropOx collapse, was monitored by ^{1}H-temperature NMR experiments, and the data revealed its occurrence, and in a reversible manner as confirmed via the recording spectra at multiple heating and cooling cycles. The system represents a first step towards the creation of temperature controlled molecular communication in aqueous environment and could potentially be expand to supramolecular systems containing multiple host and/or guests, towards the creation of molecular communication between polymers/hydrogels.

Acknowledgments

EP would like to thank his promotor prof. dr. Richard Hoogenboom for the opportunity to work on this project in the Supramolecular Chemistry Group at the university of Ghent. EP would also like to thank Dr. Yann Bernhard for his guidance throughout this project.

References

1. BURNSTOCK G. Recent Concepts of Chemical Communication between Excitable Cells. In: Dale's Principle and Communication Between Neurones. Elsevier; 1983. p. 7–35.
2. Varghese S, Elemans JAAW, Rowan AE, Nolte RJM. Molecular computing: paths to chemical Turing machines. Chem Sci. 2015;6(11):6050–8.
3. Lehn J-M. Perspectives in Chemistry-Steps towards Complex Matter. Angew Chemie Int Ed [Internet]. 2013 Mar 4 [cited 2020 May 14];52(10):2836–50. Available from: http://doi.wiley.com/10.1002/anie.201208397
4. Merindol R, Walther A. Materials learning from life: Concepts for active, adaptive and autonomous molecular systems. Vol. 46, Chemical Society Reviews. Royal Society of Chemistry; 2017. p. 5588–619.
5. Farsad N, Guo W, Eckford AW. Tabletop molecular communication: Text messages through chemical signals. PLoS One. 2013;8(12).
6. Biswas PK, Saha S, Gaikwad S, Schmittel M. Reversible Multicomponent AND Gate Triggered by Stoichiometric Chemical Pulses Commands the Self-Assembly and Actuation of Catalytic Machinery. J Am Chem Soc. 2020;(I).
7. Fedorov Y V., Tkachenko S V., Chernikova EY, Godovikov IA, Fedorova OA, Isaacs L. Photoinduced guest transformation promotes translocation of guest from hydroxypropyl-β-cyclodextrin to cucurbit[7]uril. Chem Commun. 2015;51(7):1349–52.
8. Remón P, González D, Romero MA, Basílio N, Pischel U. Chemical signal cascading in a supramolecular network. Chem Commun [Internet]. 2020; Available from: http://xlink.rsc.org/?DOI=D0CC00217H
9. De La Rosa VR, Nau WM, Hoogenboom R. Tuning temperature responsive poly(2-

alkyl-2-oxazoline)s by supramolecular host-guest interactions. Org Biomol Chem. 2015 Mar 14;13(10):3048–57.
10. Kocak G, Tuncer C, Bütün V. PH-Responsive polymers. Vol. 8, Polymer Chemistry. Royal Society of Chemistry; 2017. p. 144–76.
11. Colson YL, Grinstaff MW. Biologically responsive polymeric nanoparticles for drug delivery. Adv Mater. 2012 Jul 24;24(28):3878–86.
12. Manouras T, Vamvakaki M. Field responsive materials: Photo-, electro-, magnetic- and ultrasound-sensitive polymers. Vol. 8, Polymer Chemistry. Royal Society of Chemistry; 2017. p. 74–96.
13. Irie M. Photoresponsive polymers. Adv Polym Sci. 1990;94:26–67.
14. Espinosa-Cano E, Aguilar MR, Vázquez B, San Román J. Inflammation-Responsive Polymers. In: Smart Polymers and their Applications. Elsevier; 2019. p. 219–54.
15. Wu P, Jia Y, Qu F, Sun Y, Wang P, Zhang K, et al. Ultrasound-Responsive Polymeric Micelles for Sonoporation-Assisted Site-Specific Therapeutic Action. ACS Appl Mater Interfaces. 2017 Aug 9;9(31):25706–16.
16. Hoogenboom R. Temperature-responsive polymers: Properties, synthesis and applications. In: Smart Polymers and their Applications. Elsevier Ltd; 2014. p. 15–44.
17. Martinez K, Stash J, Benson KR, Paul JJ, Schmehl RH. Direct Observation of Sequential Electron and Proton Transfer in Excited-State ET/PT Reactions. J Phys Chem C. 2019 Feb 7;123(5):2728–35.
18. Ogoshi T, Hashizume M, Yamagishi TA, Nakamoto Y. Synthesis, conformational and host-guest properties of water-soluble pillar[5]arene. Chem Commun. 2010 May 18;46(21):3708–10.